Section 17

Gas-Solid Operations and Equipment

Mel Pell, Ph.D., *Senior Consultant, E. I. duPont de Nemours & Co.; Fellow, American Institute of Chemical Engineers. (Section Editor, Fluidized Bed Systems)*

James B. Dunson, M.S., *Principal Consultant, E. I. duPont de Nemours & Co.; Member American Institute of Chemical Engineers; Registered Professional Engineer. (Delaware) (Gas-Solid Separations)*

FLUIDIZED-BED SYSTEMS

GAS-SOLIDS SEPARATIONS

FLUIDIZED-BED SYSTEMS

Fluidization, or fluidizing, converts a bed of solid particles into an expanded, suspended mass that has many properties of a liquid. This mass has zero angle of repose, seeks its own level, and assumes the shape of the containing vessel.

Fluidized beds are used successfully in a multitude of processes both catalytic and noncatalytic. Among the catalytic uses are hydrocarbon cracking and re-forming, oxidation of naphthalene to phthalic anhydride, and ammoxidation of propylene to acrylonitrile. A few of the noncatalytic uses are roasting of sulfide ores, coking of petroleum residues, calcination of ores, incineration of sewage sludge, drying, and classification. Considerable effort and interest are now centered in the areas of coal and waste combustion to raise steam.

The size of solid particles which can be fluidized varies greatly from less than 1 μm to 6 cm (2½ in). It is generally concluded that particles distributed in sizes between 150 μm and 10 μm are the best for smooth fluidization (least formation of large bubbles). Large particles cause instability and result in slugging or massive surges. Small particles (less than 20 μm) frequently, even though dry, act as if damp, forming agglomerates or fissures in the bed, or spouting. Adding finer-sized particles to a coarse bed or coarser-sized particles to a bed of fines usually results in better fluidization.

The upward velocity of the gas is usually between 0.15 m/s (0.5 ft/s) and 6 m/s (20 ft/s). This velocity is based upon the flow through the empty vessel and is referred to as the **superficial velocity.**

For details beyond the scope of this subsection, reference should be made to Kunii and Levenspiel, *Fluidization Engineering,* 2d ed., Butterworth Heinemann, Boston, 1991; Pell, *Gas Fluidization,* Elsevier, New York, 1990; D. Geldart (ed.), *Gas Fluidization Technology,* Wiley, New York, 1986; and the vast number of papers published in periodicals, transcripts of symposia, and the American Institute of Chemical Engineers symposium series.

GAS-SOLID SYSTEMS

Several workers in the field have systematized the various types of fluidization. Several of these types are discussed in the following subsections because each adds another dimension to the understanding of the phenomena.

Types of Solids Geldart [*Powder Technol.,* **7,** 285–292 (1973)] has characterized four groups of solids that exhibit different properties when fluidized with a gas. Figure 17-1 shows the division of the classes as a function of mean particle size, $\bar{d}_{sv}$, μm, and density difference, $(\rho_s - \rho_f)$, g/cm^3, where ρ_s = particle density and ρ_f = fluid density

$$\bar{d}_{sv} = \frac{1}{\sum (x_i/d_{pi})}$$

where $\bar{d}_{sv}$ = surface volume diameter of particle and x_i = weight fraction of particles of size d_{pi}. $\bar{d}_{sv}$ is the preferred particle averaging method for fluid bed applications.

When gas is passed upward through a bed of particles of groups *A, B,* or *D,* friction causes a pressure drop expressed by the Carman-Kozeny fixed-bed correlation. As the gas velocity is increased, the pressure drop increases until it equals the weight of the bed divided by the cross-sectional area. This velocity is called minimum fluidizing velocity, U_{mf}. When this point is reached, the bed of group *A* particles will expand uniformly until at some higher velocity gas bubbles will form (minimum bubbling velocity, U_{mb}). For group *B* and group *D* particles U_{mf} and U_{mb} are essentially equal. Group *C* particles exhibit cohesive tendencies, and as the gas flow is further increased, usually "rathole"; the gas opens channels that extend from the gas distributor to the surface. If channels are not formed, the whole bed will lift as a piston. At higher velocities or with mechanical agitation or vibration,

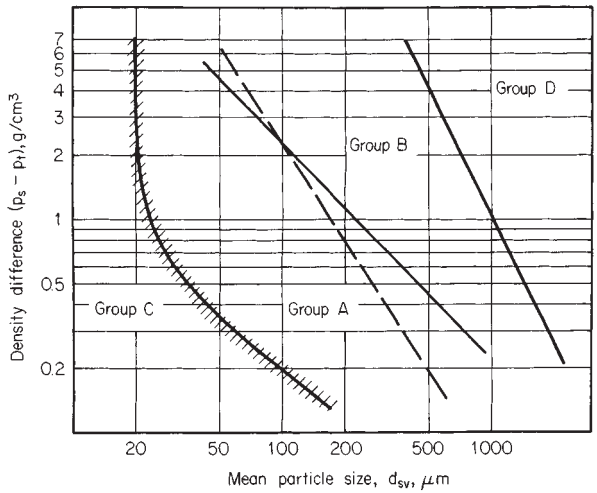

FIG. 17-1 Powder-classification diagram for fluidization by air (ambient conditions). [*From Geldart,* Powder Technol., **7,** *285–292 (1973).*]

this type of particle will fluidize but with the appearance of clumps or clusters of particles. For all groups of powder (*A, B, C,* and *D*) as the gas velocity is further increased, bed density is decreased and turbulence increased. In smaller-diameter beds, especially with group *B* and *D* powders, slugging will occur as the bubbles increase in size to greater than half of the bed diameter. Bubbles grow by vertical and lateral merging. Bubbles also increase in size as the gas velocity is increased [Whitehead, in Davidson and Harrison (eds.), *Fluidization,* Academic, London and New York, 1971]. As the gas velocity is increased further and bubbles tend to disappear and streamers of solids and gas prevail, pressure fluctuations in the bed are greatly reduced. Further increase in velocity results in dilute-phase pneumatic transport.

Phase Diagram (Zenz and Othmer) Zenz and Othmer (op. cit.) have graphically represented (Fig. 17-2) all gas-solid systems in which the gas is flowing counter to gravity as a function of pressure drop per unit of height versus velocity. Note that line *OAB* in Fig. 17-2 is the pressure-drop versus gas-velocity curve for a packed bed and *BD* the curve for a fluid bed. Zenz indicates an instability between *D* and *H* because with no solids flow all the particles will be entrained from the bed; however, if solids are added to replace those entrained, system *IJ* prevails. The area *DHIJ* will be discussed further.

Phase Diagram (Grace) Grace [*Can. J. Chem. Eng.,* **64,** 353–363 (1986); Fig. 17-3] has correlated the various types of gas-solid systems in which the gas is flowing counter to gravity in a status graph using the parameters of the Archimedes number (Ar) for the particle size and a nondimensional velocity (U^*) for the gas effects. By means of this plot, the regime of fluidization can be predicted.

Regime Diagram (Grace) Grace [*Can. J. Chem. Eng.,* **64,** 353–363 (1986); Fig. 17-4] has also sketched the way a fluid bed appears in the different regimes of fluidization resulting from increasing velocity from packed-bed operation to a transport reactor. The area that Zenz and Othmer consider to be discontinuous is called the fast fluid bed regime. Note that since beds in turbulent and faster regimes operate above the terminal velocity of some or all of the particles, solids return is necessary to maintain a bed.

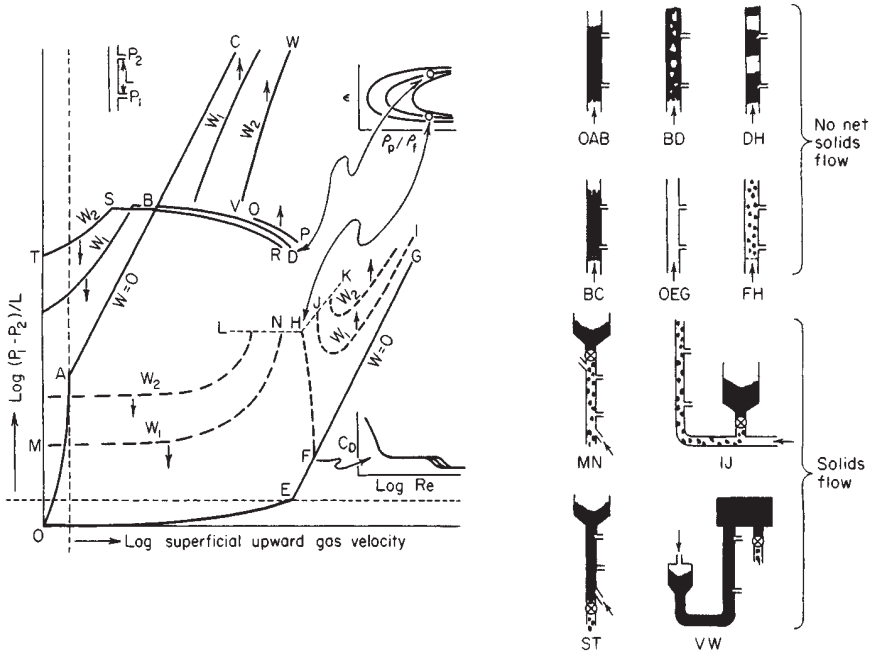

FIG. 17-2 Schematic phase diagram in the region of upward gas flow. W = mass flow solids, lb/(h · ft^2); ε = fraction voids; ρ_p = particle density, lb/ft^3; ρ_f = fluid density, lb/ft^3; Cd = drag coefficient; Re = modified Reynolds number. (*Zenz and Othmer,* Fluidization and Fluid Particle Systems, *Reinhold, New York, 1960.*)

Key:

OAB = packed bed	IJ = cocurrent flow (dilute phase)	AC = packed bed (restrained at top)	FH = dilute phase
BD = fluidized bed	ST = countercurrent flow (dense phase)	OEG = fluid only (no solids)	MN = countercurrent flow (dilute phase)
DH = slugging bed			VW = cocurrent flow (dense phase)

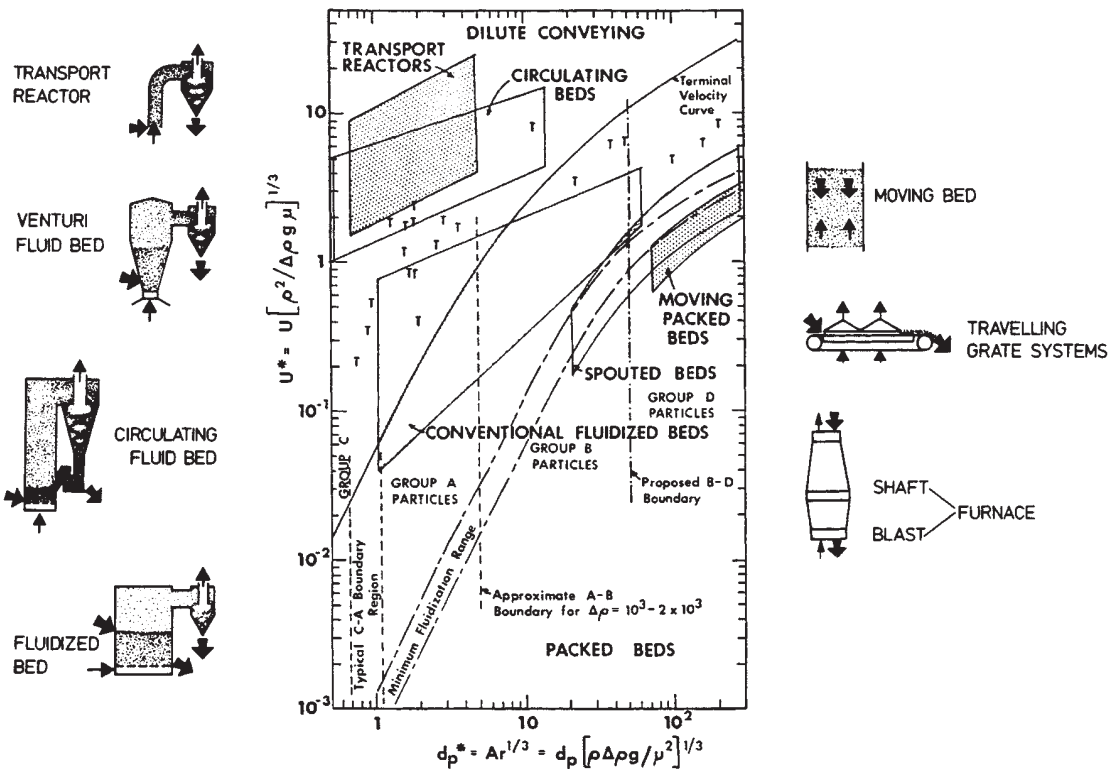

FIG. 17-3 Simplified fluid-bed status graph [*From Grace,* Can. J. Chem. Eng., ***64,*** *353–363 (1986); sketches from Reh,* Ger. Chem. Eng., ***1,*** *319–329 (1978).*]

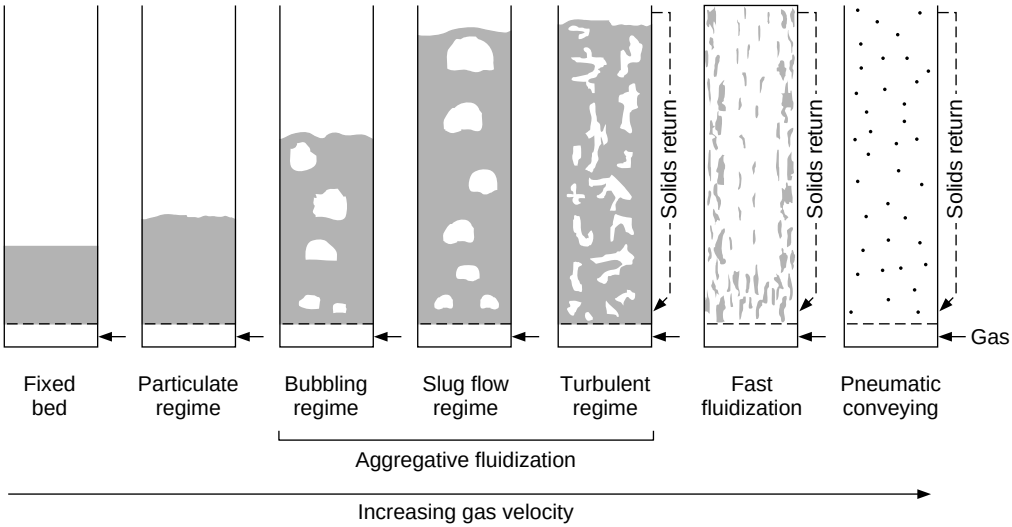

FIG. 17-4 Fluidization regimes. [*Adapted from Grace,* Can J. Chem. Eng., ***64,*** *353–363 (1986).*]

Solids Concentration versus Height From the foregoing it is apparent that there are several regimes of fluidization. These are, in order of increasing gas velocity, particulate fluidization (Geldart group *A*), bubbling (aggregative), turbulent, fast, and transport. Each of these regimes has characteristic solids concentration profiles as shown in Fig. 17-5.

Equipment Types Fluidized-bed systems take many forms. Figure 17-6 shows some of the more prevalent concepts with approximate ranges of gas velocities.

Minimum Fluidizing Velocity U_{mf}, the minimum fluidizing velocity, is frequently used in fluid-bed calculations and in quantifying one of the particle properties. This parameter is best measured in small-scale equipment at ambient conditions. The correlation by Wen and Yu [*A.I.Ch.E.J.*, 610–612 (1966)] given below can then be used to back calculate d_p. This gives a particle size that takes into account effects of size distribution and sphericity. The correlation can then be used to estimate U_{mf} at process conditions. If U_{mf} cannot be determined experimentally, use the expression below directly.

$$\mathrm{Re}_{mf} = (1135.7 + 0.0408\mathrm{Ar})^{0.5} - 33.7$$

where $\mathrm{Re}_{mf} = \bar{d}_p \rho_f U_{mf}/\mu$

$\mathrm{Ar} = \bar{d}_p^3 \rho_f(\rho_s - \rho_f)g/\mu^2$

$\bar{d}_p = 1/\sum (x_i/d_{pi})$

The flow required to maintain a complete homogeneous bed of solids in which coarse or heavy particles will not segregate from the fluidized portion is very different from the minimum fluidizing velocity. See Nienow and Chiba, *Fluidization,* 2d ed., Wiley, 1985, pp. 357–382, for a discussion of segregation or mixing mechanism as well as the means of predicting this; also see Baeyens and Geldart, *Gas Fluidization Technology,* Wiley, 1986, 97–122.

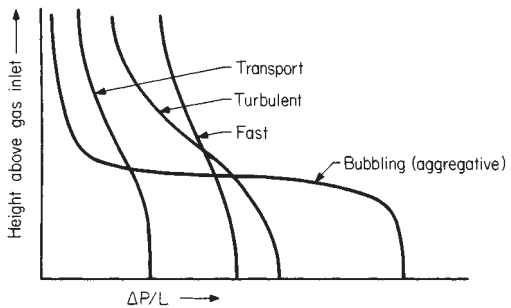

FIG. 17-5 Solids concentration versus height above distributor for regimes of fluidization.

Particulate Fluidization Fluid beds of Geldart class *A* powders that are operated at gas velocities above the minimum fluidizing velocity (U_{mf}) but below the minimum bubbling velocity (U_{mb}) are said to be particulately fluidized. As the gas velocity is increased above U_{mf}, the bed further expands. Decreasing $(\rho_s - \rho_f)$, d_p and/or increasing μ_f increases the spread between U_{mf} and U_{mb} until at some point, usually at high pressure, the bed is fully particulately fluidized. Richardson and Zaki [*Trans. Inst. Chem. Eng.,* **32,** 35 (1954)] showed that $U/U_i = \varepsilon^n$, where n is a function of system properties, ε = void fraction, U = superficial fluid velocity, and U_i = theoretical superficial velocity from the Richardson and Zaki plot when $\varepsilon = 1$.

Vibrofluidization It is possible to fluidize a bed mechanically by imposing vibration to throw the particles upward cyclically. This enables the bed to operate with either no gas upward velocity or reduced gas flow. Entrainment can also be greatly reduced compared to unaided fluidization. The technique is used commercially in drying and other applications [Mujumdar and Erdesz, *Drying Tech.,* **6,** 255–274 (1988)], and chemical reaction applications are possible. See Sec. 12 for more on drying applications of vibrofluidization.

DESIGN OF FLUIDIZED-BED SYSTEMS

The use of the fluidization technique requires in almost all cases the employment of a fluidized-bed system rather than an isolated piece of equipment. Figure 17-7 illustrates the arrangement of components of a system.

The major parts of a fluidized-bed system can be listed as follows:

1. Fluidization vessel
   - *a.* Fluidized-bed portion
   - *b.* Disengaging space or freeboard
   - *c.* Gas distributor
2. Solids feeder or flow control
3. Solids discharge
4. Dust separator for the exit gases
5. Instrumentation
6. Gas supply

Fluidization Vessel The most common shape is a vertical cylinder. Just as for a vessel designed for boiling a liquid, space must be provided for vertical expansion of the solids and for disengaging

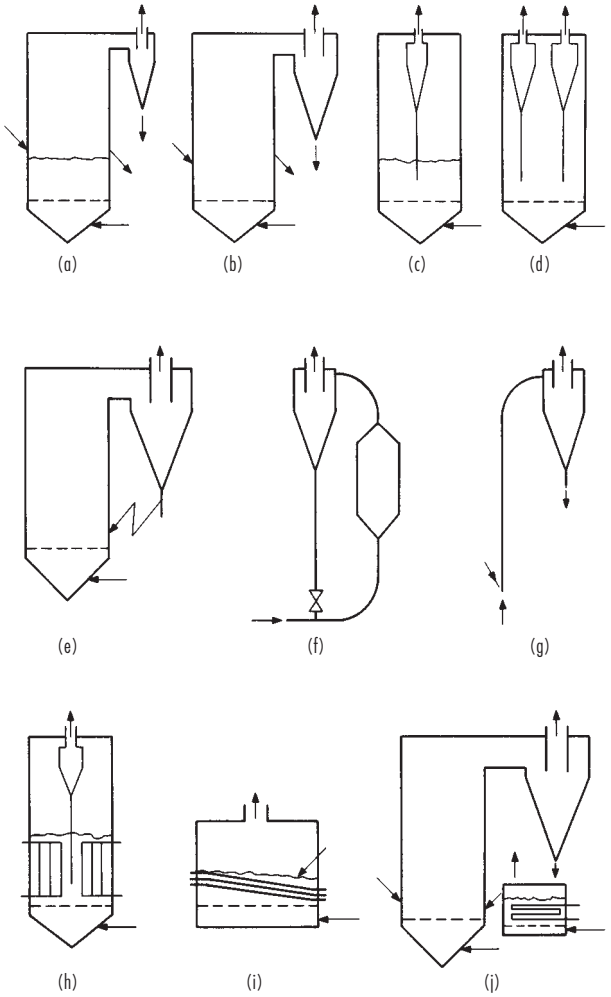

FIG. 17-6 Fluidized-bed systems. (*a*) Bubbling bed, external cyclone, $U < 20 \times U_{mf}$. (*b*) Turbulent bed, external cyclone, $20 \times U_{mf} < U < 200 \times U_{mf}$. (*c*) Bubbling bed, internal cyclones, $U < 20 \times U_{mf}$. (*d*) Turbulent bed, internal cyclones, $20 \times U_{mf} < U < 200 \times U_{mf}$. (*e*) Circulating (fast) bed, external cyclones, $U > 200 \times U_{mf}$. (*f*) Circulating bed, $U > 200 \times U_{mf}$. (*g*) Transport, $U > U_T$. (*h*) Bubbling or turbulent bed with internal heat transfer, $2 \times U_{mf} < U < 200 \times U_{mf}$. (*i*) Bubbling or turbulent bed with internal heat transfer, $2 \times U_{mf} < U < 100 \times U_{mf}$. (*j*) Circulating bed with external heat transfer, $U > 200 \times U_{mf}$.

splashed and entrained material. The volume above the bed is called the disengaging space. The cross-sectional area is determined by the volumetric flow of gas and the allowable or required fluidizing velocity of the gas at operating conditions. In some cases the lowest permissible velocity of gas is used, and in others the greatest permissible velocity is used. The maximum flow is generally determined by the carry-over or entrainment of solids, and this is related to the dimensions of the disengaging space (cross-sectional area and height).

Bed Bed height is determined by a number of factors, either individually or collectively, such as:

1. Gas-contact time
2. *L/D* ratio required to provide staging
3. Space required for internal heat exchangers
4. Solids-retention time

Generally, bed heights are not less than 0.3 m (12 in) or more than 15 m (50 ft).

Although the reactor is usually a vertical cylinder, there is no real limitation on shape. The specific design features vary with operating

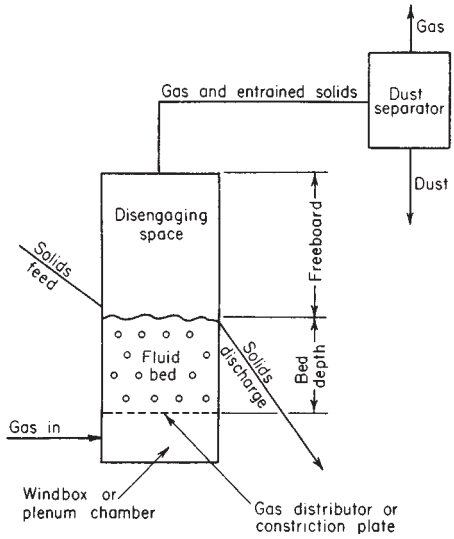

FIG. 17-7 Noncatalytic fluidized-bed system.

conditions, available space, and use. The lack of moving parts lends toward simple, clean design.

Many fluidized-bed units operate at elevated temperatures. For this use, refractory-lined steel is the most economical design. The refractory serves two main purposes: (1) it insulates the metal shell from the elevated temperatures, and (2) it protects the metal shell from abrasion by the bed and particularly the splashing solids at the top of the bed resulting from bursting bubbles. Depending on specific conditions, several different refractory linings are used [Van Dyck, *Chem. Eng. Prog.*, 46–51 (December 1979)]. Generally, for the moderate temperatures encountered in catalytic cracking of petroleum, a reinforced-gunnite lining has been found to be satisfactory. This also permits the construction of larger units than would be permissible if self-supporting ceramic domes were to be used for the roof of the reactor.

When heavier refractories are required because of operating conditions, insulating brick is installed next to the shell and firebrick is installed to protect the insulating brick. Industrial experience in many fields of application has demonstrated that such a lining will successfully withstand the abrasive conditions for many years without replacement. Most serious refractory wear occurs with coarse particles at high gas velocities and is usually most pronounced near the operating level of the fluidized bed.

Gas leakage behind the refractory has plagued a number of units. Care should be taken in the design and installation of the refractory to reduce the possibility of the formation of "chimneys" in the refractories. A small flow of solids and gas can quickly erode large passages in soft insulating brick or even in dense refractory. Gas stops are frequently attached to the shell and project into the refractory lining. Care in design and installation of openings in shell and lining is also required.

In many cases, cold spots on the reactor shell will result in condensation and high corrosion rates. Sufficient insulation to maintain the shell and appurtenances above the dew point of the reaction gases is necessary. Hot spots can occur where refractory cracks allow heat to permeate to the shell. These can sometimes be repaired by pumping castable refractory into the hot area from the outside.

The violent motion of a fluidized bed requires ample foundations and sturdy supporting structure for the reactor. Even a relatively small differential movement of the reactor shell with the lining will materially shorten refractory life. The lining and shell must be designed as a unit. Structural steel should not be supported from a vessel that is subject to severe vibration.

Freeboard and Entrainment The freeboard or disengaging height is the distance between the top of the fluid bed and the gas-exit

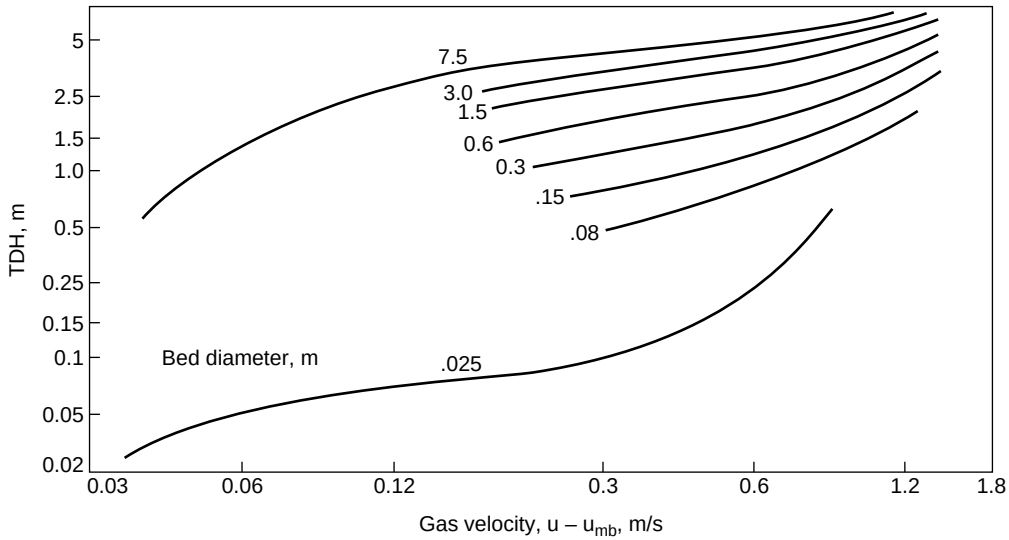

FIG. 17-8 Estimating transport disengaging height (TDH).

nozzle in bubbling- or turbulent-bed units. The distinction between bed and freeboard is difficult to determine in fast and transport units (see Fig. 17-5).

At least two actions can take place in the freeboard: classification of solids and reaction of solids and gases.

As a bubble reaches the upper surface of a fluidized bed, the gas breaks through the thin upper envelope composed of solid particles entraining some of these particles. The crater-shaped void formed is rapidly filled by flowing solids. When these solids meet at the center of the void, solids are geysered upward. The downward pull of gravity and the upward pull of the drag force of the upward-flowing gas act on the particles. The larger and denser particles return to the top of the bed, and the finer and lighter particles are carried upward. The distance above the bed at which the entrainment becomes constant is the transport disengaging height, TDH. Cyclones and vessel gas outlets are usually located above TDH. Figure 17-8 graphically estimates TDH as a function of velocity and bed size.

The higher the concentration of an entrainable component in the bed, the greater its rate of entrainment. Finer particles have a greater rate of entrainment than coarse ones. These principles are embodied in the method of Geldart (*Gas Fluidization Tech.,* Wiley, 1986, pp. 123–153) via the equation, $E(i) = K^*(i)x(i)$, where $E(i)$ = entrainment rate for size i, kg/m^2 s; $K^*(i)$ = entrainment rate constant for particle size i; and $x(i)$ = weight fraction for particle size i. K^* is a function of operating conditions given by $K^*(i)/(P_f u) = 23.7 \exp [-5.4\ U_t(i)/U]$. The composition and the total entrainment are calculating by summing over the entrainable fractions. An alternative is to use the method of Zenz as reproduced by Pell (*Gas Fluidization,* Elsevier, 1990, pp. 69–72).

In batch classification, the removal of fines (particles less than any arbitrary size) can be correlated by treating as a second-order reaction $K = (F/\theta)[1/x(x - F)]$, where K = rate constant, F = fines removed in time θ, and x = original concentration of fines.

Gas Distributor The gas distributor has a considerable effect on proper operation of the fluidized bed. Basically there are two types: (1) for use when the inlet gas contains solids and (2) for use when the inlet gas is clean. In the latter case, the distributor is designed to prevent back flow of solids during normal operation, and in many cases it is designed to prevent back flow during shutdown. In order to provide distribution, it is necessary to restrict the gas or gas and solids flow so that pressure drops across the restriction amount to from 0.5 kPa (2 in of water) to 20 kPa (3 lbf/in^2).

The bubbling action of the bed produces local pressure fluctuations. A temporary condition of low pressure in one section of the bed due to bubbles can combine with higher pressure in another section with fewer bubbles to produce permanent flow maldistribution. The grid should be designed for a pressure drop of at least ⅓ the bed weight for upflow distributors and about 1/10 the bed weight for downflow spargers. In units with shallow beds such as dryers or where distribution is less crucial, lower distributor pressure drops can be used.

When both solids and gases pass through the distributor, such as in catalytic-cracking units, a number of variations are or have been used, such as concentric rings in the same plane, with the annuli open (Fig. 17-9a); concentric rings in the form of a cone (Fig. 17-9b); grids of T bars or other structural shapes (Fig. 17-9c); flat metal perforated plates supported or reinforced with structural members (Fig. 17-9d); dished and perforated plates concave both upward and downward (Fig. 17-9e and f). The last two forms are generally more economical.

In order to generate the required pressure drop, a high velocity through the grid openings may be needed. It is best to limit this velocity to less than 70 m/s to minimize attrition of the bed material. It is common industrial practice to put a shroud of pipe over the opening so that the velocity can be kept high for pressure drop but is reduced for entry to the bed. The technique is applied to both plate and pipe spargers.

Pressure drop through a pipe or a drilled plate is given by:

$$\Delta P = \frac{u^2 \rho_f}{0.64 \times 2g}$$

where u = velocity in the hole at inlet conditions
ρ_f = fluid density in the hole at inlet conditions
ΔP = pressure drop in consistent units (may be lbs/ft^2)

Experience has shown that the concave-upward type is a better arrangement than the concave-downward type, as it tends to increase the flow of gases in the outer portion of the bed. This counteracts the normal tendency of higher gas flows in the center of the bed.

Structurally, distributors must withstand the differential pressure across the restriction during normal and abnormal flow. In addition, during a shutdown all or a portion of the bed will be supported by the distributor until sufficient back flow of the solids has occurred both to reduce the weight of solids above the distributor and to support some of this remaining weight by transmitting the force to the walls and bottom of the reactor. During startup considerable upward thrust can be exerted against the distributor as the settled solids under the distributor are carried up into the normal reactor bed.

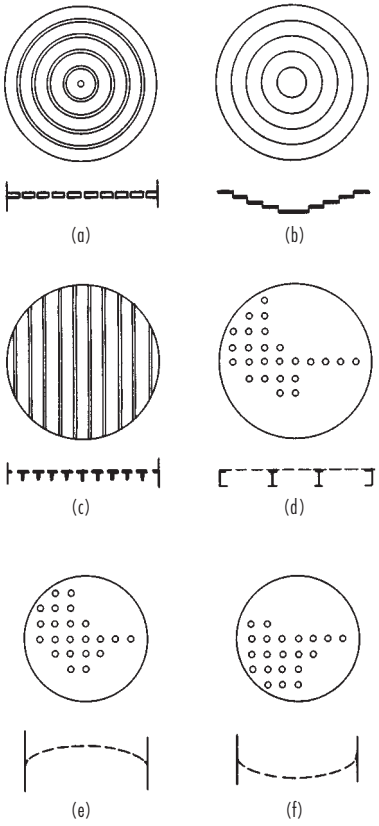

FIG. 17-9 Gas distribution for gases containing solids.

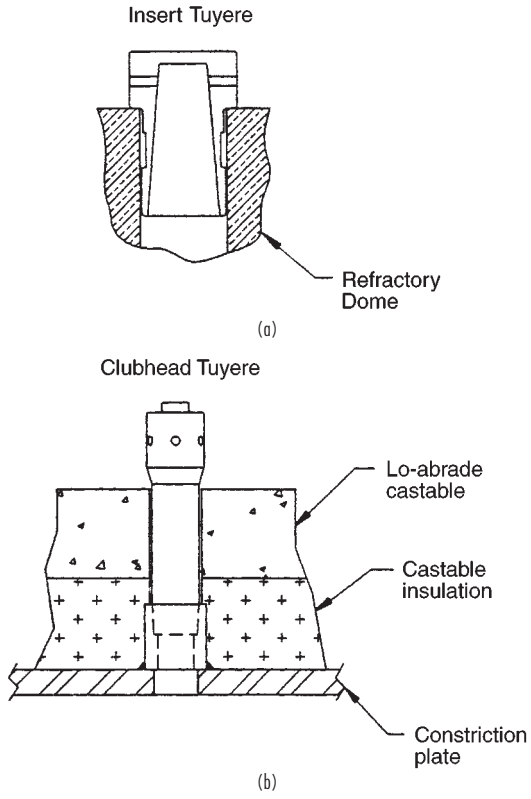

FIG. 17-10 Gas inlets designed to prevent backflow of solids. (*a*) Insert tuyere; (*b*) clubhead tuyere. (*Dorr-Oliver, Inc.*)

When the feed gas is devoid of or contains only small quantities of fine solids, more sophisticated designs of gas distributors can be used to effect economies in initial cost and maintenance. This is most pronounced when the inlet gas is cold and noncorrosive. When this is the case, the plenum chamber gas distributor, and distributor supports can be fabricated of mild steel by using normal temperature design factors. The first commercial fluidized-bed ore roaster [Mathews, *Trans. Can. Inst. Min. Metall.*, **L11,** 97 (1949)], supplied by the Dorr Co. (now Dorr-Oliver Inc.) in 1947 to Cochenour-Willans, Red Lake, Ontario, was designed with a mild-steel constriction plate covered with castable refractory to insulate the plate from the calcine and also to provide cones in which refractory balls were placed to act as ball checks. The balls eroded unevenly, and the castable cracked. However, when the unit was shut down by closing the air-control valve, the runback of solids was negligible because of bridging. If, however, the unit was shut down by deenergizing the centrifugal blower motor, the higher pressure in the reactor would relieve through the blower and fluidizing gas plus solids would run back through the constriction plate. Figure 17-10 illustrates two designs of gas inlets which have been successfully used to prevent flowback of solids. For best results, irrespective of the design, the gas flow should be stopped and pressure-relieved from the bottom upward through the bed.

Some units have been built and successfully operated with simple slot-type distributors made of heat-resistant steel. This requires a heat-resistant plenum chamber but eliminates the frequently encountered problem of corrosion caused by condensation of acids and water vapor on the cold metal of the distributor.

When the inlet gas is hot, such as in dryers or in the upper distributors of multibed units, ceramic arches or heat-resistant metal grates are generally used.

Self-supporting ceramic domes have been in successful use for many years as gas distributors when temperatures range up to 1100°C. Some of these domes are fitted with alloy-steel orifices to regulate air distribution. However, the ceramic arch presents the same problem as the dished head positioned concave downward. Either the holes in the center must be smaller so that the sum of the pressure drops through the distributor plus the bed is constant across the whole cross section, or the top of the arch must be flattened so that the bed depth in the center and outside is equal. This is especially important when shallow beds are used.

It is important to consider thermal effects in design of the grid to

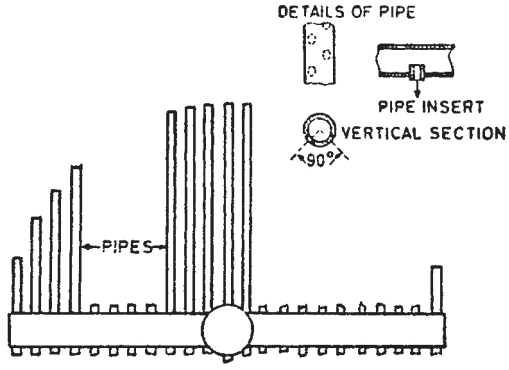

FIG. 17-11 Multiple-pipe gas distributor. [*From Stemerding, de Groot, and Kuypers,* Soc. Chem. Ind. J. Symp. Fluidization Proc., *35–46, London (1963).*]

shell seal. Bypassing of the grid at the seal point is a common problem caused by situations such as uneven expansion of metal and ceramic parts, a cold plenum and hot solids in contact with the grid plate at the same time, and startup and shutdown scenarios.

When the atmosphere in the bed is sufficiently benign, a sparger-type distributor may be used. See Fig. 17-11.

In some cases, it is impractical to use a plenum chamber under the constriction plate. This condition arises when a flammable or explosive mixture of gases is being introduced to the reactor. One solution is to pipe the gases to a multitude of individual gas inlets in the floor of the reactor. In this way it may be possible to maintain the gas velocities in the pipes above the flame velocity or to reduce the volume of gas in each pipe to the point at which an explosion can be safely contained. Another solution is to provide separate inlets for the different gases and depend on mixing in the fluidized bed. The inlets should be fairly close to one another, as lateral gas mixing in fluidized beds is poor.

Much attention has been given to the effect of gas distribution on bubble growth in the bed and the effect of this on catalyst utilization, space-time yield, etc. It would appear that the best gas distributor would be a porous membrane. This type of distributor is seldom practical for commercial units because of both structural limitations and the need for absolutely clean gas. Practically, the limitations on hole spacing are dependent on particle size of solids, materials of construction, and type of distributor. If easily worked metals are used, punching, drilling, and welding are not expensive operations and permit the use of large numbers of holes. The use of tuyeres or bubble caps permits horizontal distribution of the gas so that a smaller number of gas-inlet ports can still achieve good gas distribution. If a ceramic arch is used, generally only one hole per brick is permissible and brick dimensions must be reasonable.

Scale-Up

Bubbling or Turbulent Beds Scale-up of noncatalytic fluidized beds when the reaction is fast, as in roasting or calcination, is straightforward and is usually carried out on an area basis. Small-scale tests are made to determine physical limitations such as sintering, agglomeration, solids-holdup time required, etc. Slower ($k < 1$/s) catalytic or more complex reactions in which several gas interchanges are required are usually scaled up in several steps, from laboratory to commercial size. The hydrodynamics of gas-solids flow and contacting is quite different in small-diameter high-L/D fluid beds as compared with large-diameter moderate-L/D beds. In small-diameter beds, bubbles tend to be small and cannot grow larger than the vessel diameter. In larger, deeper units, bubbles can grow very large. The large bubbles have less surface for mass transfer to the solids than the same volume of small bubbles. The large bubbles also rise through the bed more quickly.

The size of a bubble as a function of height was given by Darton et al. [*Trans. Inst. Chem. Eng.*, **55,** 274–280 (1977)] as

$$d_b = \frac{0.54(u - u_{mb})^{0.4}(h + 4\sqrt{A_t/N_o})^{0.8}}{g^{0.2}}$$

where d_b = bubble diameter, m
h = height above the grid, m
A_t/N_o = grid area per hole

Bubble growth will be limited by the containing vessel and the bubble hydrodynamic stability. Bubbles in group-B systems can grow to several meters in diameter. Bubbles in group-A materials with high fines may reach a maximum stable bubble size of only several cm.

Furthermore, the solids and gas back mixing is much less in high-L/D beds, either slugging or bubbling, as compared with low-L/D beds. Thus, the conversion or yield in large unstaged reactors is sometimes considerably lower than in small high-L/D units. To overcome some of the problems of scale-up, staged units are used (see Fig. 17-12). It is generally concluded than an unstaged 1-m- (40-in-) diameter unit will achieve about the same conversion as a large industrial unit. The validity of this conclusion is dependent on many variables, including bed depth, particle size, and size distribution, temperature, and pressure. A brief history of fluidization, fluidized-bed scale-up, and modeling will illustrate the problems.

Fluidized beds were used in Europe in the 1920s to gasify coal. Scale-up problems either were insignificant or were not publicized. During World War II, catalytic cracking of oil to produce gasoline was successfully commercialized by scaling up from pilot-plant size (a few centimeters in diameter) to commercial size (several meters in diameter). It is fortunate that the kinetics of the cracking reactions are fast, that the ratio of crude oil to catalyst is determined by thermal balance and the required catalyst circulation rates, and that the crude feed point was in the plug-flow riser. The first experience of problems with scale-up was associated with the production of gasoline from natural gas by using the Fischer-Tropsch process. Some 0.10-m- (4-in-), 0.20-m- (8-in-), and 0.30-m- (12-in-) diameter pilot-plant results were scaled to a 7-m-diameter commercial unit, where the yield was only about 50 percent of that achieved in the pilot units. The Fischer-Tropsch synthesis is a relatively slow reaction; therefore, gas-solid contacting is very important. Since this unfortunate experience or perhaps because of it, much effort has been given to the scale-up of fluidized beds. Many models have been developed; these basically are

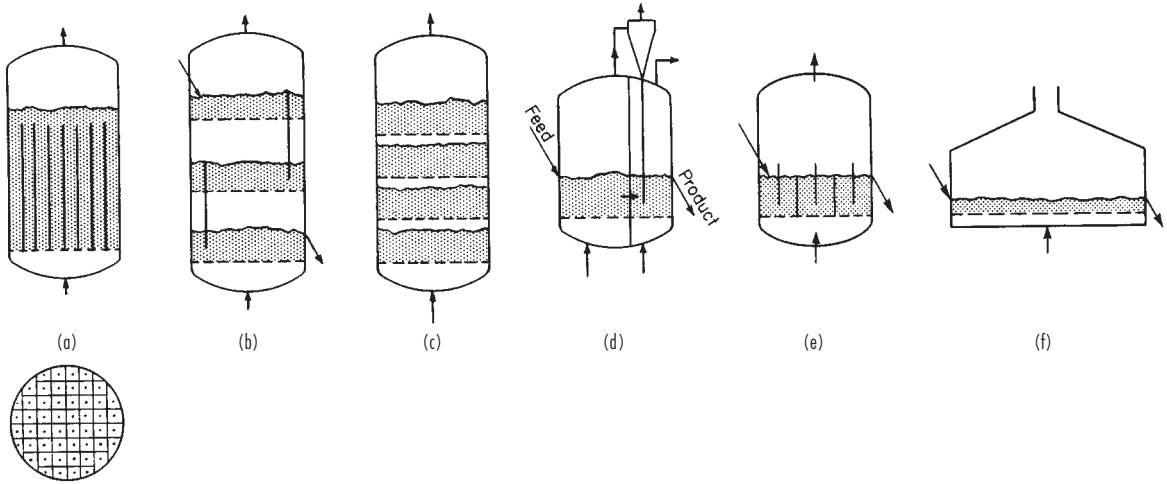

FIG. 17-12 Methods of providing staging in fluidized beds.

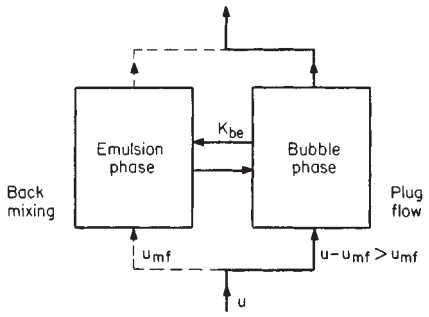

FIG. 17-13 Two-phase model according to May [Chem. Eng. Prog., ***55,*** *12, 5, 49–55 (1959)*] and Van Deemter [Chem. Eng. Sci., ***13,*** *143–154 (1961)*]. U = superficial velocity, U_{mf} = minimum fluidizing velocity, E = axial dispersion coefficient, and K_{be} = mass-transfer coefficient.

of two types, the two-phase model [May, *Chem. Eng. Prog.*, **55,** 12, 5, 49–55 (1959); and Van Deemter, *Chem. Eng. Sci.*, **13,** 143–154 (1961)] and the bubble model (Kunii and Levenspiel, *Fluidization Engineering*, Wiley, New York, 1969). The two-phase model according to May and Van Deemter is shown in Fig. 17-13. In these models all or most of the gas passes through the bed in plug flow in the bubbles which do not contain solids (catalyst). The solids form a dense suspension-emulsion phase in which gas and solids mix according to an axial dispersion coefficient (E). Cross flow between the two phases is predicted by a mass-transfer coefficient.

Conversion of a gaseous reactant can be given by $C/C_0 = \exp[-Na \times Nr/(Na + Nr)]$ where C = the exit concentration, C_0 = the inlet concentration, Na = diffusional driving force and Nr = reaction driving force. Conversion is determined by both reaction and diffusional terms. It is possible for reaction to dominate in a lab unit with small bubbles and for diffusion to dominate in a plant size unit. It is this change of limiting regime that makes scaleup so difficult. Refinements of the basic model and predictions of mass-transfer and axial-dispersion coefficients are the subject of many papers [Van Deemter, *Proc. Symp. Fluidization,* Eindhoven (1967); de Groot, ibid.; Van Swaaij; and Zuidiweg, *Proc. 5th Eur. Symp. React. Eng., Amsterdam,* B9–25 (1972); DeVries, Van Swaaij, Mantovani, and Heijkoop, ibid., B9–59 (1972); Werther, *Ger. Chem. Eng.,* **1,** 243–251 (1978); and Pell, *Gas Fluidization,* Elsevier, 75–81 (1990).

The bubble model (Kunii and Levenspiel, *Fluidization Engineering*, Wiley, New York, 1969; Fig. 17-14) assumes constant-sized bubbles (effective bubble size d_b) rising through the suspension phase. Gas is transferred from the bubble void to the mantle and wake at

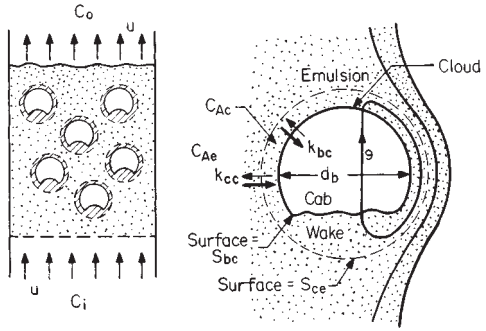

FIG. 17-14 Bubbling-bed model of Kunii and Levenspiel. d_b = effective bubble diameter, C_{Ab} = concentration of A in bubble, C_{Ac} = concentration of A in cloud, C_{Ae} = concentration of A in emulsion, q = volumetric gas flow into or out of bubble, k_{bc} = mass-transfer coefficient between bubble and cloud, and k_{ce} = mass-transfer coefficient between cloud and emulsion. (*From Kunii and Levenspiel,* Fluidization Engineering, *Wiley, New York, 1969, and Krieger, Malabar, Fla., 1977.*)

mass-transfer coefficient K_{bc} and from the mantle and wake to the emulsion phase at mass-transfer coefficient K_{ce}. Experimental results have been fitted to theory by means of adjusting the effective bubble size. As mentioned previously, bubble size changes from the bottom to the top of the bed, and thus this model is not realistic though of considerable use in evaluating reactor performance. Several bubble models using bubbles of increasing size from the distributor to the top of the bed and gas interchange between the bubbles and the emulsion phase according to Kunii and Levenspiel have been proposed [Kato and Wen, *Chem. Eng. Sci.*, **24,** 1351–1369 (1969); and Fryer and Potter, in Keairns (ed.), *Fluidization Technology,* vol. I, Hemisphere, Washington, 1975, pp. 171–178].

There are several methods available to reduce scaleup loss. These are summarized in Fig. 17-15. The efficiency of a fluid bed reactor usually decreases as the size of the reactor increases. This can be minimized by the use of high velocity, fine solids, staging methods, and a high L/D. High velocity maintains the reactor in the turbulent mode, where bubble breakup is frequent and backmixing is infrequent. A fine catalyst leads to smaller maximum bubble sizes by promoting instability of large bubbles. Maintaining high L/D minimizes backmixing, as does the use of baffles in the reactor. By these techniques, Mobil was able to scale up its methanol to gasoline technology with little difficulty. [Krambeck, Avidan, Lee and Lo, *A.I.Ch.E.J.*, 1727–1734 (1987)].

Another way to examine scaleup of hydrodynamics is to build a cold or hot scale model of the commercial design. Validated scaling criteria have been developed and are particularly effective for group B and D materials [Glicksman, Hyre and Woloshun, *Powder Tech.*, 177–199 (1993)].

Circulating or Fast Beds The circulating or fast fluidized bed carries the principles given above to the maximum extent. Velocity is increased until solids are entrained from the bed at a massive rate. Thus, solids extend to the exit and may constitute up to 10 percent of the freeboard volume. There are no bubbles, mass transfer rates are high, and there is little backmixing. The high velocity means high gas throughput, minimizing reactor cost. Scaleup is less of a problem than with bubbling beds.

The system is characterized by an external cyclone return system that is usually as large as the reactor itself. The axial solids density profile is relatively flat, as indicated in Figs. 17-4 and 17-5. There is a radial solids density profile called core annular flow. In the center of the reactor, gas flow may be double the average, and the solids are in dilute flow, traveling at $U_g - U_t$, their expected slip velocity. Near the wall, the solids are close to their minimum bubbling density and are likely to be in downflow. Engineering methods for evaluating the hydrodynamics of the circulating bed are given by Kunii and Levenspiel (*Fluidization Engineering,* 2d ed., Butterworth, 1991, pp. 195–

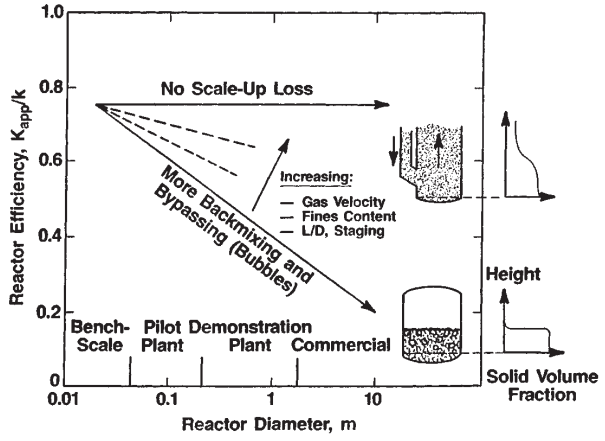

FIG. 17-15 Reducing scaleup loss (*From Krambeck, Avidan, Lee and Lo,* A.I.Ch.E.J., *1727–1734, 1987.*)

209) and Werther (*Circulating Fluid Bed Technology IV,* in press, 1994).

Transport Transport units can be scaled up on the principles of pneumatic conveying. Mass and heat transfer can be predicted on both the slip velocity during acceleration and the slip velocity at full acceleration. The slip velocity is increased as the solids concentration is increased.

Heat Transfer Heat-exchange surfaces have been used to provide means of removing or adding heat to fluidized beds. Usually, these surfaces are provided in the form of vertical tubes manifolded at top and bottom or in trombone shape manifolded exterior to the vessel.

Other shapes such as horizontal bayonets have been used. In any such installations adequate provision must be made for abrasion of the exchanger surface by the bed.

The prediction of the heat-transfer coefficient is covered in Secs. 5 and 11. Normally, the transfer rate is between 5 and 25 times that for the gas alone.

Heat transfer from solids to gas and gas to solids usually results in a coefficient of about 6 to 20 J/(m²·s·K) [3 to 10 Btu/(h·ft²·°F)]. However, the large area of the solids per cubic foot of bed, 5000 m²/m³ (15,000 ft²/ft³) for 60-μm particles of 600 kg/m³ (40 lb/ft³) bulk density, results in the rapid approach of gas and solids temperatures. With a fairly good distributor, essential equalization of temperatures occurs within 2 to 6 cm (1 to 3 in) of the top of the distributor.

Bed thermal conductivities in the vertical direction have been measured in the laboratory in the range of 40 to 60 kJ/(m²·s·K) [20,000 to 30,000 Btu/(h·ft²·°F·ft)]. Horizontal conductivities for 3-mm (⅛-in) particles in the range of 2 kJ/(m²·s·K) [1000 Btu/(h·ft²·°F·ft)] have been measured in large-scale experiments.

Except in extreme *L/D* ratios, the temperature in the fluidized bed is uniform—generally the temperature at any point being within 5 K (10°F) of any other point.

Temperature Control Because of the rapid equalization of temperatures in fluidized beds, temperature control can be accomplished in a number of ways.

1. *Adiabatic.* Control gas flow and/or solids feed rate so that the heat of reaction is removed as sensible heat in off gases and solids or heat supplied by gases or solids.
2. *Solids circulation.* Remove or add heat by circulating solids.
3. *Gas circulation.* Recycle gas through heat exchangers to cool or heat.
4. *Liquid injection.* Add volatile liquid so that the latent heat of vaporization equals excess energy.
5. *Cooling or heating surfaces in bed.*

Solids Mixing Solids are mixed in fluidized beds by means of solids entrained in the lower portion of bubbles, and the shedding of these solids from the wake of the bubble (Rowe and Patridge, "Particle Movement Caused by Bubbles in a Fluidized Bed," Third Congress of European Federation of Chemical Engineering, London, 1962). Thus, no mixing will occur at incipient fluidization, and mixing increases as the gas rate is increased. Naturally, particles brought to the top of the bed must displace particles toward the bottom of the bed. Generally, solids upflow is greater in the center of the bed and downward at the wall.

At high ratios of fluidizing velocity to minimum fluidizing velocity, tremendous solids circulation from top to bottom of the bed assures rapid mixing of the solids. For all practical purposes, beds with *L/D* ratios of from 4 to 0.1 can be considered to be completely mixed continuous-reaction vessels insofar as the solids are concerned.

Batch mixing using fluidization has been successfully employed in many industries. In this case there is practically no limitation to vessel dimensions.

All the foregoing pertains to solids of approximately the same physical characteristics. There is evidence that solids of widely different characteristics will classify one from the other at certain gas flow rates [Geldart, Baeyens, Pope, and van de Wijer, *Powder Technol.,* **30**(2), 195 (1981)]. Two fluidized beds, one on top of the other, may be formed, or a lower static bed with a fluidized bed above may result. The latter frequently occurs when agglomeration takes place because of either fusion in the bed or poor dispersion of sticky feed solids. Increased gas flows sometimes overcome the problem; however, improved feeding techniques or a change in operating conditions may be required. Another solution is to remove agglomerates either continuously or periodically from the bottom of the bed.

Gas Mixing The mixing of gases as they pass vertically up through the bed has never been considered a problem. However, horizontal mixing is very poor and requires effective distributors if two gases are to be mixed in the fluidized bed.

In bubbling beds operated at velocities of less than about 5 to 11 times U_{mf} the gases will flow upward in both the emulsion and the bubble phases. At velocities greater than about 5 to 11 times U_{mf} the downward velocity of the emulsion phase is sufficient to carry the contained gas downward. The back mixing of gases increases as U/U_{mf} is increased until the circulating or fast regime is reached where the back mixing decreases as the velocity is further increased.

Size Enlargement Under proper conditions, particles of solids can be caused to grow. That is sometimes advantageous and at other times disadvantageous. Growth is associated with the liquefaction or softening of some portion of the bed material (i.e., addition of soda ash to calcium carbonate feed in lime reburning, tars in fluidized-bed coking, or lead or zinc roasting cause agglomeration of dry particles in much the same way as binders act in rotary pelletizers). The motion of the particles, one against the other, in the bed results in spherical pellets. If the size of these particles is not controlled, segregation of the large particles from the bed will occur. Control can be achieved by crushing a portion of the bed product and recycling it to form nuclei for new growth.

In drying solutions or slurries of solutions, the location of the feed-injection nozzle (spray nozzle) has a great effect on the size of particle formed in the bed. Also of importance are the operating temperature, relative humidity of the off gas, and gas velocity. Particle growth can occur as agglomeration or as an "onion skinning."

Size Reduction Three major size-reduction mechanisms occur in the fluidized bed. These are attrition, impact, and thermal decrepitation.

Because of the random motion of the solids, some abrasion of the surface occurs. This is generally quite small, usually amounting to about 0.25 to 1 percent of the solids per day.

In areas of high gas velocities, greater rates of attrition will occur as well as fracture of particles by impact. This type of jet grinding is employed in some of the coking units to control particle size [Dunlop, Griffin and Moser, *J. Chem. Eng. Prog.*, **54,** 39–43, (1958)]. It also occurs to a lesser degree at the point of gas introduction when the pressure drop to assure gas distribution is taken across an orifice or pipe that discharges directly into the bed.

Thermal decrepitation occurs frequently when crystals are rearranged because of transition from one form to another or when new compounds are formed (i.e., calcination of limestone). Sometimes the strains in cases such as this are sufficient to reduce the particle to the basic crystal size.

All these mechanisms will cause completion of fractures that were started before the introduction of the solids into the fluidized bed.

Standpipes, Solids Feeders, and Solids Flow Control In the case of catalytic-cracking units in which the addition of catalyst is small and need not be steady, the makeup catalyst may be fed from pressurized hoppers into one of the conveying lines. The main solids-flow-control problem is to maintain balanced inventories of catalyst in and controlled flow from and to the reactor and regenerator. This flow of solids from an oxidizing atmosphere to a reducing one, or vice versa, usually necessitates stripping gases from the interstices of the solids as well as gases adsorbed by the particles. Steam is usually used for this purpose. The point of removal of the solids from the fluidized bed is usually under a lower pressure than the point of feed introduction into the carrier gas.

The pressure is higher at the bottom of the solids draw-off pipe due to the relative flow of gas counter to the solids flow. The gas may either be flowing downward more slowly than the solids or upward. The standpipe may be fluidized, or the solids may be in moving packed bed flow with no expansion. Gas is introduced at the bottom (best for group B) or at about 3-m intervals along the standpipe (best for group A). The increasing pressure causes gas inside and between

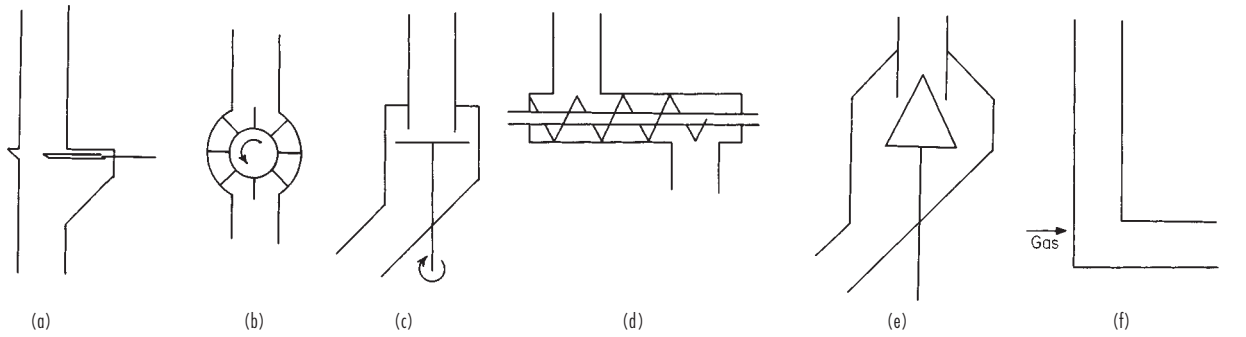

FIG. 17-16 Solids-flow-control devices. (*a*) Slide valve. (*b*) Rotary valve. (*c*) Table feeder. (*d*) Screw feeder. (*e*) Cone valve. (*f*) L Valve.

the particles to be compressed. Unless aeration gas is added, the solids could defluidize and become a moving fixed bed with a lower-pressure head than that of fluidized solids. In any event, the pressure drop across the solids control valve should be designed for 3 psi or more to safely prevent backflow. See Zenz, *Powder Tech.*, 105–113 (1986).

Several designs of valves for solids flow control are used. These should be chosen with care to suit the specific conditions. Usually, block valves are used in conjunction with the control valves. Figure 17-16 shows schematically some of the devices used for solids flow control. Not shown in Fig. 17-16 is the flow-control arrangement used in the Exxon Research & Engineering Co. model IV catalytic-cracking units. This device consists of a U bend. A variable portion of regenerating air is injected into the riser leg. Changes in air-injection rate change the fluid density in the riser and thereby achieve control of the solids flow rate. Catalyst circulation rates of 1200 kg/s (70 tons/min) have been reported.

When the solid is one of the reactants, such as in ore roasting, the flow must be continuous and precise in order to maintain constant conditions in the reactor. Feeding of free-flowing granular solids into a fluidized bed is not difficult. Standard commercially available solids-weighing and -conveying equipment can be used to control the rate and deliver the solids to the feeder. Screw conveyors, dip pipes, seal legs, and injectors are used to introduce the solids into the reactor proper (Fig. 17-16). Difficulties arise and special techniques must be used when the solids are not free-flowing, such as is the case with most filter cakes. One solution to this problem was developed at Cochenour-Willans. After much difficulty in attempting to feed a wet and sometimes frozen filter cake into the reactor by means of a screw feeder, experimental feeding of a water slurry of flotation concentrates was attempted. This trial was successful, and this method has been used in almost all cases in which the heat balance, particle size of solids, and other considerations have permitted. Gilfillan et al. (*J. Chem. Metall. Min. Soc. S. Afr.*, May 1954) and Soloman and Beal (*Uranium in South Africa, 1946–56*) present complete details on the use of this system for feeding.

When slurry feeding is impractical, recycling of solids product to mix with the feed, both to dry and to achieve a better-handling material, has been used successfully. Also, the use of a rotary table feeder mounted on top of the reactor, discharging through a mechanical disintegrator, has been successful. The wet solids generally must be broken up into discrete particles of very fine agglomerates either by mechanical action before entering the bed or by rapidly vaporizing water. If lumps of dry or semidry solids are fed, the agglomerates do not break up but tend to fuse together. As the size of the agglomerate is many times the size of the largest individual particle, these agglomerates will segregate out of the bed, and in time the whole of the fluidized bed may be replaced with a static bed of agglomerates.

Solids Discharge The type of discharge mechanism utilized is dependent upon the necessity of sealing the atmosphere inside the fluidized-bed reactor and the subsequent treatment of the solids. The simplest solids discharge is an overflow weir. This can be used only when the escape of fluidizing gas does not present any hazards due to nature or dust content or when the leakage of gas into the fluidized-bed chamber from the atmosphere into which the bed is discharged is permitted. Solids will overflow from a fluidized bed through a port even though the pressure above the bed is maintained at a slightly lower pressure than the exterior pressure. When it is necessary to restrict the flow of gas through the opening, a simple flapper valve is frequently used. Overflow to combination seal and quench tanks (Fig. 17-17) is used when it is permissible to wet the solids and when disposal or subsequent treatment of the solids in slurry form is desirable. The FluoSeal is a simple and effective way of sealing and purging gas from the solids when an overflow-type discharge is used (Fig. 17-18).

Either trickle (flapper) or star (rotary) valves are effective sealing devices for solids discharge. Each functions with a head of solids above it. Bottom of the bed discharge is also acceptable via a slide valve with a head of solids.

Seal legs are frequently used in conjunction with solids-flow-control valves to equalize pressures and to strip trapped or adsorbed gases from the solids. The operation of a seal leg is shown schematically in Fig. 17-19. The solids settle by gravity from the fluidized bed into the seal leg or standpipe. Seal and/or stripping gas is introduced near the bottom of the leg. This gas flows both upward and downward. Pressures indicated in the illustration have no absolute value but are only relative. The legs are designed for either fluidized or settled solids.

The L valve is shown schematically in Fig. 17-20. It can act as a seal and as a solids-flow control valve. However, control of solids rate is only practical for solids that deaerate quickly (Geldart B and D). The

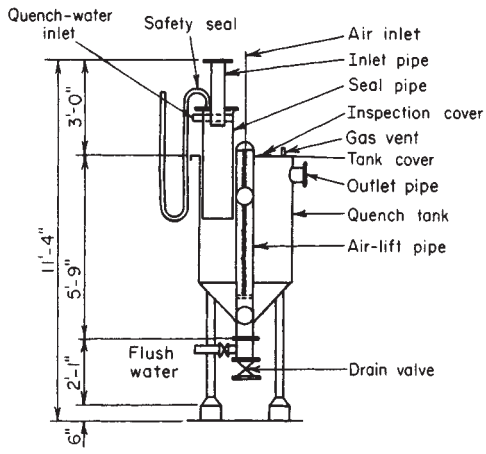

FIG. 17-17 Quench tank for overflow or cyclone solids discharge. [*Gilfillan et al., "The FluoSolids Reactor as a Source of Sulphur Dioxide,"* J. Chem. Metall. Min. Soc. S. Afr. (*May 1954*).]

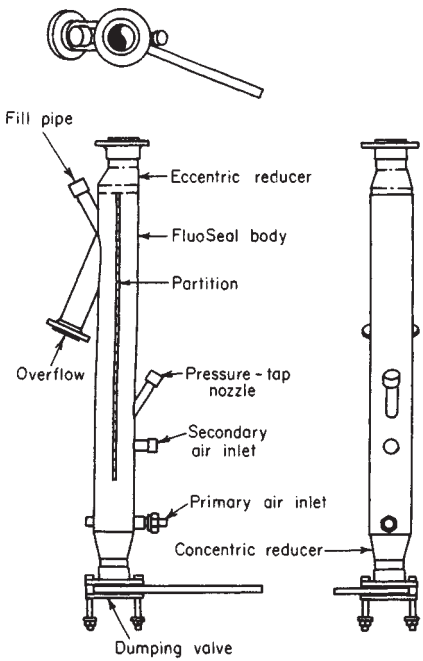

FIG. 17-18 Dorrco FluoSeal, type UA. (*Dorr-Oliver Inc.*)

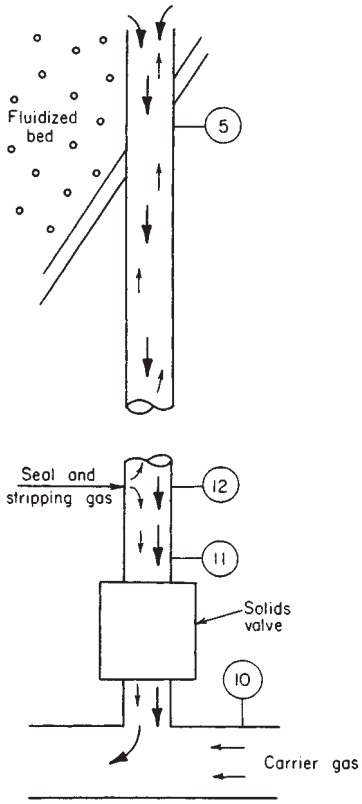

FIG. 17-19 Fluidized-bed seal leg.

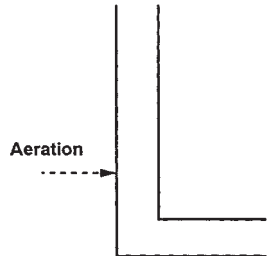

FIG. 17-20 L valve.

height at which aeration is added in Fig. 17-20 is usually one exit pipe diameter above the centerline of the exit pipe. For L-valve design equations, see Yang and Knowlton [*Powder Tech.*, **77,** 49–54 (1993)].

In the sealing mode, the leg is usually fluidized. Gas introduced below the normal solids level and above the discharge port will flow upward and downward. The relative flow in each direction is self-adjusting, depending upon the differential pressure between the point of solids feed and discharge and the level of solids in the leg. The length and diameter of the discharge spout are selected so that the undisturbed angle of repose of the solids will prevent discharge of the solids. As solids are fed into the leg, height H of solids increases. This in turn reduces the flow of gas in an upward direction and increases the flow of gas in a downward direction. When the flow of gas downward and through the solids-discharge port reaches a given rate, the angle of repose of the solids is upset and solids discharge commences. Usually, the level of solids above the point of gas introduction will float. When used as a flow controller, the vertical leg is best run in the packed bed mode. The solids flow rate is controlled by varying the aeration gas flow.

In most catalytic-reactor systems, no solids removal is necessary as the catalyst is retained in the system and solids loss is in the form of fines that are not collected by the dust-recovery system.

Dust Separation It is usually necessary to recover the solids carried by the gas leaving the disengaging space or freeboard of the fluidized bed. Generally, cyclones are used to remove the major portion of these solids (see "Gas-Solids Separation"). However, in a few cases, usually on small-scale units, filters are employed without the use of cyclones to reduce the loading of solids in the gas. For high-temperature usage, either porous ceramic or sintered metal has been employed. Multiple units must be provided so that one unit can be blown back with clean gas while one or more are filtering.

Cyclones are arranged generally in any one of the arrangements shown in Fig. 17-21. The effect of cyclone arrangement on the height of the vessel and the overall height of the system is apparent. Details regarding cyclone design and collection efficiencies are to be found in another portion of this section.

Discharging of the cyclone into the fluidized bed requires some care. It is necessary to seal the bottom of the cyclone so that the collection efficiency of the cyclone will not be impaired by the passage of appreciable quantities of gas up through the solids-discharge port. This is usually done by sealing the dip leg in the fluid bed. Experience has shown, particularly in the case of deep beds, that the bottom of the dip pipe must be protected from the action of large gas bubbles which, if allowed to pass up the leg, would carry quantities of fine solids up into the cyclone and cause momentarily high losses. This can be done by attaching a plate larger in diameter than the pipe to the bottom (see Fig. 17-22*e*).

Example 1: Length of Seal Leg The length of the seal leg can be estimated as shown in the following example.

Given: Fluid density of bed at 0.3-m/s (1-ft/s) superficial gas velocity = 1100 kg/m^3 (70 lb/ft^3).

Fluid density of cyclone product at 0.15 m/s (0.5 ft/s) = 650 kg/m^3 (40 lb/ft^3).

Settled bed depth = 1.8 m (6 ft)

Fluidized-bed depth = 2.4 m (8 ft)

Pressure drop through cyclone = 1.4 kPa (0.2 lbf/in^2)

In order to assure seal at startup, the bottom of the seal leg is 1.5 m (5 ft) above the constriction plate or submerged 0.9 m (3 ft) in the fluidized bed.

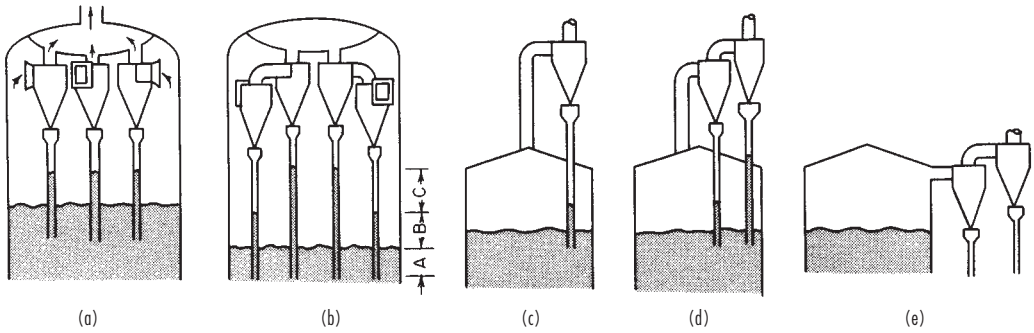

FIG. 17-21 Fluidized-bed cyclone arrangements. (*a*) Single-stage internal cyclone. (*b*) Two-stage internal cyclone. (*c*) Single-stage external cyclone; dust returned to bed. (*d*) Two-stage external cyclone; dust returned to bed. (*e*) Two-stage external cyclone; dust collected externally.

The pressure at the solids outlet of a gas cyclone is usually about 0.7 kPa (0.1 lbf/in^2) lower than the pressure at the discharge of the leg. Total pressure to be balanced by the fluid leg in the cyclone dip leg is

$$(0.9 \times 1100 \times 9.81)/1000 + 1.4 + 0.7 = 11.8 \text{ Kpa}$$

$$[(3 \times 70)/144 + 0.2 + 0.1 = 1.7 \text{ lb/in}^2]$$

Height of solids in dip leg = $(11.8 \times 1000)/(650 \times 9.81) = 1.9$ m [$(1.7 \times 144)/40 = 6.1$ ft]; therefore, the bottom of the separator pot on the cyclone must be at least 1.9 + 1.5 or 3.4 m (6.1 + 5 or 11.1 ft) above the gas distributor. To allow for upsets, changes in size distribution, etc., use 4.6 m (15 ft).

In addition to the open dip leg, various other devices have been used to seal cyclone solids returns, especially for second-stage cyclones. A number of these are shown in Fig. 17-22. One of the most frequently used is the trickle valve (17-22*a*). There is no general agreement as to whether this valve should discharge below the bed level or in the freeboard. In any event, the legs must be large enough to carry momentarily high rates of solids and must provide seals to overcome cyclone pressure drops as well as to allow for differences in fluid density of bed and cyclone products. It has been reported that, in the case of catalytic-cracking catalysts, the fluid density of the solids collected by the primary cyclone is essentially the same as that in the fluidized bed because the particles in the bed are so small, nearly all are entrained. However, as a general rule the fluidized density of solids collected by the first cyclone is less than the fluidized density of the bed. Each succeeding cyclone collects finer and less dense solids.

As cyclones are less effective as the particle size decreases, secondary collection units are frequently required, i.e., filters, electrostatic precipitators, and scrubbers. When dry collection is not required, elimination of cyclones is possible if allowance is made for heavy solids loads in the scrubber (see "Gas-Solids Separations"; see also Sec. 14).

Instrumentation

Temperature Measurement This is usually simple, and standard temperature-sensing elements are adequate for continuous use. Because of the high abrasion wear on horizontal protection tubes, vertical installations are frequently used. In highly corrosive atmospheres in which metallic protection tubes cannot be used, short, heavy ceramic tubes have been used successfully.

Pressure Measurement Although successful pressure-measurement probes or taps have been fabricated by using porous materials, the most universally accepted pressure tap consists of a purged tube projecting into the bed as nearly vertically as possible. Minimum internal diameters are 1 to 2 cm (½ to 1 in). A purge rate of at least 0.9 m/s (3 ft/s) is usually required. Pressure measurements taken at various heights in the bed are used to determine bed level.

Bed density is determined directly from $\Delta P/L$, the pressure drop inside the bed itself ($\Delta P/L$ in units of weight/area $\times L$). The overall bed weight is obtained from ΔP taken between the grid and the freeboard. Nominal bed height is the length required to have the overall weight at the measured density. Of course, splashing and entrainment will place solids well above the nominal bed height in most cases.

The pressure-drop signal is noisy due to bubble effects and the generally statistical nature of fluid bed flow parameters. A fast fourier transform of the pressure drop signal transforms the perturbations to a frequency-versus-amplitude plot with a maximum at about 5 Hz and frequencies generally tailing off above 20 Hz. Changes in frequency and amplitude are associated with changes in the quality of the fluidization. Experienced operators can frequently predict performance from changes in the ΔP signal.

Flow Measurement Measurement of flow rates of clean gases presents no problem. Flow measurement of dirty gases is usually

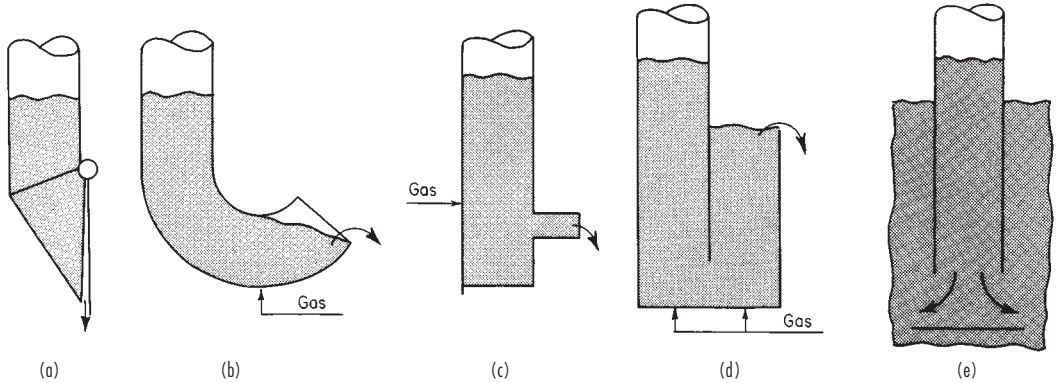

FIG. 17-22 Cyclone solids-return seals. (*a*) Trickle valve. (*Ducon Co., Inc.*) (*b*) J valve. (*c*) L valve. (*d*) Fluid-seal pot. (*e*) "Dollar" plate. *a*, *b*, *c*, and *d* may be used above the bed; *a* and *e* are used below the bed.

avoided. The flow of solids is usually controlled but not measured except externally to the system. Solids flows in the system are usually adjusted on an inferential basis (temperature, pressure level, catalyst activity, gas analysis, etc.). In many roasting operations the color of the calcine indicates solids feed rate.

USES OF FLUIDIZED BEDS

There are many uses of fluidized beds. A number of applications have become commercial successes; others are in the pilot-plant stage, and others in bench-scale stage. Generally, the fluidized bed is used for gas-solids contacting; however, in some instances the presence of the gas or solid is used only to provide a fluidized bed to accomplish the end result. Uses or special characteristics follow:

I. Chemical reactions
   - *A.* Catalytic
   - *B.* Noncatalytic
     1. Homogeneous
     2. Heterogeneous

II. Physical contacting
   - *A.* Heat transfer
     1. To and from fluidized bed
     2. Between gases and solids
     3. Temperature control
     4. Between points in bed
   - *B.* Solids mixing
   - *C.* Gas mixing
   - *D.* Drying
     1. Solids
     2. Gases
   - *E.* Size enlargement
   - *F.* Size reduction
   - *G.* Classification
     1. Removal of fines from solids
     2. Removal of fines from gas
   - *H.* Adsorption-desorption
   - *I.* Heat treatment
   - *J.* Coating

Chemical Reactions

Catalytic Reactions This use has provided the greatest impetus for use, development, and research in the field of fluidized solids. Some of the details pertaining to this use are to be found in the preceding pages of this section. Reference should also be made to Sec. 23.

Cracking. The evolution of fluidized catalytic cracking (FCC) since the early 1940s has resulted in several configurations depending upon the particular use and designer.

The high rate of transfer of solids between the regenerator and the reactor permits a balancing of the exothermic burning of carbon and tars in the regenerator and the endothermic cracking of petroleum in the reactor, so that temperature in both units can usually be controlled without resorting to auxiliary heat-control mechanisms. The high rate of catalyst circulation also permits the maintenance of the catalyst at a constantly high activity. The original regenerators were considered to be backmixed units. Newer systems have staged regenerators to improve conversion (see Fig. 17-23). The use of the riser reactor (transport or fast fluid bed) results in much lower gas and solids back mixing and an approach to plug flow.

The first fluid catalytic-cracking unit was placed in operation in Baytown, Texas, in 1942. This was a low-pressure, 115- to 120-kPa (2- to 3-psig) unit operating in what is now called the turbulent fluidization mode, 1.2 to 1.8 m/s (4 to 6 ft/s). Even before the startup of the first model I, it was realized that by lowering the velocity, a dense, aggregative fluidized bed, 300 to 400 kg/m^3 (20 to 25 lb/ft^3), would be formed, allowing completion of reaction and regeneration. Pressure was increased to 240 to 320 kPa (20 to 30 psig). In the 1960s more active catalysts resulted in the use of riser cracking. Recently, heavier crude feedstocks have produced higher coke yields. This has necessitated addition of catalyst cooling to the regeneration step as shown in Fig. 17-24. Many companies participated in the development of the

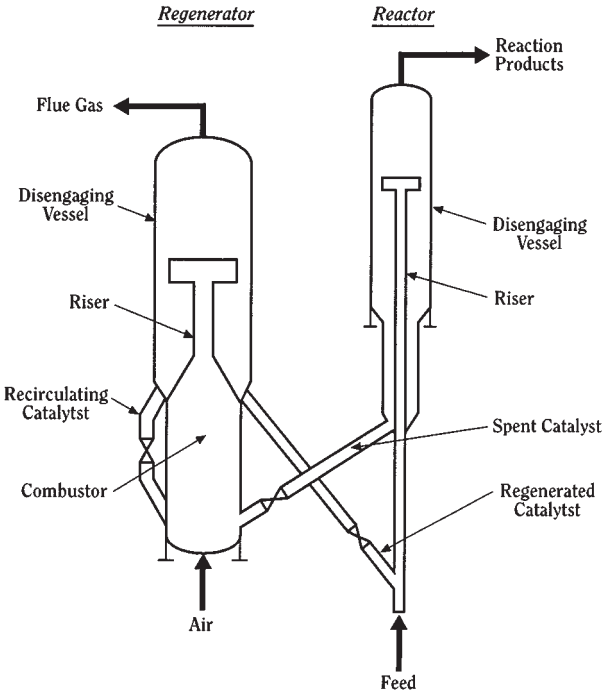

FIG. 17-23 UOP fluid cracking unit. (*Reprinted with permission of UOP.*)

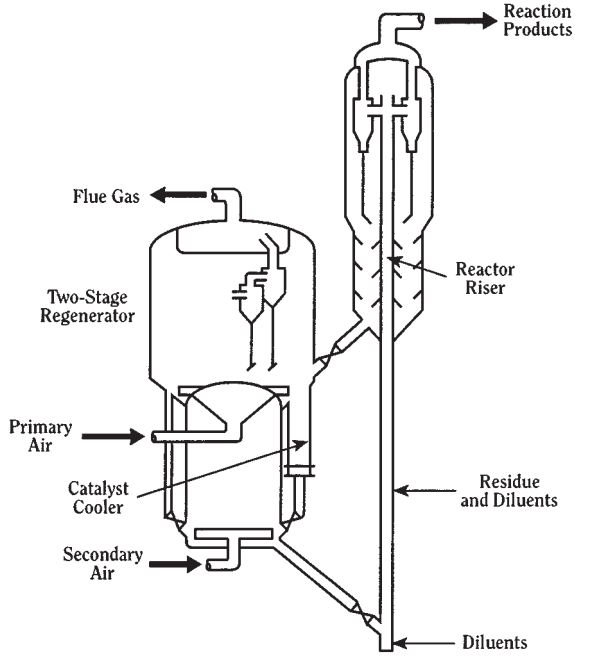

FIG. 17-24 Modern FCC unit configured for high-efficiency regeneration and extra catalyst cooling. (*Reprinted with permission of UOP. RCC is a service mark of Ashland Oil Inc.*)

cat cracker, including Exxon Research & Engineering Co., Universal Oil Products Companies, Kellogg Co., Texaco Development Corp., Gulf Research Development Co., and Shell Oil Company. Many of the companies provide designs and/or licenses to operate to others. For further details, see Luckenbach, Reichle, Gladrow, and Worley, "Cracking, Catalytic," in McKetta (ed.), *Encyclopedia of Chemical Processing and Design,* vol. 13, Marcel Dekker, New York, 1981, pp. 1–132.

Alkyl chlorides. Olefins are chlorinated to alkyl chlorides in a single fluidized bed. HCl reacts with O_2 over a copper chloride catalyst to form chlorine. The chlorine reacts with the olefin to form the alkyl chloride. The process developed by the Shell Development Co. uses a recycle of catalyst fines in aqueous HCl to control the temperature [*Chem. Proc.,* **16,** 42 (1953)].

Phthalic anhydride. Naphthalene is oxidized by air to phthalic anhydride in a bubbling fluidized reactor. Even though the naphthalene feed is in liquid form, the reaction is highly exothermic. Temperature control is achieved by removing heat through vertical tubes in the bed to raise steam [Graham and Way, *Chem. Eng. Prog.,* **58,** 96 (January 1962)].

Acrylonitrile. Acrylonitrile is produced by reacting propylene, ammonia, and oxygen (air) in a single fluidized bed of a complex catalyst. Known as the SOHIO process, this process was first operated commercially in 1960. In addition to acrylonitrile, significant quantities of HCN and acetonitrile are also produced. This process is also exothermic. Temperature control is achieved by raising steam inside vertical tubes immersed in the bed [Veatch, *Hydrocarbon Process. Pet. Refiner,* **41,** 18 (November 1962)].

Fischer-Tropsch synthesis. The scale-up of a bubbling-bed reactor to produce gasoline from CO and H_2 was unsuccessful (see "Design of Fluidized-Bed Systems: Scale-Up"). However, Kellogg Co. developed a successful Fischer-Tropsch synthesis reactor based on a dilute-phase or transport-reactor concept. Kellogg, in its design, prevented gas bypassing by using the transport reactor and maintained temperature control of the exothermic reaction by inserting heat exchangers in the transport line. This process has been very successful and repeatedly expanded at the South African Synthetic Oil Limited (SASOL) plant in the Republic of South Africa, where politics and economics favor the conversion of coal to gasoline and other hydrocarbons. Refer to Jewell and Johnson, U.S. Patent 2,543,974, Mar. 6, 1951. Recently, the process has been modified to a simpler, less expensive turbulent bed catalytic reactor system [Silverman et al., *Fluidization V,* Engineering Foundation 1986, pp. 441–448).

The first commercial fluidized bed polyethylene plant was constructed by Union Carbide in 1968. Modern units operate at 100°C and 32 MPa (300 psig). The bed is fluidized with ethylene at about 0.5 m/s and probably operates near the turbulent fluidization regime. The excellent mixing provided by the fluidized bed is necessary to prevent hot spots, since the unit is operated near the melting point of the product. A model of the reactor (Fig. 17-25) that couples kinetics to the hydrodynamics was given by Choi and Ray, *Chem. Eng. Sci.,* **40,** 2261, 1985.

Additional catalytic processes. Nitrobenzene is hydrogenated to aniline (U.S. Patent 2,891,094). Melamine and isophthalonitrile are produced in catalytic fluidized-bed reactors. Badger has announced a process to produce maleic anhydride by the partial oxidation of butane (Schaffel, Chen, and Graham, "Fluidized Bed Catalytic Oxidation of Butane to Maleic Anhydride," presented at Chemical Engineering World Congress, Montreal, 1981). Dupont has announced a circulating bed process for production of maleic anhydride (Contractor, *Circulating Fluidized Bed Tech. II,* Pergamon, 1988, pp. 467–474). Mobil Oil has developed a commercial process to convert methanol to gasoline. (Grimmer et al., *Methane Conversion,* Elsevier, 1988, pp. 273–291).

Noncatalytic Reactions

Homogeneous reactions. Homogeneous noncatalytic reactions are normally carried out in a fluidized bed to achieve mixing of the gases and temperature control. The solids of the bed act as a heat sink or source and facilitate heat transfer from or to the gas or from or to heat-exchange surfaces. Reactions of this type include chlorination of hydrocarbons or oxidation of gaseous fuels.

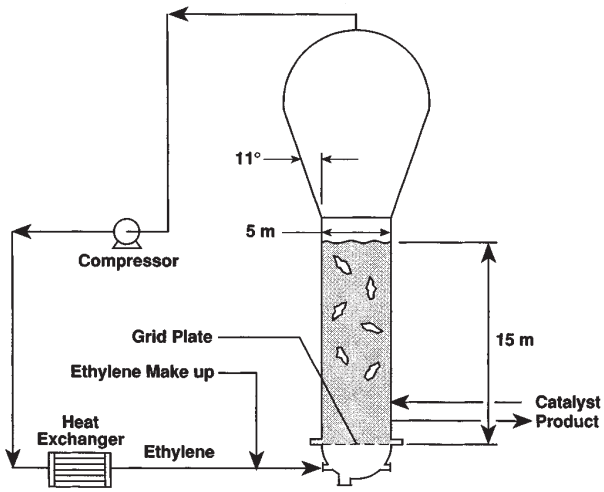

FIG. 17-25 High-pressure polyethylene reactor.

Heterogeneous reactions. This category covers the greatest commercial use of fluidized beds other than petroleum cracking. The roasting of sulfide, arsenical, and/or antimonial ores to facilitate the release of gold or silver values; the roasting of pyrite, pyrrhotite, or naturally occurring sulfur ores to provide SO_2 for sulfuric acid manufacture; and the roasting of copper, cobalt, and zinc sulfide ores to solubilize the metal values are the major metallurgical uses. Figure 17-26 shows basic items in the system.

Thermally efficient **calcination** of lime dolomite and clay can be carried out in a multicompartment fluidized bed (Fig. 17-27). Fuels are burned in a fluidized bed of the product to produce the required heat. Bunker C oil, natural gas, and coal are used in commercial units. Temperature control is accurate enough to permit production of lime of very high availability with close control of slaking characteristics. Also, half calcination of dolomite is an accepted practice. The requirement of large crystal size for the limestone limits application. Small-sized crystals in the limestone result in low yields due to high dust losses.

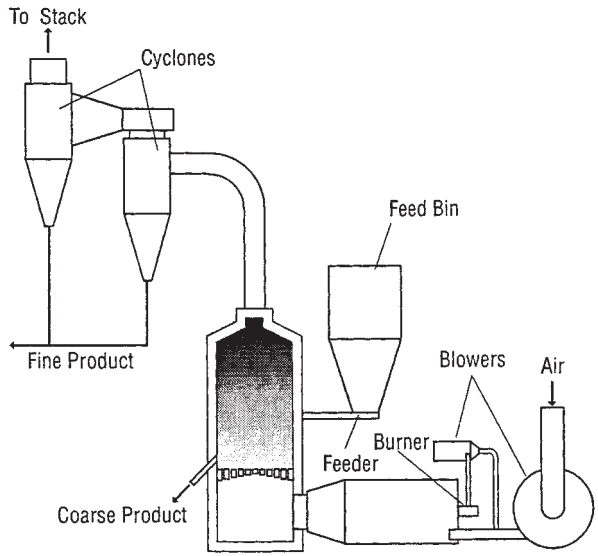

FIG. 17-26 Single-stage FluoSolids roaster or dryer. (*Dorr-Oliver, Inc.*)

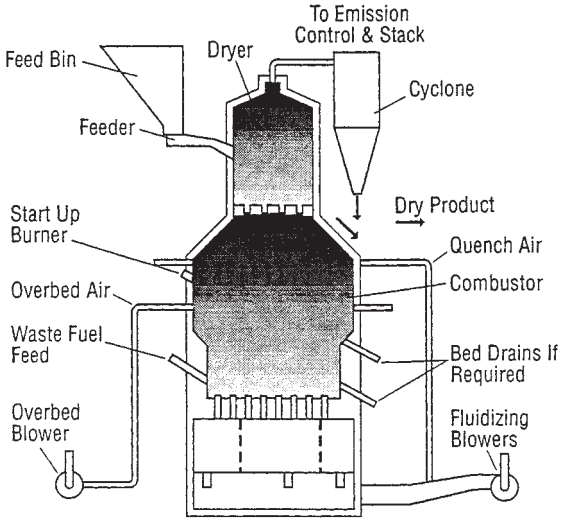

FIG. 17-27 FluoSolids multicompartment fluidized bed. (*Dorr-Oliver, Inc.*)

Phosphate rock is calcined to remove carbonaceous material before being digested with sulfuric acid. Several different fluidization processes have been commercialized for the direct reduction of hematite to high-iron, low-oxide products. Foundry sand is also calcined to remove organic binders and release fines.

The calcination of $Al(OH)_3$ to Al_2O_3 in a circulating fluidized process produces a high-grade product. The process combines the use of circulating, bubbling, and transport beds to achieve high thermal efficiency. See Fig. 17-28.

An interesting feature of these high-temperature-calcination applications is the direct injection of either heavy oil, natural gas, or fine coal into the fluidized bed. Combustion takes place at well below flame temperatures without atomization. Considerable care in the design of the fuel- and air-supply system is necessary to take full advantage of the fluidized bed, which serves to mix the air and fuel.

Coal can be burned in fluidized beds in an environmentally acceptable manner by adding limestone or dolomite to the bed to react with the SO_2 to form $CaSO_4$. Because of moderate combustion temperature, about 800 to 900°C, NO_x, which results from the oxidation of nitrogen compounds contained in the coal, is kept at a low level. NO_x is increased by higher temperatures and higher excess oxygen. Two-stage air addition reduces NO_x.

Several concepts of fluidized-bed combustion have been or are being developed. Atmospheric fluidized-bed combustion (AFBC), in which most of the heat-exchange tubes are located in the bed, is illustrated in Fig. 17-29. This type of unit is most commonly used for industrial applications up to about 50 metric tons/h of steam generation. Larger units are generally of the circulating bed type as shown in Fig. 17-30. **Circulating fluidized bed combustors** have many advantages. The velocity is significantly higher for greater throughput. Since all the solids are recycled, fine limestone and coal can be fed, which gives better limestone utilization and greater laitude in specifying coal sizing. Because of erosion due to high velocity coarse solids, heat-transfer surface is usually not designed into the bottom of the combustion zone. Figure 17-30 shows a commercial 110 MWe unit. Pressurized fluidized-bed combustion (PFBC) is, as the name implies, operated at above atmospheric pressures. The beds and heat-transfer surface are stacked to conserve space and to reduce the size of the pressure vessel. This type of unit is usually conceived as a cogeneration unit. Steam raised in the boilers would be employed to drive turbines or for other uses, and the hot pressurized gases after cleaning would be let down through an expander coupled to a compressor to supply the compressed combustion air and/or electric generator. A 71 MWe unit is shown in Fig. 17-31. Also see Sec. 27, "Energy Sources: Conversion and Utilization."

Incineration The majority of over 400 units in operation are used for the incineration of biological sludges. These units can be designed to operate autogenously with wet sludges containing as little as 6 MJ/kg (2600 Btu/lb) heating value (Fig. 17-32). Depending on the calorific value of the feed, heat can be recovered as steam either by means of waste-heat boilers or by a combination of waste-heat boilers and the heat-exchange surface in the fluid bed.

Several units are used for sulfite-paper-mill waste-liquor disposal. At least six units are used for oil-refinery wastes, which sometimes include a mixture of liquid sludges, emulsions, and caustic waste

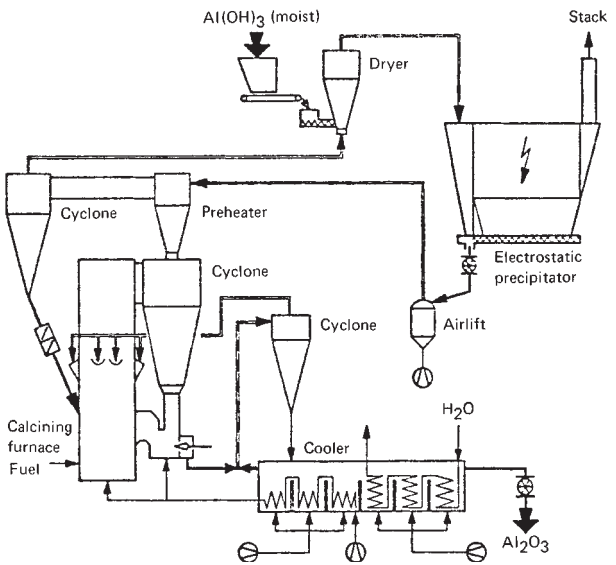

FIG. 17-28 Circulating-fluid-bed calciner. (*Lurgi Corp.*)

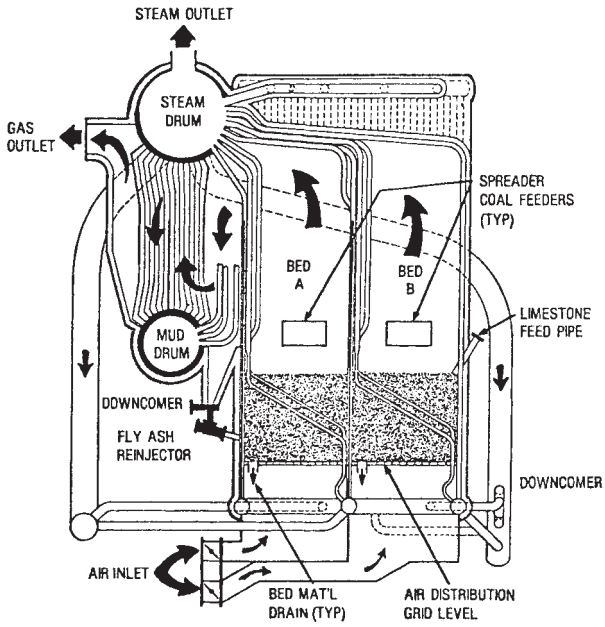

FIG. 17-29 Fluidized-bed steam generator at Georgetown University; 12.6-kg/s (100,000-lb/h) steam at 4.75-MPa (675-psig) pressure. (*From Georgetown Univ. Q. Tech. Prog. Rep. METC/DOE/10381/135, July–September 1980.*)

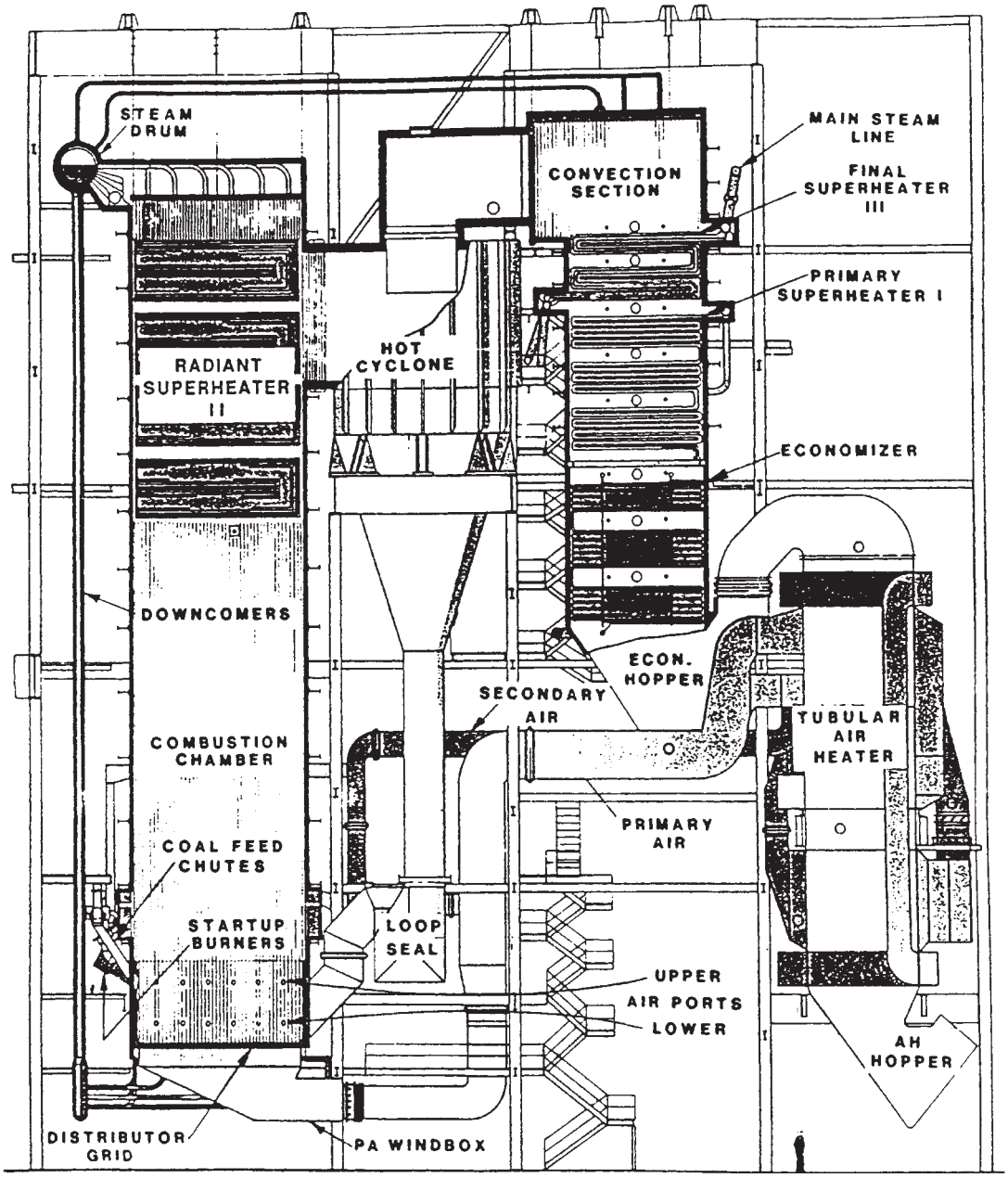

FIG. 17-30 Side view of 110 MWe Nucla CFB boiler. (*Source: Pyropower Corporation.*)

[Flood and Kernel, *Chem. Proc.* (Sept. 8, 1973)]. Miscellaneous uses include the incineration of sawdust, carbon-black waste, pharmaceutical waste, grease from domestic sewage, spent coffee grounds, and domestic garbage.

Toxic or hazardous wastes can be disposed of in fluidized beds by either chemical capture or complete destruction. In the former case, bed material, such as limestone, will react with halides, sulfides, metals, etc., to form stable compounds which can be landfilled. Contact times of up to 5 or 10 s at 1200 K (900°C) to 1300 K (1000°C) assure complete destruction of most compounds.

Physical Contacting

Drying Fluidized-bed units for drying solids, particularly coal, cement, rock, and limestone, are in general acceptance. Economic considerations make these units particularly attractive when large tonnages of solids are to be handled. Fuel requirements are 3.3 to 4.2 MJ/kg (1500 to 1900 Btu/lb of water removed), and total power for blowers, feeders, etc., is about 0.08 kWh/kg of water removed. The maximum-sized feed is 6 cm (1½ in) × 0 coal. One of the major advantages of this type of dryer is the close control of conditions so that a predetermined amount of free moisture may be left with the solids to

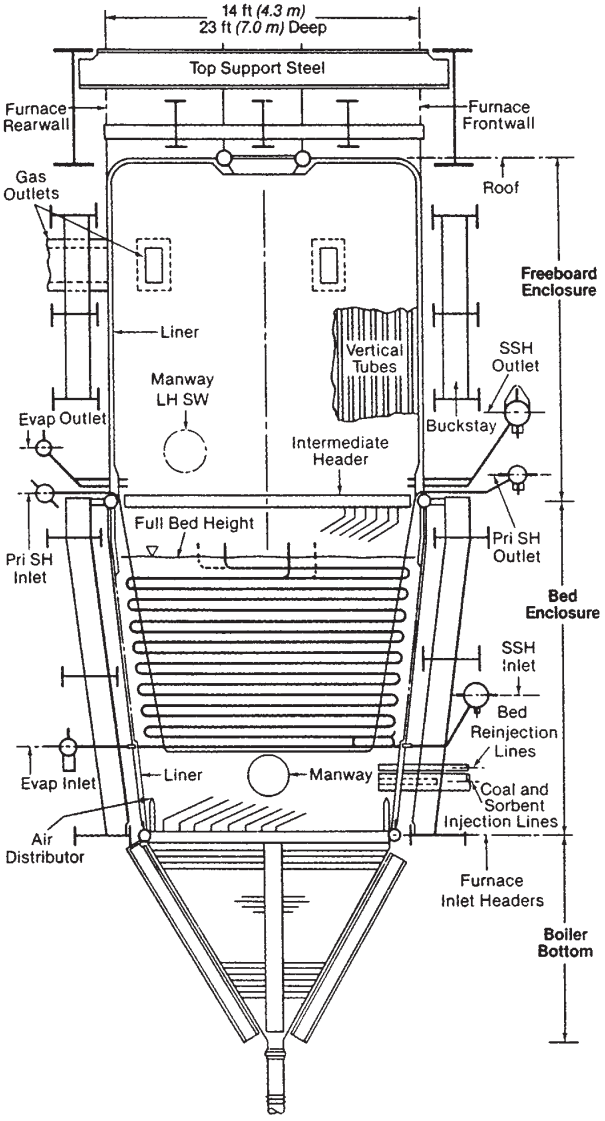

FIG. 17-31 71 MWe PFBC unit. (*From* Steam, *40th ed., 29-9, Babcock & Wilcox, 1992*).

prevent dusting of the product during subsequent material-handling operations. The fluidized-bed dryer is also used as a classifier so that both drying and classification operations are accomplished simultaneously.

Wall and Ash [*Ind. Eng. Chem.*, **41,** 1247 (1949)] state that, in drying 4.8-mm (–4 mesh) dolomite with combustion gases at a superficial velocity of 1.2 m/s (4 ft/s), the following removals of fines were achieved:

Particle size	% removed
–65 + 100 mesh	60
–100 + 150 mesh	79
–150 + 200 mesh	85
–200 + 325 mesh	89
–325 mesh	89

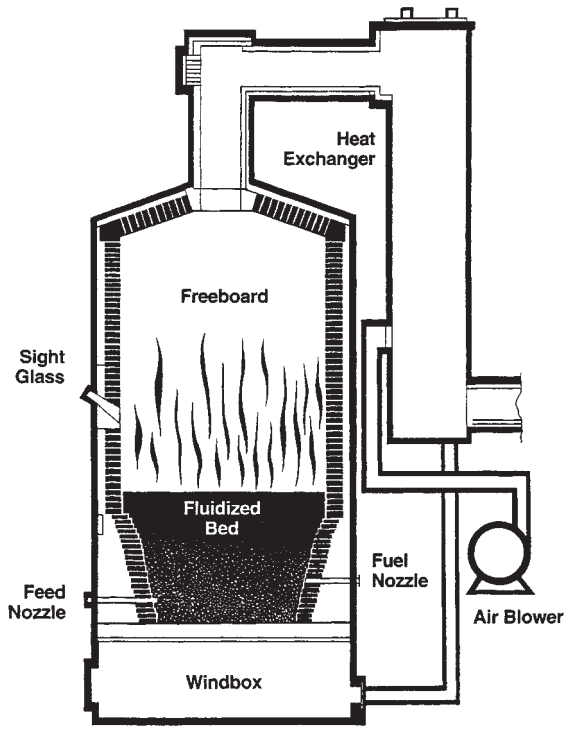

FIG. 17-32 Hot windbox incinerator/reactor with air preheating. (*Dorr-Oliver, Inc.*)

Classification The separation of fine particles from coarse can be effected by use of a fluidized bed (see "Drying"). However, for economic reasons (i.e., initial cost, power requirements for compression of fluidizing gas, etc.), it is doubtful except in special cases if a fluidized-bed classifier would be built for this purpose alone.

It has been proposed that fluidized beds be used to remove fine solids from a gas stream. This is possible under special conditions.

Adsorption-Desorption An arrangement for gas fractionation is shown in Fig. 17-33.

The effects of adsorption and desorption on the performance of fluidized beds are discussed elsewhere. Adsorption of carbon disulfide

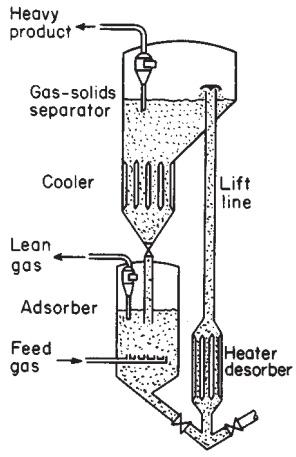

FIG. 17-33 Fluidized bed for gas fractionation. [*Sittig,* Chem. Eng. (*May 1953*).]

vapors from air streams as great as 300 m^3/s (540,000 ft^3/min) in a 17-m- (53-ft-) diameter unit has been reported by Avery and Tracey ("The Application of Fluidized Beds of Activated Carbon to Recover Solvent from Air or Gas Streams," Tripartate Chemical Engineering Conference, Montreal, Sept. 24, 1968).

Heat Treatment Heat treatment can be divided into two types, treatment of fluidizable solids and treatment of large, usually metallic objects in a fluid bed. The former is generally accomplished in multicompartment units to conserve heat (Fig. 17-27). The heat treatment of large metallic objects is accomplished in long, narrow heated beds. The objects are conveyed through the beds by an overhead conveyor system. Fluid beds are used because of the high heat-transfer rate and uniform temperature. See Reindl, "Fluid Bed Technology," *American Society for Metals*, Cincinnati, Sept. 23, 1981; Fennell, *Ind. Heat.*, **48,** 9, 36 (September 1981).

Coating Fluidized beds of thermoplastic resins have been used to facilitate the coating of metallic parts. A properly prepared, heated metal part is dipped into the fluidized bed, which permits complete immersion in the dry solids. The heated metal fuses the thermoplastic, forming a continuous uniform coating.

GAS-SOLIDS SEPARATIONS

This subsection is concerned with the application of particle mechanics (see Sec. 5, "Fluid and Particle Mechanics") to the design and application of dust-collection systems. It includes wet collectors, or scrubbers, for particle collection. Scrubbers designed for purposes of mass transfer are discussed in Secs. 14 and 18. Equipment for removing entrained liquid mist from gases is described in Sec. 18.

Nomenclature

Except where otherwise noted here or in the text, either consistent system of units (SI or U.S. customary) may be used. Only SI units may be used for electrical quantities, since no comparable electrical units exist in the U.S. customary system. When special units are used, they are noted at the point of use.

Symbols	Definition	SI units	U.S. customary units	Special units
B_c	Width of rectangular cyclone inlet duct	m	ft	
B_e	Spacing between wire and plate, or between rod and curtain, or between parallel plates in electrical precipitators	m	ft	
B_s	Width of gravity settling chamber	m	ft	
C°	Dry scrubber pollutant gas equilibrium concentration over sorbent			
C_1	Dry scrubber pollutant gasinlet concentration			
C_2	Dry scrubber pollutant gasoutlet concentration			
c_d	Dust concentration in gas stream	g/m^3		grains/ft^3
c_h	Specific heat of gas	J/(k·K)	Btu/(lbm·°F)	
c_{hb}	Specific heat of collecting body	J/(kg·K)	Btu/(lbm·°F)	
c_{hp}	Specific heat of particle	J/(kg·K)	Btu/(lbm·°F)	
D_b	Diameter or other representative dimension of collector body or device	m	ft	
D_{b1},D_{b2}	Other characteristic dimensions of collector body or device	m	ft	
D_c	Cyclone diameter	m	ft	
D_d	Outside diameter of wire or discharge electrode of concentric-cylinder type of electrical precipitator	m	ft	
D_e	Diameter of cyclone gas exit duct	m	ft	
D_o	Volume/surface-mean-drop diameter			µm
D_p	Diameter of particle	m	ft	µm
D_{pth}	Cut diameter, diameter of particles of which 50% of those present are collected	m	ft	µm
d_P	Particle diameter of fraction number c'	m	ft	
D_t	Inside diameter of collecting tube of concentric-cylinder type of electrical precipitator	m	ft	
D_v	Diffusion coefficient for particle	m^2/s	ft^2/s	
DI	Decontamination index = $\log_{10}[1/(1-\eta)]$	Dimensionless	Dimensionless	
e	Natural (napierian) logarithmic base	2.718 . . .	2.718 . . .	
E	Potential difference	V		
E_c	Potential difference required for corona discharge to commence	V		
E_d	Voltage across dust layer	V		
E_s	Potential difference required for sparking to commence	V		
E_L	Cyclone collection efficiency at actual loading			
E_O	Cyclone collection efficiency at low loading			
F_E	Effective friction loss across wetted equipment in scrubber	kPa		in water
F_k	Packed bed friction loss			
g_c	Conversion factor		32.17 (lbm/lbf)(ft/s^2)	
g_L	Local acceleration due to gravity	m/s^2	ft/s^2	
H_c	Height of rectangular cyclone inlet duct	m	ft	
H_s	Height of gravity settling chamber	m	ft	
I	Electrical current per unit of electrode length	A/m		

Nomenclature (*Continued*)

Symbols	Definition	SI units	U.S. customary units	Special units
j	Corona current density at dust layer	A/m^2		
k_ρ	Density of gas relative to its density at 0°C, 1 atm	Dimensionless	Dimensionless	Dimensionless
k_t	Thermal conductivity of gas	W/(m·K)	Btu/(s·ft·°F)	
k_{tb}	Thermal conductivity of collecting body	W/(m·K)	Btu/(s·ft·°F)	
k_{tp}	Thermal conductivity of particle	W/(m·K)	Btu/(s·ft·°F)	
K	Empirical proportionality constant for cyclone pressure drop or friction loss	Dimensionless	Dimensionless	
K_1	Resistance coefficient of "conditioned" filter fabric	kPa/(m/min)	in water/(ft/min)	
K_2	Resistance coefficient of dust cake on filter fabric	$\frac{\text{kPa}}{(\text{m/min})(\text{g/m}^2)}$	$\frac{\text{in water}}{(\text{ft/min})(\text{lbm/ft}^2)}$	
K_a	Proportionality constant, for target efficiency of a single fiber in a bed of fibers	Dimensionless	Dimensionless	
K_c	Resistance coefficient for "conditioned" filter fabric			$\frac{\text{in water}}{(\text{ft/min})(\text{cP})}$
K_d	Resistance coefficient for dust cake on filter fabric		$\frac{\text{in water}}{(\text{ft/min})(\text{gr/ft}^2)(\text{cP})}$	
K_e	Electrical-precipitator constant	s/m	s/ft	
K_F	Resistance coefficient for clean filter cloth			$\frac{\text{in water}}{(\text{ft/min})(\text{cP})}$
K_o	"Energy-distance" constant for electrical discharge in gases	m		
K_m	Stokes-Cunningham correction factor	Dimensionless	Dimensionless	Dimensionless
L	Thickness of fibrous filter or of dust layer on surface filter	m	ft	
L_e	Length of collecting electrode in direction of gas flow	m	ft	
L_s	Length of gravity settling chamber in direction of gas flow	m	ft	
ln	Natural logarithm (logarithm to the base e)	Dimensionless	Dimensionless	Dimensionless
M	Molecular weight	kg/mol	lbm/mol	
n	Exponent	Dimensionless	Dimensionless	Dimensionless
N_{Kn}	Knudsen number = λ_m/D_b	Dimensionless	Dimensionless	
N_{Ma}	Mach number	Dimensionless	Dimensionless	
N_o	Number of elementary electrical charges acquired by a particle	Dimensionless	Dimensionless	
N_{Re}	Reynolds number = $(D_p\rho V_o/\mu)$ or $(D_p\rho u_t/\mu)$	Dimensionless	Dimensionless	
N_{sc}	Interaction number = $18\,\mu/K_m\rho_p D_c$	Dimensionless	Dimensionless	
N_{sd}	Diffusional separation number	Dimensionless	Dimensionless	
N_{sec}	Electrostatic-attraction separation number	Dimensionless	Dimensionless	
N_{sei}	Electrostatic-induction separation number	Dimensionless	Dimensionless	
N_{sf}	Flow-line separation number	Dimensionless	Dimensionless	
N_{sg}	Gravitational separation number	Dimensionless	Dimensionless	
N_{si}	Inertial separation number	Dimensionless	Dimensionless	
N_{st}	Thermal separation number	Dimensionless	Dimensionless	
N_t	Number of transfer units = $\ln[1/(1-\eta)]$	Dimensionless	Dimensionless	
N_s	Number of turns made by gas stream in a cyclone separator	Dimensionless	Dimensionless	
Δp	Gas pressure drop	kPa	lbf/ft^2	in water
Δp_i	Gas pressure drop in cyclone or filter			in water
p_F	Gauge pressure of water fed to scrubber	kPa		lbf/in^2
P_G	Gas-phase contacting power	MJ/1000 m^3		hp/(1000 ft^3/min)
P_L	Liquid-phase contacting power	MJ/1000 m^3		hp/(1000 ft^3/min)
P_M	Mechanical contacting power	MJ/1000 m^3		hp/(1000 ft^3/min)
P_T	Total contacting power	MJ/1000 m^3		hp/(1000 ft^3/min)
q	Gas flow rate	m^3/s	ft^3/s	
Q_G	Gas flow rate		ft^3/s	ft^3/min
Q_L	Liquid flow rate		ft^3/s	gal/min
Q_p	Electrical charge on particle	C		
r	Radius; distance from centerline of cyclone separator; distance from centerline of concentric-cylinder electrical precipitator	m	ft	
t_m	Time			min
T	Absolute gas temperature	K	°R	
T_b	Absolute temperature of collecting body	K	°R	

Nomenclature (*Concluded*)

Symbols	Definition	SI units	U.S. customary units	Special units
u_s	Velocity of migration of particle toward collecting electrode	m/s	ft/s	
u_t	Terminal settling velocity of particle under action of gravity	m/s	ft/s	ft/s
v_m	Average cyclone inlet velocity, based on area A_c	m/s	ft/s	ft/s
v_p	Actual particle velocity	m/s	ft/s	
V_f	Filtration velocity (superficial gas velocity through filter)	m/min		ft/min
V_o	Gas velocity	m/s	ft/s	
V_s	Average gas velocity in gravity settling	m/s	ft/s	
V_{ct}	Tangential component of gas velocity in cyclone	m/s	ft/s	
w	Loading of collected dust on filter	g/m^2	lbm/ft^2	gr/ft^2
	Greek symbols			
α	Empirical constant in equation of scrubber performance curve	$\left[\frac{\text{MJ}}{1000\ \text{m}^3}\right]^{-\gamma}$		$\left[\frac{\text{hp}}{100\ \text{ft}^3/\text{min}}\right]^{-\gamma}$
γ	Empirical constant in equation of scrubber performance curve	Dimensionless		Dimensionless
δ	Dielectric constant	Dimensionless		
δ_g	Dielectric constant at 0°C, 1 atm	Dimensionless		
δ_o	Permittivity of free space	F/m		
δ_b	Dielectric constant of collecting body	Dimensionless		
δ_p	Dielectric constant of particle	Dimensionless		
Δ	Fractional free area (for screens, perforated plates, grids)	Dimensionless	Dimensionless	
ε	Elementary electrical charge	1.60210×10^{-19} C		
ε_b	Characteristics potential gradient at collecting surface	V/m		
ε_v	Fraction voids in bed of solids	Dimensionless	Dimensionless	Dimensionless
ζ	$= 1 + 2\frac{(\delta - 1)}{(\delta + 2)}$ ranges from a value of 1 for materials with a dielectric constant of 1 to 3 for conductors	Dimensionless		
η	Collection efficiency, weight fraction of entering dispersoid collected	Dimensionless	Dimensionless	Dimensionless
η_o	Target efficiency of an isolated collecting body, fraction of dispersoid in swept volume collected on body	Dimensionless	Dimensionless	Dimensionless
η_t	Target efficiency of a single collecting body in an array of collecting bodies, fraction of dispersoid in swept volume collected on body	Dimensionless	Dimensionless	Dimensionless
λ_i	Ionic mobility of gas	(m/s)/(V/m)		
λ_p	Particle mobility = $u_e/\mathscr{E}$	(m/s)/(V/m)		
μ	Gas viscosity	Pa·s	lbm/(s·ft)	cP
μ_L	Liquid viscosity			cP
ρ	Gas density	g/m^3	lb/ft^3	
ρ_d	Resistivity of dust layer	Ω·m		
ρ_L	Liquid density		lbm/ft^3	lbm/ft^3
ρ_s	True (*not* bulk) density of solids or liquid drops	kg/m^3	lbm/ft^3	lbm/ft^3
ρ'	Density of gas relative to its density at 25°C, 1 atm	Dimensionless	Dimensionless	Dimensionless
σ	Ion density	Number/m^3		
σ_{avg}	Average ion density	Number/m^3		
σ_L	Liquid surface tension			dyn/cm
ϕ_s	Particle shape factor = (surface of sphere)/(surface of particle of same volume)	Dimensionless	Dimensionless	Dimensionless
	Script symbols			
$\mathscr{E}$	Potential gradient	V/m		
$\mathscr{E}_c$	Potential gradient required for corona discharge to commence	V/m		
$\mathscr{E}_i$	Average potential gradient in ionization stage	V/m		
$\mathscr{E}_o$	Electrical breakdown constant for gas	V/m		
$\mathscr{E}_p$	Average potential gradient in collection stage	V/m		
$\mathscr{E}_s$	Potential gradient required for sparking to commence	V/m		

General References: Burchsted, Kahn, and Fuller, *Nuclear Air Cleaning Handbook,* ERDA 76-21, Oak Ridge, Tenn., 1976. Cadle, *The Measurement of Airborne Particles,* Wiley, New York, 1975. Davies, *Aerosol Science,* Academic, New York, 1966. Davies, *Air Filtration,* Academic, New York, 1973. Dennis, *Handbook on Aerosols,* ERDA TID-26608, Oak Ridge, Tenn., 1976. Drinker and Hatch, *Industrial Dust,* 2d ed., McGraw-Hill, New York, 1954. Friedlander, *Smoke, Dust, and Haze,* Wiley, New York, 1977. Fuchs, *The Mechanics of Aerosols,* Pergamon, Oxford, 1964. Green and Lane, *Particulate Clouds: Dusts, Smokes, and Mists,* Van Nostrand, New York, 1964. Lapple, *Fluid and Particle Mechanics,* University of Delaware, Newark, 1951. Licht, *Air Pollution Control Engineering—Basic Calculations for Particle Collection,* Marcel Dekker, New York, 1980. Liu, *Fine Particles—Aerosol Generation, Measurement, Sampling, and Analysis,* Academic, New York, 1976. Lunde and Lapple, *Chem. Eng. Prog.,* **53,** 385 (1957). Lundgren et al., *Aerosol Measurement,* University of Florida, Gainesville, 1979. Mercer, *Aerosol Technology in Hazard Evaluation,* Academic, New York, 1973. Nonhebel, *Processes for Air Pollution Control,* CRC Press, Cleveland, 1972. Shaw, *Fundamentals of Aerosol Science,* Wiley, New York, 1978. Stern, *Air Pollution: A Comprehensive Treatise,* vols. 3 and 4, Academic, New York, 1977. Strauss, *Industrial Gas Cleaning,* 2d ed., Pergamon, New York, 1975. Theodore and Buonicore, *Air Pollution Control Equipment: Selection, Design, Operation, and Maintenance,* Prentice-Hall, Englewood Cliffs, N.J., 1982. White, *Industrial Electrostatic Precipitation,* Addison-Wesley, Reading, Mass., 1963. White and Smith, *High-Efficiency Air Filtration,* Butterworth, Washington, 1964. ASME Research Committee on Industrial and Municipal Wastes, *Combustion Fundamentals for Waste Incineration,* American Society of Mechanical Engineers, 1974. Buonicore and Davis (eds.), *Air Pollution Engineering Manual,* Air & Waste Management Association, Van Nostrand Reinhold, 1992. Burchsted, Fuller, and Kahn, *Nuclear Air Cleaning Handbook,* ORNL for the U.S. Energy Research and Development Administration, NTIS Report ERDA 76-21, 1976. Dennis (ed.), *Handbook on Aerosols,* GCA for the U.S. Energy Research and Development Administration, NTIS Report TID-26608, 1976. Stern, *Air Pollution,* 3d ed., Academic Press, 1977 (supplement 1986).

PURPOSE OF DUST COLLECTION

Dust collection is concerned with the removal or collection of solid dispersoids in gases for purposes of:

1. Air-pollution control, as in fly-ash removal from power-plant flue gases
2. Equipment-maintenance reduction, as in filtration of engine-intake air or pyrites furnace-gas treatment prior to its entry to a contact sulfuric acid plant
3. Safety- or health-hazard elimination, as in collection of siliceous and metallic dusts around grinding and drilling equipment and in some metallurgical operations and flour dusts from milling or bagging operations
4. Product-quality improvement, as in air cleaning in the production of pharmaceutical products and photographic film
5. Recovery of a valuable product, as in collection of dusts from dryers and smelters
6. Powdered-product collection, as in pneumatic conveying; the spray drying of milk, eggs, and soap; and the manufacture of high-purity zinc oxide and carbon black

PROPERTIES OF PARTICLE DISPERSOIDS

An understanding of the fundamental properties and characteristics of gas dispersoids is essential to the design of industrial dust-control equipment. Figure 17-34 shows characteristics of dispersoids and other particles together with the types of gas-cleaning equipment that are applicable to their control. Two types of solid dispersoids are shown: (1) dust, which is composed of particles larger than 1 μm; and (2) fume, which consists of particles generally smaller than 1 μm. Dusts usually result from mechanical disintegration of matter. They may be redispersed from the settled, or bulk, condition by an air blast. Fumes are submicrometer dispersoids formed by processes such as combustion, sublimation, and condensation. Once collected, they cannot be redispersed from the settled condition to their original state of dispersion by air blasts or mechanical dispersion equipment.

The primary distinguishing characteristic of gas dispersoids is particle size. The generally accepted unit of particle size is the micrometer, μm. (Prior to the adoption of the SI system, the same unit was known as the micron and was designated by μ.) The particle size of a gas dispersoid is usually taken as the diameter of a sphere having the same mass and density as the particle in question. Another common method is to designate the screen mesh that has an aperture corresponding to the particle diameter; the screen scale used must also be specified to avoid confusion.

From the standpoint of collector design and performance, the most important size-related property of a dust particle is its dynamic behavior. Particles larger than 100 μm are readily collectible by simple inertial or gravitational methods. For particles under 100 μm, the range of principal difficulty in dust collection, the resistance to motion in a gas is viscous (see Sec. 6, "Fluid and Particle Mechanics"), and for such particles, the most useful size specification is commonly the Stokes settling diameter, which is the diameter of the spherical particle of the same density that has the same terminal velocity in viscous flow as the particle in question. It is yet more convenient in many circumstances to use the "aerodynamic diameter," which is the diameter of the particle of unit density (1 g/cm^3) that has the same terminal settling velocity. Use of the aerodynamic diameter permits direct comparisons of the dynamic behavior of particles that are actually of different sizes, shapes, and densities [Raabe, *J. Air Pollut. Control Assoc.,* **26,** 856 (1976)].

When the size of a particle approaches the same order of magnitude as the mean free path of the gas molecules, the settling velocity is greater than predicted by Stokes' law because of molecular slip. The slip-flow correction is appreciable for particles smaller than 1 μm and is allowed for by the Cunningham correction for Stokes' law (Lapple, op. cit.; Licht, op. cit.). The Cunningham correction is applied in calculations of the aerodynamic diameters of particles that are in the appropriate size range.

Although solid fume particles may range in size down to perhaps 0.001 μm, fine particles effectively smaller than about 0.1 μm are not of much significance in industrial dust and fume sources because their aggregate mass is only a very small fraction of the total mass emission. At the concentrations present in such sources (e.g., production of carbon black) the coagulation, or flocculation, rate of the ultrafine particles is extremely high, and the particles speedily grow to sizes of 0.1 μm or greater. The most difficult collection problems are thus concerned with particles in the range of about 0.1 to 2 μm, in which forces for deposition by inertia are small. For collection of particles under 0.1 μm, diffusional deposition becomes increasingly important as the particle size decreases.

In a gas stream carrying dust or fume, some degree of particle flocculation will exist, so that both discrete particles and clusters of adhering particles will be present. The discrete particles composing the clusters may be only loosely attached to each other, as by van der Waals forces [Lapple, *Chem. Eng.,* **75**(11), 149 (1968)]. Flocculation tends to increase with increases in particle concentration and may strongly influence collector performance.

PARTICLE MEASUREMENTS

Measurements of the concentrations and characteristics of dust dispersed in air or other gases may be necessary (1) to determine the need for control measures, (2) to establish compliance with legal requirements, (3) to obtain information for collector design, and (4) to determine collector performance.

Atmospheric-Pollution Measurements The dust-fall measurement is one of the common methods for obtaining a relative long-period evaluation of particulate air pollution. Stack-smoke densities are often graded visually by means of the Ringelmann chart. Plume opacity may be continuously monitored and recorded by a photoelectric device which measures the amount of light transmitted through a stack plume. Equipment for local atmospheric-dust-concentration measurements fall into five general types: (1) the impinger, (2) the hot-wire or thermal precipitator, (3) the electrostatic precipitator, (4) the filter, and (5) impactors and cyclones. The filter is the most widely used, in the form of either a continuous tape, or a number of filter disks arranged in an automatic sequencing device, or a single, short-term, high-volume sampler. Samplers such as these are commonly used to obtain mass emission and particle-size distribution. Impactors and small cyclones are commonly used as size-discriminating samplers and are usually followed by filters for the determination of the finest

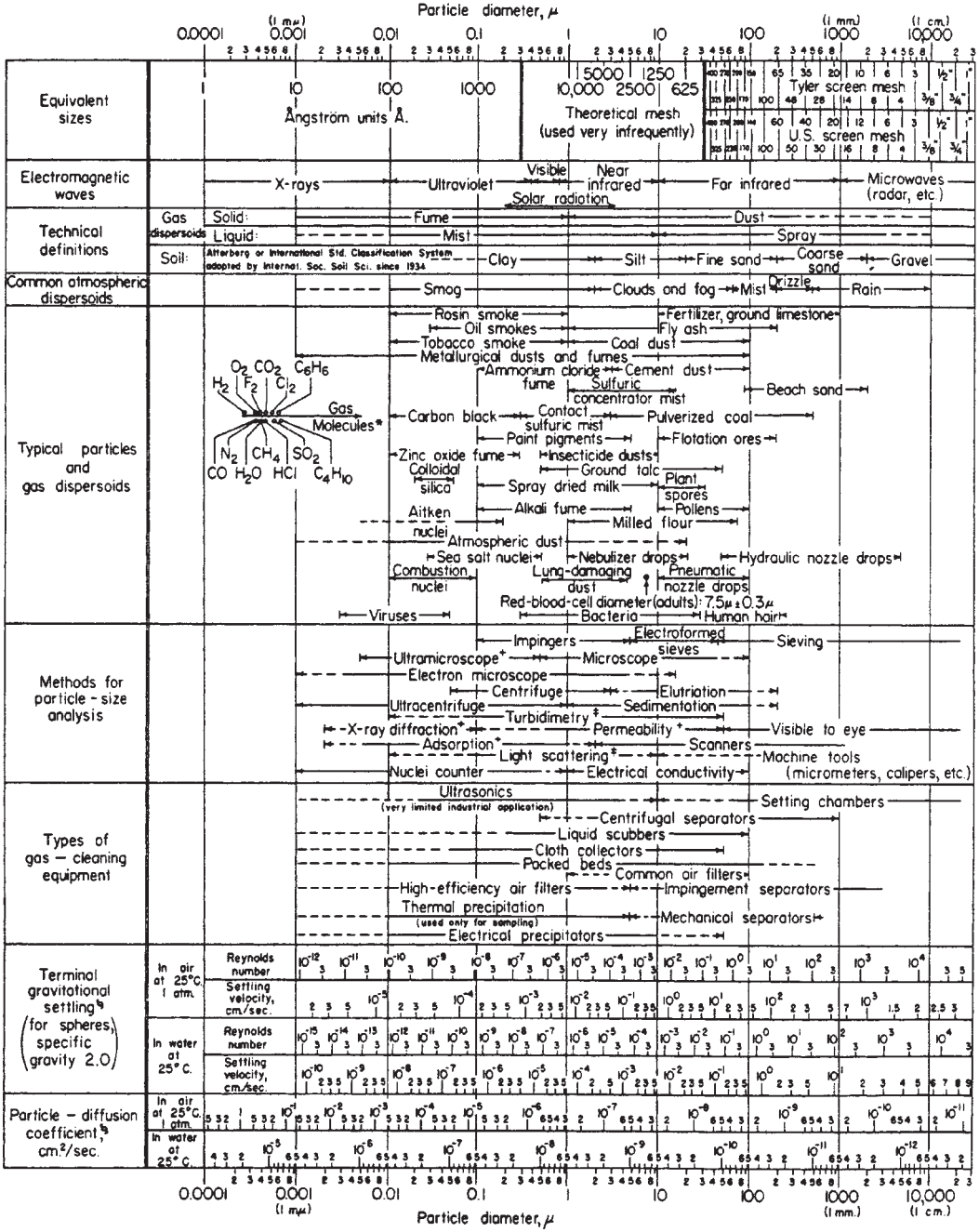

* Molecular diameters calculated from viscosity data at 0° C.

\+ Furnishes average particle diameter but no size distribution.

‡ Size distribution may be obtained by special calibration.

§ Stokes–Cunningham factor included in values given for air but not included for water.

FIG. 17-34 Characteristics of particles and particle dispersoids. (*Courtesy of the Stanford Research Institute; prepared by C. E. Lapple.*)

fraction of the dust (Lundgren et al., *Aerosol Measurement,* University of Florida, Gainesville, 1979; and Dennis, *Handbook on Aerosols,* U.S. ERDA TID-26608, Oak Ridge, Tenn., 1976).

Process-Gas Sampling In sampling process gases either to determine dust concentration or to obtain a representative dust sample, it is necessary to take special precautions to avoid inertial segregation of the particles. To prevent such classification, a traverse of the duct may be required, and at each point the sampling nozzle must face

directly into the gas stream with the velocity in the mouth of the nozzle equal to the local gas velocity at that point. This is called "isokinetic sampling." If the sampling velocity is too high, the dust sample will contain a lower concentration of dust than the mainstream, with a greater percentage of fine particles; if the sampling velocity is too low, the dust sample will contain a higher concentration of dust with a greater percentage of coarse particles [Lapple, *Heat. Piping Air Cond.,* **16,** 578 (1944); *Manual of Disposal of Refinery Wastes,* vol. V, American Petroleum Institute, New York, 1954; and Dennis, op. cit.].

Particle-Size Analysis Methods for particle-size analysis are shown in Fig. 17-34, and examples of size-analysis methods are given in Table 17-1. More detailed information may be found in Lapple, *Chem. Eng.,* **75**(11), 140 (1968); Lapple, "Particle-Size Analysis," in *Encyclopedia of Science and Technology,* 5th ed., McGraw-Hill, New York, 1982; Cadle, *The Measurement of Airborne Particles,* Wiley, New York, 1975; Lowell, *Introduction to Powder Surface Area,* 2d ed., Wiley, New York, 1993; and Allen, *Particle Size Measurement,* 4th ed, Chapman and Hall, London, 1990. Particle-size distribution may be presented on either a frequency or a cumulative basis; the various methods are discussed in the references just cited. The most common method presents a plot of particle size versus the cumulative weight percent of material larger or smaller than the indicated size, on logarithmic-probability graph paper.

For determination of the aerodynamic diameters of particles, the most commonly applicable methods for particle-size analysis are those based on inertia: aerosol centrifuges, cyclones, and inertial impactors (Lundgren et al., *Aerosol Measurement,* University of Florida, Gainesville, 1979; and Liu, *Fine Particles—Aerosol Generation, Measurement, Sampling, and Analysis,* Academic, New York, 1976). Impactors are the most commonly used. Nevertheless, impactor measurements are subject to numerous errors [Rao and Whitby, *Am. Ind. Hyg. Assoc. J.,* **38,** 174 (1977); Marple and Willeke, "Inertial Impactors," in Lundgren et al., *Aerosol Measurement;* and Fuchs, "Aerosol Impactors," in Shaw, *Fundamentals of Aerosol Science,* Wiley, New York, 1978]. Reentrainment due to particle bouncing and blowoff of deposited particles makes a dust appear finer than it actually is, as does the breakup of flocculated particles. Processing cascade-impactor data also presents possibilities for substantial errors (Fuchs, *The Mechanics of Aerosols,* Pergamon, Oxford, 1964) and is laborious as well. Lawless (Rep. No. EPA-600/7-78-189, U.S. EPA, 1978) discusses problems in analyzing and fitting cascade-impactor data to obtain dust-collector efficiencies for discrete particle sizes.

The measured diameters of particles should as nearly as possible represent the effective particle size of a dust as it exists in the gas stream. When significant flocculation exists, it is sometimes possible to use measurement methods based on gravity settling.

For dust-control work, it is recommended that a preliminary qualitative examination of the dust first be made without a detailed particle count. A visual estimate of particle-size distribution will often provide sufficient guidance for a preliminary assessment of requirements for collection equipment.

MECHANISMS OF DUST COLLECTION

The basic operations in dust collection by any device are (1) separation of the gas-borne particles from the gas stream by deposition on a collecting surface; (2) retention of the deposit on the surface; and (3) removal of the deposit from the surface for recovery or disposal. The separation step requires (1) application of a force that produces a differential motion of a particle relative to the gas and (2) a gas retention time sufficient for the particle to migrate to the collecting surface. The principal mechanisms of aerosol deposition that are applied in dust collectors are (1) gravitational deposition, (2) flow-line interception, (3) inertial deposition, (4) diffusional deposition, and (5) electrostatic deposition. Thermal deposition is only a minor factor in practical dust-collection equipment because the thermophoretic force is small. Table 17-2 lists these six mechanisms and presents the characteristic

TABLE 17-1 Particle Size Analysis Methods and Equipment

Method	Brand names	Size range	Sample size, g
Quantitative image analysis	American Innovation Videometric, Analytical Measuring Systems Quickstep & Optomax, Artec Omnicon Automatix, Boeckeler, Buehler Omnimat, Compix Imaging Systems, Data Teanslation—Global Lab, Image, Hamamatsu C-1000, Hitech Olympus Cue-3, Joyce-Loebl Magiscan, Leco AMF System, Leico Quantimet, LeMont Oasys, Millipore_MC, Nachet 1500, Nicon Microphot, Oncor Instrument System, Optomax V, Outokumpu Imagist, Shapespeare Juliet, Tracor Northern, Carl Zeiss Videoplan	1–1000 μm	0.001
Sieves:		4–100 mm	500
Punched Plate	Many		
Woven wire	Many	20 μm–125 mm	25–200
Micromesh	Buckbee Mears, Veco, Endecottes	5–500 + μm	1–5
Sieving machines (Air jet, sonic wet and dry)	Alpine, ATM, Gilson, Gradex, Hosokawa, Retsch, Seishin		
Sedimentation	*Pipette*—Gilson, *Photosedimentometer—gravitational,* Paar; *centrifugal,* Joyce Loebl, Brookhaven, Horiba, Seishin, Shimadzu; *x-ray absorption*—gravitational, Quantachrome, Micromeretics; *centrifugal,* Brookhaven	Gravitational 1–100 μm Centrifugal 0.05–5 mm	0.1–5+ g
Classification	Air-Bahco, Water-Warmain Cyclosizer	5–500 μm	5–100 g
Field scanning (light)	Cilas, Coulter, Insitec, Fritsch, Horiba, Leeds & Northrup (Microtrac), Malvern, Nitto, Seishin, Shimadzu, Sympatec	0.04–3500 μm	<1 g (wet) >20 g (on-line)
Field scanning (ultrasonics)	Sympatec OPUS, Pen-Kem		On-line
Stream scanning	Brinkmann, Climet, Coulter, Dantec, Erdco, Faley, Flowvision, Hiac/Royco, Kowa, Lasentec, Malvern, Met One, Particle Measuring Systems, Polytec, Procedyne, Rion, Spectrex	0.2–10,000 μm	0.1–10 g (also on-line)
Zeta potential	Zeta Plus, Micromeretics, Zeta sizer	0.001–30 μm	0.1–1 μm
Photon correlation Spectroscopy	Malvern, Nicomp, Brookhaven, Coulter, Photol		

NOTE: This table was compiled with the assistance of T. Allen, DuPont Particle Science and Technology, and is not intended to be comprehensive. Many other fine suppliers of particle analysis equipment are available.

TABLE 17-2 Summary of Mechanisms and Parameters in Aerosol Deposition

Deposition	Origin of force field	Deposition mechanism measureable in terms of: Basic parameter	Deposition mechanism measureable in terms of: Specific modifying parameters	System parameters
Flow-line interception*	Physical gradient*	$N_{sf} = \left(\frac{D_p}{D_b}\right)$	$N_{sc} = \left(\frac{N_{sf}^2}{N_{st} N_{sd}}\right) = \left(\frac{18\mu}{K_m \rho_p D_v}\right)^{\dagger}$	Geometry: (D_{b1}/D_b), (D_{b2}/D_b), etc. ϵ_v Δ
Inertial deposition	Velocity gradient	$N_{st} = \left(\frac{K_m \rho s D_p^2 V_o}{18\mu D_b}\right)$		
Diffusional deposition	Concentration gradient	$N_{sd} = \left(\frac{D_v}{V_o D_b}\right)$		
Gravity settling	Elevation gradient	$N_{sg} = \left(\frac{u_t}{V_o}\right)$		Flow pattern: N_{Re}‡ N_{Ma} N_{Kn}
Electrostatic precipitation	Electric-field gradient§ *a.* Attraction *b.* Induction	$N_{sec} = \left(\frac{K_m Q_p \epsilon_b}{\mu D_p V_o}\right)$ $N_{sei} = \left(\frac{\delta_p - 1}{\delta_p + 2}\right)\left(\frac{K_m D_p^2 \delta_o \epsilon_b 2}{\mu D_b V_o}\right)$	δ_p, δ_b¶	Surface accommodation
Thermal precipitation	Temperature gradient	$N_{st} = \left(\frac{T - T_b}{T}\right)\left(\frac{\mu}{K_m \rho D_b V_o}\right)\left(\frac{k_t}{2k_t + k_{tp}}\right)$	(T_b/T), (T_p/T),† (N_{Pr}), (k_{tp}/k_t), (k_{tb}/k_t),¶ (c_{hp}/c_h), (c_{hb}/c_h)¶	

SOURCE: Lunde and Lapple, *Chem. Eng. Prog.*, **53,** 385 (1957).

*This has also commonly been termed "direct interception" and in conventional analysis would constitute a physical boundary condition imposed upon the particle path induced by action of other forces. By itself it reflects deposition that might result with a hypothetical particle having finite size but no mass or elasticity.

†This parameter is an alternative to N_{sf}, N_{si}, or N_{ad} and is useful as a measure of the interactive effect of one of these on the other two. It is comparable with the Schmidt number.

‡When applied to the inertial deposition mechanism, a convenient alternative is $(K_m \rho_s/18\rho) = N_{si}/(N_{sf}^2 N_{Re})$.

§In cases in which the body charge distribution is fixed and known, ϵ_b may be replaced with Q_{bs}/δ_o.

¶Not likely to be significant contributions.

parameters of their operation [Lunde and Lapple, *Chem. Eng. Prog.*, **53,** 385 (1957)]. The actions of the inertial-deposition, flow-line-interception, and diffusional-deposition mechanisms are illustrated in Fig. 17-35 for the case of a collecting body immersed in a particle-laden gas stream.

Two other deposition mechanisms, in addition to the six listed, may be in operation under particular circumstances. Some dust particles may be collected on filters by sieving when the pore diameter is less than the particle diameter. Except in small membrane filters, the sieving mechanism is probably limited to surface-type filters, in which a layer of collected dust is itself the principal filter medium.

The other mechanism appears in scrubbers. When water vapor diffuses from a gas stream to a cold surface and condenses, there is a net hydrodynamic flow of the noncondensable gas directed toward the surface. This flow, termed the Stefan flow, carries aerosol particles to the condensing surface (Goldsmith and May, in Davies, *Aerosol Science,* Academic, New York, 1966) and can substantially improve the performance of a scrubber. However, there is a corresponding Stefan flow directed away from a surface at which water is evaporating, and this will tend to repel aerosol particles from the surface.

In addition to the deposition mechanisms themselves, methods for preliminary conditioning of aerosols may be used to increase the effectiveness of the deposition mechanisms subsequently applied. One such conditioning method consists of imposing on the gas high-intensity acoustic vibrations to cause collisions and flocculation of the aerosol particles, producing large particles that can be separated by simple inertial devices such as cyclones. This process, termed "sonic (or acoustic) agglomeration," has attained only limited commercial acceptance.

Another conditioning method, adaptable to scrubber systems, consists of inducing condensation of water vapor on the aerosol particles as nuclei, increasing the size of the particles and making them more susceptible to collection by inertial deposition.

Most forms of dust-collection equipment use more than one of the collection mechanisms, and in some instances the controlling mechanism may change when the collector is operated over a wide range of conditions. Consequently, collectors are most conveniently classified by type rather than according to the underlying mechanisms that may be operating.

PERFORMANCE OF DUST COLLECTORS

The performance of a dust collector is most commonly expressed as the collection efficiency η, the weight ratio of the dust collected to the dust entering the apparatus. However, the collection efficiency is usually related exponentially to the properties of the dust and gas and the operating conditions of most types of collectors and hence is an insensitive function of the collector operating conditions as its value approaches 1.0. Performance in the high-efficiency range is better expressed by the penetration $1 - \eta$, the weight ratio of the dust escaping to the dust entering. Particularly in reference to collection of radioactive aerosols, it is common to express performance in terms of the reciprocal of the penetration $1/(1 - \eta)$, which is termed the "decontamination factor." The number of transfer units N_t, which is equal to $\ln [1/(1 - \eta)]$ in the case of dust collection, was first proposed for use by Lapple (Wright, Stasny, and Lapple, "High Velocity Air Filters," WADC Tech. Rep. 55-457, ASTIA No. AD-142075, October 1957) and is more commonly used than the DI. Because of the exponential form of the relationship between efficiency and process variables for most dust collectors, the use of N_t (or DI) is particularly suitable for correlating collector performance data.

In comparing alternative collectors for a given service, a figure of merit is desirable for ranking the different devices. Since power consumption is one of the most important characteristics of a collector, the ratio of N_t to power consumption is a useful criterion. Another is the ratio of N_t to capital investment.

Mechanism	Model	Separation number	Description
Inertial interception	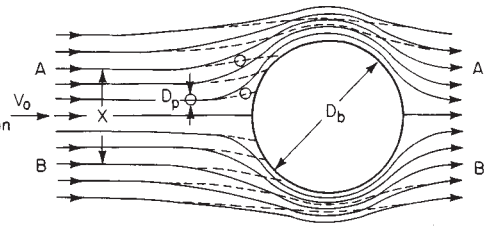	$N_{si} = \frac{K_m \rho_p D_p^2 V_o}{18 \mu D_b}$	On approaching a collecting body (fiber or liquid droplet), a particle carried along by the gas stream tends to follow the stream but may strike the obstruction because of its inertia. Solid lines represent the fluid streamlines around a body of diameter D_b, and the dotted lines represent the paths of particles that initially followed the fluid streamlines. X is the distance between the limiting streamlines A and B. The fraction of particles initially present in a volume swept by the body that is removed by inertial interception is represented by the quantity X/D_b for a cylindrical collector and $(X/D_b)^2$ for a spherical collector.
Brownian diffusion	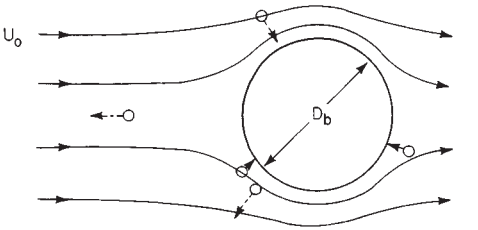	$N_{sd} = \frac{D_v}{V_o D_b}$	Smaller particles, particularly those below about 0.3 μm in diameter, exhibit considerable Brownian movement and do not move uniformly along the gas streamline. These particles diffuse from the gas to the surface of the collecting body and are collected.
Flow-line interception	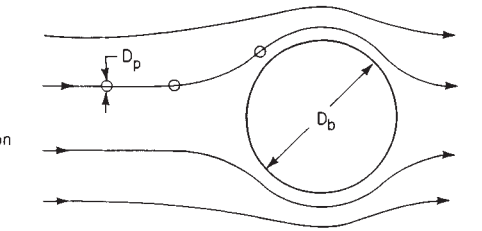	$N_{sf} = \frac{D_p}{D_b}$	If a fluid streamline passes within one particle radius of the collecting body, a particle traveling along the streamline will touch the body and may be collected without the influence of inertia or brownian diffusion.

Fluid streamline
Particle path

FIG. 17-35 Particle deposition on collector bodies.

DUST-COLLECTOR DESIGN

In dust-collection equipment, most or all of the collection mechanisms may be operating simultaneously, their relative importance being determined by the particle and gas characteristics, the geometry of the equipment, and the fluid-flow pattern. Although the general case is exceedingly complex, it is usually possible in specific instances to determine which mechanism or mechanisms may be controlling. Nevertheless, the difficulty of theoretical treatment of dust-collection phenomena has made necessary simplifying assumptions, with the introduction of corresponding uncertainties. Theoretical studies have been hampered by a lack of adequate experimental techniques for verification of predictions. Although theoretical treatment of collector performance has been greatly expanded in the period since 1960, few of the resulting performance models have received adequate experimental confirmation because of experimental limitations.

The best-established models of collector performance are those for fibrous filters and fixed-bed granular filters, in which the structures and fluid-flow patterns are reasonably well defined. These devices are also adapted to small-scale testing under controlled laboratory conditions. Realistic modeling of full-scale electrostatic precipitators and scrubbers is incomparably more difficult. Confirmation of the models has been further limited by a lack of monodisperse aerosols that can be generated on a scale suitable for testing equipment of substantial sizes. When a polydisperse test dust is used, the particle-size distributions of the dust both entering and leaving a collector must be determined with extreme precision to avoid serious errors in the determination of the collection efficiency for a given particle size.

The design of industrial-scale collectors still rests essentially on empirical or semiempirical methods, although it is increasingly guided by concepts derived from theory. Existing theoretical models frequently embody constants that must be evaluated by experiment and that may actually compensate for deficiencies in the models.

DUST-COLLECTION EQUIPMENT

Gravity Settling Chambers The gravity settling chamber is probably the simplest and earliest type of dust-collection equipment, consisting of a chamber in which the gas velocity is reduced to enable dust to settle out by the action of gravity. Its simplicity lends it to almost any type of construction. Practically, however, its industrial utility is limited to removing particles larger than 325 mesh (43-μm diameter). For removing smaller particles, the required chamber size is generally excessive.

Gravity collectors are generally built in the form of long, empty, horizontal, rectangular chambers with an inlet at one end and an outlet at the side or top of the other end. By assuming a low degree of turbulence relative to the settling velocity of the dust particle in question, the performance of a gravity settling chamber is given by

$$\eta = \frac{u_t L_s}{H_s V_s} = \frac{u_t B_s L_s}{q} \qquad (\text{for } \eta \leqq 1.0) \qquad (17\text{-}1)$$

where V_s = average gas velocity. Expressing u_t in terms of particle size (equivalent spherical diameter), the smallest particle that can be completely separated out corresponds to $\eta = 1.0$ and, assuming Stokes' law, is given by

$$D_{p,\min} = \sqrt{\frac{18\mu H_s V_s}{g_L L_s(\rho_s - \rho)}}$$

$$= \sqrt{\frac{18\mu q}{g_L B_s L_s(\rho_s - \rho)}} \qquad (17\text{-}2)$$

where ρ = gas density and ρ_s = particle density. For a given volumetric air-flow rate, collection efficiency depends on the total plan cross section of the chamber and is independent of the height. The height need be made only large enough so that the gas velocity V_s in the chamber is not so high as to cause reentrainment of separated dust. Generally V_s should not exceed about 3 m/s (10 ft/s).

Horizontal plates arranged as shelves within the chamber will give a marked improvement in collection. This arrangement is known as the Howard dust chamber (Fume Arrester, U.S. Patent 896,111, 1908). The disadvantage of the unit is the difficulty of cleaning owing to the close shelf spacing and warpage at elevated temperatures.

The pressure drop through a settling chamber is small, consisting primarily of entrance and exit losses. Because low gas velocities are used, the chamber is not subject to abrasion and may therefore be used as a precleaner to remove very coarse particles and thus minimize abrasion on subsequent equipment.

Impingement Separators Impingement separators are a class of inertial separators in which particles are separated from the gas by inertial impingement on collecting bodies arrayed across the path of the gas stream, as shown on Fig. 17-35. Fibrous-pad inertial impingement separators for the collection of wet particles are the main application in current technology, as is described in Sec. 18 and Fig. 17-48. With the growing need for very high performance dust collectors, there is little application anymore for impingement collectors that catch large amounts of dry dust.

Cyclone Separators The most widely used type of dust-collection equipment is the cyclone, in which dust-laden gas enters a cylindrical or conical chamber tangentially at one or more points and leaves through a central opening (Fig. 17-36). The dust particles, by virtue of their inertia, will tend to move toward the outside separator wall, from which they are led into a receiver. A cyclone is essentially a settling chamber in which gravitational acceleration is replaced by centrifugal acceleration. At operating conditions commonly employed, the centrifugal separating force or acceleration may range from 5 times gravity in very large diameter, low-resistance cyclones, to 2500 times gravity in very small, high-resistance units. The immediate entrance to a cyclone is usually rectangular.

Fields of Application Within the range of their performance capabilities, cyclone collectors offer one of the least expensive means of dust collection from the standpoint of both investment and operation. Their major limitation is that unless very small units are used, their efficiency is low for collection of particles smaller than 5 μm. Although cyclones may be used to collect particles larger than 200 μm, gravity settling chambers or simple inertial separators (such as gas-reversal chambers) are usually satisfactory and less subject to abrasion. In special cases in which the dust is highly flocculated or high dust concentrations (over 230 g/m^3, or 100 gr/ft^3) are encountered, cyclones will remove dusts having small particle sizes. In certain instances efficiencies as high as 98 percent have been attained on dusts having ultimate particle sizes of 0.1 to 2.0 μm because of the predominant effect of flocculation.

Cyclones are used to remove both solids and liquids from gases and have been operated at temperatures as high as 1000°C and pressures as high as 50,700 kPa (500 atm).

Flow Pattern In a cyclone the gas path involves a double vortex with the gas spiraling downward at the outside and upward at the inside. When the gas enters the cyclone, its velocity undergoes a redistribution so that the tangential component of velocity increases with decreasing radius as expressed by $V_{ct} \sim r^{-n}$. The spiral velocity in a cyclone may reach a value several times the average inlet-gas velocity. Theoretical considerations indicate that n should be equal to 1.0 in the absence of wall friction. Actual measurements [Shepherd and Lapple, *Ind. Eng. Chem.*, **31,** 972 (1939); **32,** 1246 (1940)], however, indicate that n may range from 0.5 to 0.7 over a large portion of the cyclone radius. Ter Linden [*Inst. Mech. Eng. J.*, **160,** 235 (1949)] found n to be 0.52 for tangential velocities measured in the cylindrical portion of the cyclone at positions ranging from the radius of the gas-outlet pipe to the radius of the collector. Although the velocity approaches zero at the wall, the boundary layer is sufficiently thin that pitot-tube measurements show relatively high tangential velocities there, as shown in Fig. 17-37. The radial velocity V_r is directed toward the center throughout most of the cyclone, except at the center, where it is directed outward.

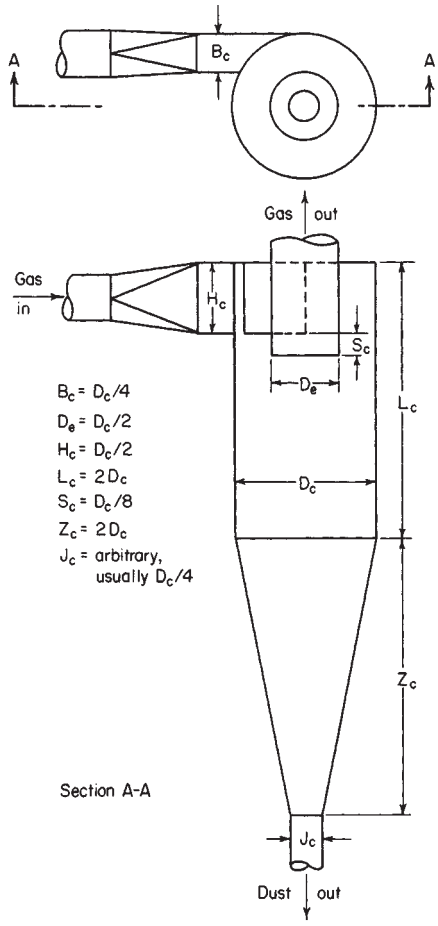

FIG. 17-36 Cyclone-separator proportions.

Superimposed on the "double spiral," there may be a "double eddy" [Van Tongeran, *Mech. Eng.*, **57,** 753 (1935); and Wellmann, *Feuerungstechnik*, **26,** 137 (1938)] similar to that encountered in pipe coils. Measurements on cyclones of the type shown in Fig. 17-36 indicate, however, that such double-eddy velocities are small compared with the spiral velocity (Shepherd and Lapple, op. cit.). Recent analyses of flow patterns can be found in Hoffman et al., *Powder Tech.*, **70,** 83 (1992); and Trefz and Muschelknautz, *Chem. Eng. Tech.*, **16,** 153 (1993).

Cyclone Efficiency The methods described below for pressure drop and efficiency calculations were given by Zenz in *Manual on Disposal of Refinery Wastes—Atmospheric Emissions*, chap. 11 (1975), American Petroleum Institute Publ. 931 and improved by the Particulate Solid Research Inc. (PSRI), Chicago.

Cyclones work by using centrifugal force to increase the gravity field experienced by the solids. They then settle to the wall under the influence of their increased weight. Settling is improved as the path the solids traverse under centrifugal flow is increased. This path is

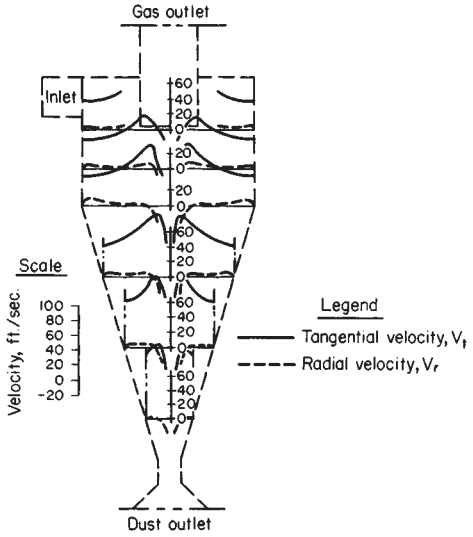

FIG. 17-37 Variation of tangential velocity and radial velocity at different points in a cyclone. [*Ter Linden,* Inst. Mech. Eng. J., ***160,*** *235 (1949).*]

equated with the number of spirals the solids make in the cyclone barrel. Figure 17-38 gives the number of spirals N_s as a function of the maximum velocity in the cyclone. The maximum velocity may be seen either at the inlet or outlet depending on design.

The equation for D_{pth}, the theoretical size particle removed by the cyclone, is

$$D_{pth} = \sqrt{\frac{9\mu_g B_c}{\pi N_s v_{in}(\rho_p - \rho_g)}}$$

When consistent units are used, the particle size will either be in meters or feet. The equation contains effects of cyclone size, velocity, viscosity, and density of solids. In practice, a design curve as given in Fig. 17-39 uses D_{pth} as the size at which 50 percent of solids of a given size are collected by the cyclone. The material entering the cyclone is divided into fractional sizes, and the collection efficiency for each size is determined. The total efficiency of collection is the sum of the collection efficiencies of the cuts.

The above applies for very dilute systems, usually on the order of 1 grain/ft^3, or 2.3 g/m^3 where a grain equals 1/7000 of a pound. When an appreciable amount of solids are present, the efficiency increases

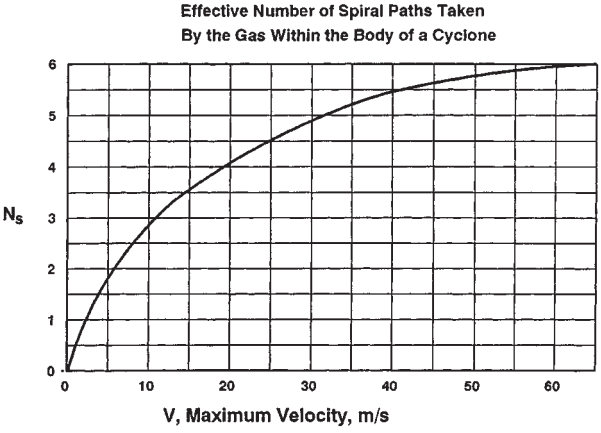

FIG. 17-38 N_s versus velocity—where the larger of either the inlet or outlet velocity is used.

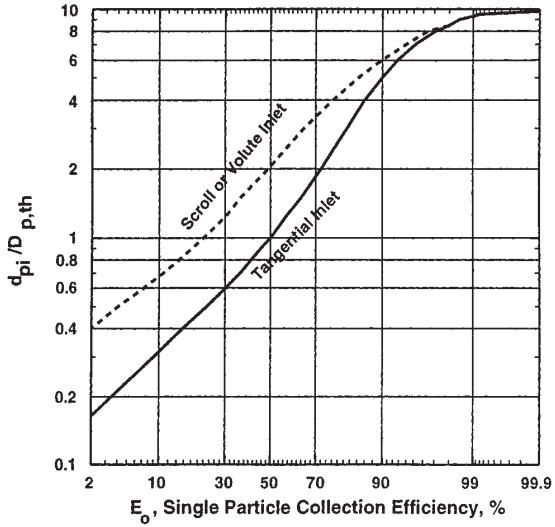

FIG. 17-39 Single particle collection efficiency curve. (*Courtesy of PSRI, Chicago.*)

dramatically. This may be due to the coarse particles colliding with fines as they settle, which takes the fines to the wall more quickly. Other explanations are that the solids have a lower drag coefficient or tend to flocculate in multiparticle environments. At very high loadings, it is believed the gas simply cannot hold that much solid material in suspension at high gravities, and the bulk of the solids simply "condenses" out of the gas stream.

The phenomenon is represented by Figs. 17-40 and 17-41 for Geldart-type A and B solids, respectively (see beginning of Sec. 17). The initial efficiency of a particle size cut is found on the chart, and the parametric line is followed to the proper overall solids loading. The efficiency for that cut size is then read from the graph.

Pressure Drop Pressure drop is first determined by summing five flow losses associated with the cyclone.

1. Inlet contraction,

$$\Delta P = 0.5\rho_g(v_{in}^2 - v_{vessel}^2 + Kv_{in}^2)$$

where K is taken from Table 17-3. Using SI units gives the pressure drop in Pa. In English units, the factor of 32.2 for g must be included. This loss is primarily associated with cyclones inside a vessel. If the cyclone is connected outside a vessel, the *dp* tap may measure acceleration, and this term should not be used for total *dp*.

TABLE 17-3 *K* versus Area Ratio

Area ratio	*K*
0	.50
0.1	.47
0.2	.43
0.3	.395
0.4	.35

2. Particle acceleration,

$$\Delta P = Lv_{in}(v_{pin} - v_{pvessel})$$

For small particles, the velocity is taken as equal to the gas velocity and L is the loading, kg/m^3.

3. Barrel friction. The inlet diameter d_{in} is taken as 4 × (inlet area)/inlet perimeter. Then,

$$\Delta P = \frac{2f\rho_g v_{in}^2 \pi D_c N_s}{d_{in}}$$

where the Reynolds number for determining the friction factor f is based on the inlet area.

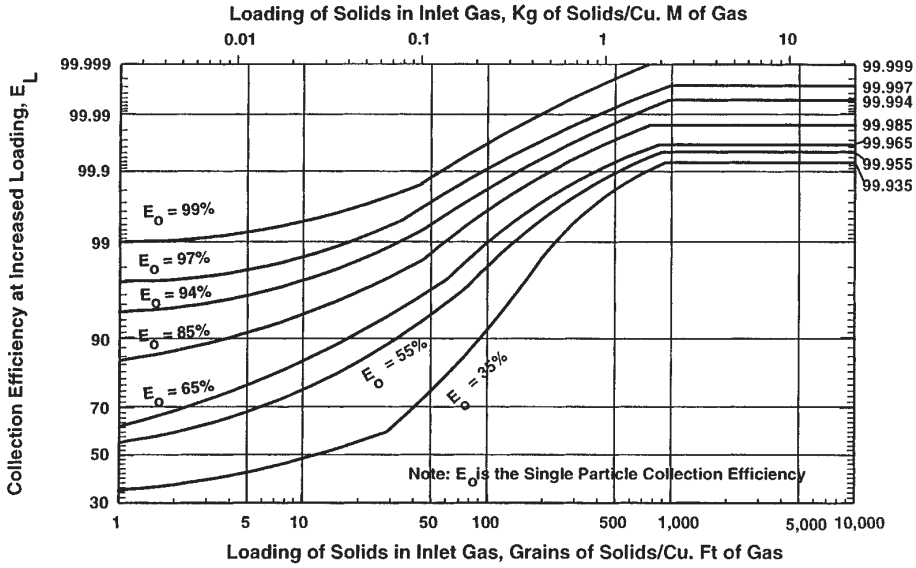

FIG. 17-40 Effect of inlet loading on collection efficiency for Geldart Group A and Group C particles. (*Courtesy of PSRI, Chicago.*)

4. Gas flow reversal,

$$\Delta P = \frac{\rho_g v_{\text{in}}^2}{2}$$

5. Exit contraction,

$$\Delta P = 0.5\rho_g(v_{\text{exit}}^2 - v_c^2 + Kv_{\text{exit}}^2)$$

where K is determined from Table 17-3 based on the area ratio of barrel and exit tube of the cyclone.

The total pressure drop is the sum of the 5 individual pressure drops.

However, the actual pressure drop observed turns out to be a function of the solids loading. The pressure drop is high when the gas is free of solids and then *decreases* as the solids loading increases up to about 3 kg/m^3 (0.2 lb/ft^3). The cyclone *dp* then begins to increase with loading. The cause of the initial decline is that the presence of solids decreases the tangential velocity of the gas [Yuu, *Chem. Eng. Sci.*, **33,** 1573 (1978)]. Figure 17-42 gives the actual pressure drop based on the loading. When solids are absent, the observed pressure drop can be 2.5 times the calculated pressure drop.

Cyclone Design Factors Cyclones are generally designed to meet specified pressure-drop limitations. For ordinary installations, operating at approximately atmospheric pressure, fan limitations generally dictate a maximum allowable pressure drop corresponding to a cyclone inlet velocity in the range of 8 to 30 m/s (25 to 100 ft/s). Consequently, cyclones are usually designed for an inlet velocity of 15 m/s (50 ft/s), though this need not be strictly adhered to.

In the removal of dusts, collection efficiency can be changed by only a relatively small amount by a variation in operating conditions.

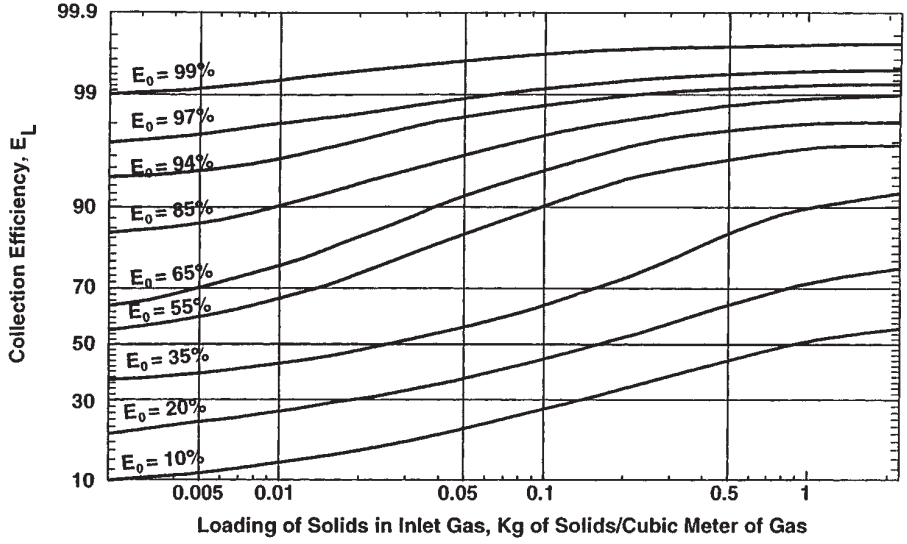

FIG. 17-41 Effect of inlet loading on collection efficiency (Geldart Group B and Group D) particles. (*Courtesy of PSRI, Chicago.*)

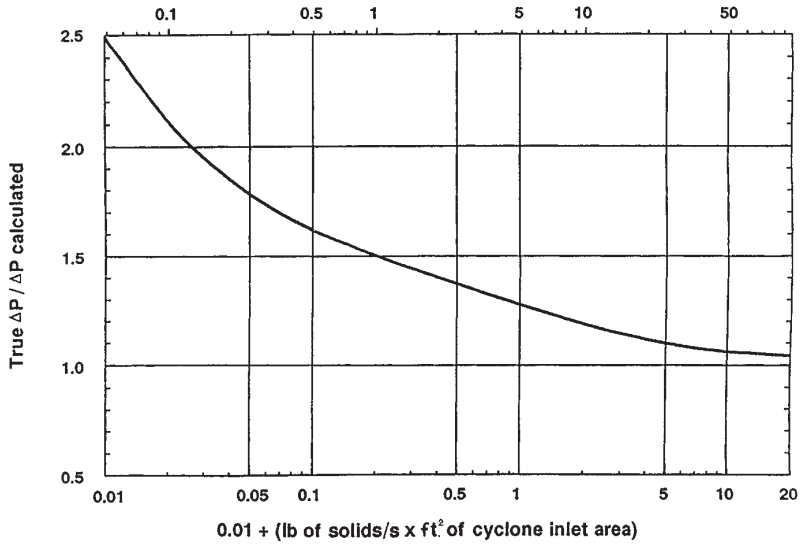

FIG. 17-42 Effect of cyclone inlet loading on pressure drop. (*Courtesy of PSRI, Chicago.*)

The primary design factor that can be utilized to control collection efficiency is the cyclone diameter, a smaller-diameter unit operating at a fixed pressure drop having the higher efficiency [Anderson, *Chem. Metall.,* **40,** 525 (1933); Drijver, *Wärme,* **60,** 333 (1937); and Whiton, *Power,* **75,** 344 (1932); *Chem. Metall.,* **39,** 150 (1932)]. Small-diameter cyclones, however, will require a multiple of units in parallel for a specified capacity. In such cases the individual cyclones can discharge the dust into a common receiving hopper [Whiton, *Trans. Am. Soc. Mech. Eng.,* **63,** 213 (1941)]. The final design involves a compromise between collection efficiency and complexity of equipment. It is customary to design a single cyclone for a given capacity, resorting to multiple parallel units only if the predicted collection efficiency is inadequate for a single unit.

Reducing the gas outlet diameter will increase both collection efficiency and pressure drop. To exit the cyclone, gas must enter the cyclonic flow associated with the outlet tube. If the outlet diameter is reduced, the outlet vortex increases in length to compensate. Therefore, when the outlet area is less than the inlet area, the length of the cyclone must increase. Too short a cyclone is associated with erosion of the cone and reentrainment of solids into the exit flow. Table 17-4 below gives this increase as a function of outlet-to-inlet area. The length is measured centrally along a cylinder 10 cm larger than the inner diameter of the outlet tube to prevent interference with the cone. If the cone interferes, the barrel must be lengthened. The minimum cone angle should be 60° or greater with steeper angles appropriate to materials that are cohesive.

The inlet is usually rectangular and sometimes circular. In either case, projection of the flow path should never interfere with the outlet tube. If a very heavy solids loading is anticipated, the barrel diameter should be increased slightly.

Collection efficiency is normally increased by increasing the gas throughput (Drijver, op. cit.). However, if the entering dust is flocculated, increased gas velocities may cause deflocculation in the cyclone, so that efficiency remains the same or actually decreases. Also, variations in design proportions that result in increased collection efficiency with dispersed dusts may be detrimental with flocculated dusts. Kalen and Zenz [*Am. Inst. Chem. Eng. Symp. Ser.,* **70** (137), 388 (1974)] report that collection efficiency increases with increasing gas inlet velocity up to a minimum tangential velocity at which dust is either reentrained or not deposited because of saltation. Koch and Licht [*Chem. Eng.,* **84**(24), 80 (1977)] estimate that for typical cyclones the saltation velocity is consistent with cyclone inlet velocities in the range of 15 to 27 m/s (50 to 90 ft/s). C. E. Lapple (private communication) reports that in cyclone tests with talc dust collection efficiency increased steadily as the inlet velocity was increased up to the maximum of 52 m/s (170 ft/s). With ilmenite dust, which was much more strongly flocculated, efficiency decreased over the same inlet-velocity range. In later experiments with well-dispersed talc dust, collection efficiency continued to increase at inlet velocities up to the maximum used, 82 m/s (270 ft/s). Another effect of increasing the cyclone inlet gas velocity is that friable materials may disintegrate as they hit the cyclone wall at high velocity. Thus, the increase in efficiency associated with increased velocity may be more than lost due to generation of fine attrited material that the cyclone cannot contain.

TABLE 17-4 Required Cyclone Length as a Function of Area Ratio

A_{out}/A_{in}	Length below outlet tube/D_c
>1.0	2.0
0.8	2.2
0.6	2.6
0.4	3.2

Cyclones in series may be justified under some circumstances:

1. The dust has a broad size distribution, including particles under 10 to 15 μm as well as larger and possibly abrasive particles. A large low-velocity cyclone may be used to remove the coarse particles ahead of a unit with small-diameter multiple tubes.
2. The dust is composed of fine particles but is highly flocculated or tends to flocculate in preceding equipment and in the cyclones themselves. Efficiencies predicted on the basis of ultimate particle size will be highly conservative.
3. The dust is relatively uniform, and the efficiency of the second-stage cyclone is not greatly lower than that of the first stage.
4. Dependable operation is critical. Second-stage or even third-stage cyclones may be used as backup.

A cyclone will operate equally well on the suction or pressure side of a fan if the dust receiver is airtight. Probably the greatest single cause for poor cyclone performance, however, is the leakage of air into the dust outlet of the cyclone. A slight air leak at this point can result in a tremendous drop in collection efficiency, particularly with fine dusts. For a cyclone under pressure, air leakage at this point is objectionable primarily because of the local dust nuisance created. For batch operation, an airtight hopper or receiver may be used. For continuous withdrawal of collected dust, a rotary star valve, a double-lock valve, or a screw conveyor may be used, the latter only with fine dusts. A collapsible open-ended rubber tube can be used for cyclones operating under slight negative pressure; mechanical flapgate valves and

fluidized seal legs can be used (see "Fluidized-Bed Systems: Solids Discharge"). Special pneumatic unloading devices can also be used with dusts. In any case it is essential that sufficient unloading and receiving capacity be provided to prevent collected material from accumulating in the cyclone.

Generally cone-and-disk baffles, helical guide vanes, etc., placed inside a cyclone, will have a detrimental effect on performance. A few of these devices do have some merit, however, under special circumstances. Although an inlet vane will reduce pressure drop, it causes a correspondingly greater reduction in collection efficiency. Its use is recommended only when collection efficiency is normally so high as to be a secondary consideration and when it is desired to decrease the resistance of an existing cyclone system for purposes of increased air-handling capacity or when floor-space or headroom requirements are controlling factors. If an inlet vane is used, it is advantageous to increase the gas-exit-duct length inside the cyclone chamber. A disk or cone baffle located beneath the gas-outlet duct may be beneficial if air in-leakage at the dust outlet cannot be avoided. A heavy chain suspended from the gas-outlet duct has been found beneficial to minimize dust buildup on the cyclone walls. Such a chain should be suspended from a swivel so that it is free to rotate without twisting. At present there are no known devices that will recover the gas spiral-velocity energy in the gas-outlet duct. Substantially all devices that have been reported to reduce pressure drop do so by reducing spiral velocities in the cyclone chamber and consequently result in reduced collection efficiency.

At low dust loadings the pressure in the dust receiver of a single cyclone will generally be lower than in the gas-outlet duct. Increased dust loadings will increase the pressure in the dust receiver. Such devices as cones, disks, and inlet vanes will generally cause the pressure in the dust receiver to exceed that in the gas-outlet duct. A cyclone will operate as well in a horizontal position as in a vertical position. However, departure from the normal vertical position results in an increasing tendency to plug the dust outlet. If the dust outlet becomes plugged, collection efficiency will, of course, be low. If the cyclone exit duct must be reduced to tie in with proposed duct sizes, the transition should be made at least five diameters downstream from the cyclone and preferably after a bend. In the event that the transition must be made closer to the cyclone, a Greek cross should be installed in the transition piece in order to avoid excessive pressure drop.

Commercial Equipment Simple cyclones are available in a wide variety of shapes ranging from long, slender units to short, large-diameter units. The body may be conical or cylindrical, and entrances may be involute or tangential and round or rectangular.

In Fig. 17-43 are shown some of the special types of commercial cyclones. In the Multiclone a spiral motion is imparted to the gas by

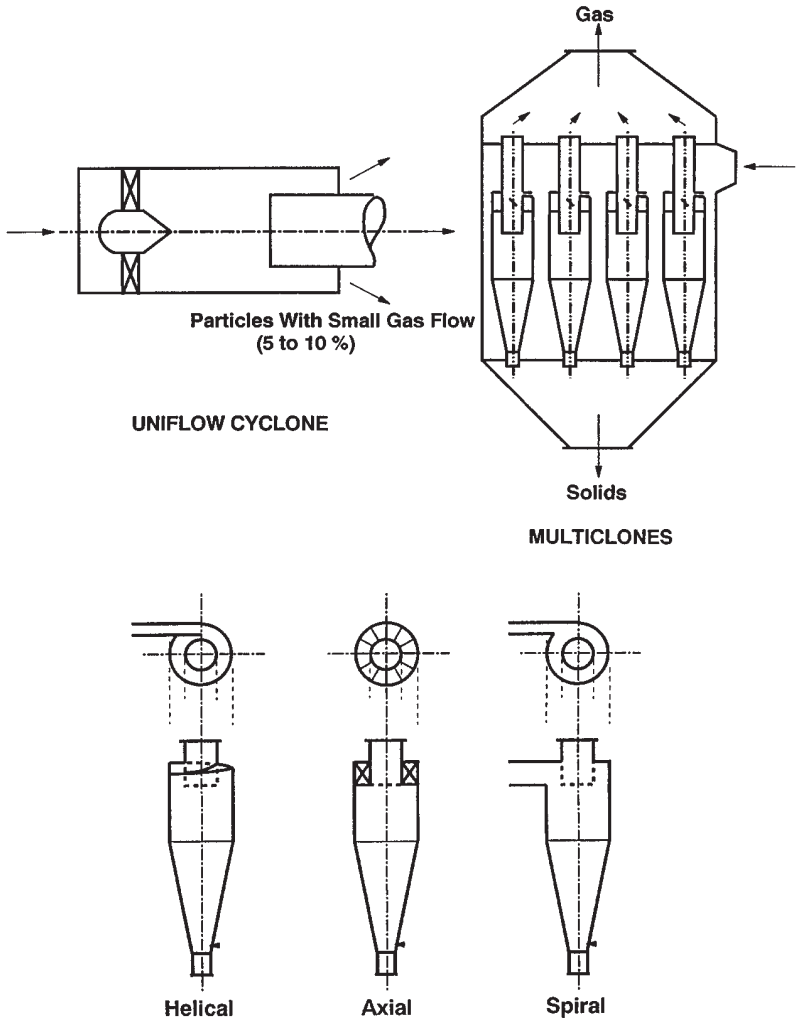

FIG. 17-43 Some commercial cyclone design alternatives. (*Courtesy of PSRI, Chicago.*)

annular vanes, and it is furnished in multiple units of 15.2- and 22.9-cm (6- and 9-in) diameter. Its largest field of application has been in the collection of fly ash from steam boilers. The tubes are commonly constructed of cast iron and other abrasion-resistant alloys.

In addition to the conventional reverse-flow cyclones, some use is made of uniflow, or straight-through, cyclones, in which the gas and solids discharge at the same end (Fig. 17-44). These devices act as concentrators; the concentrated dust, together with 5 to 20 percent of the inlet gas, is discharged at the periphery, while the clean gas passes out axially. The purge gas and concentrated dust enter a conventional cyclone for final separation. The straight-through cyclones are usually multiple-tube units.

Mechanical Centrifugal Separators A number of collectors in which the centrifugal field is supplied by a rotating member are commercially available. In the typical unit shown in Fig. 17-45, the exhauster or fan and dust collector are combined as a single unit. The blades are especially shaped to direct the separated dust into an annular slot leading to the collection hopper while the cleaned gas continues to the scroll.

Although no comparative data are available, the collection efficiency of units of this type is probably comparable with that of the single-unit high-pressure-drop-cyclone installation. The clearances are smaller and the centrifugal fields higher than in a cyclone, but these advantages are probably compensated for by the shorter gas path and the greater degree of turbulence with its inherent reentrainment tendency. The chief advantage of these units lies in their compactness, which may be a prime consideration for large installations or plants requiring a large number of individual collectors. Caution should be exercised when attempting to apply this type of unit to a dust that shows a marked tendency to build up on solid surfaces, because of the high maintenance costs that may be encountered from plugging and rotor unbalancing.

Particulate Scrubbers Wet collectors, or scrubbers, form a class of devices in which a liquid (usually water) is used to assist or accomplish the collection of dusts or mists. Such devices have been in use for well over 100 years, and innumerable designs have been or are offered commercially or constructed by users. Wet-film collectors logically form a separate subcategory of devices. They comprise inertial collectors in which a film of liquid flows over the interior surfaces, preventing reentrainment of dust particles and flushing away the deposited dust. Wetted-wall cyclones are an example [Stairmand, *Trans. Inst. Chem. Eng.*, **29,** 356 (1951)]. Wet-film collectors have not been studied systematically but can probably be expected to perform much as do equivalent dry inertial collectors, except for the benefit of reduced reentrainment.

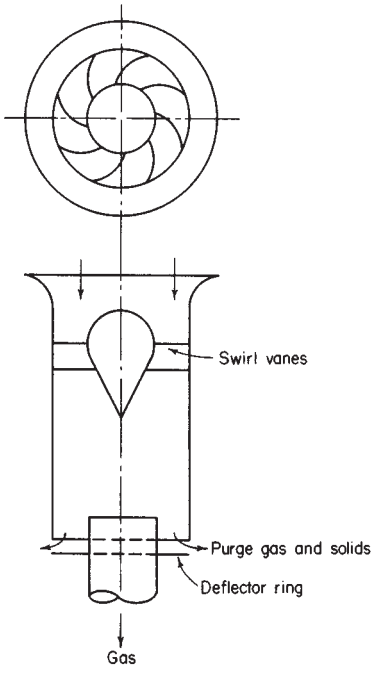

FIG. 17-44 Uniflow cyclone. [*Ter Linden,* Inst. Mech. Eng. J., ***160,*** *233 (1949).*]

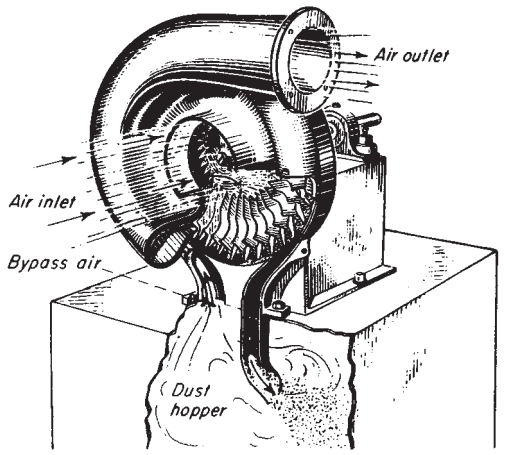

FIG. 17-45 Typical mechanical centrifugal separator. Type D Rotoclone (cutaway view). (*American Air Filter Co., Inc.*)

In particulate scrubbers, the liquid is dispersed into the gas as a spray, and the liquid droplets are the principal collectors for the dust particles. Depending on their design and operating conditions, particulate scrubbers can be adapted to collecting fine as well as coarse particles. Collection of particles by the drops follows the same principles illustrated in Fig. 17-35. Various investigations of the relative contributions of the various mechanisms have led to the conclusion that the predominant mechanism is inertial deposition. Flow-line interception is only a minor mechanism in the collection of the finer dust particles by liquid droplets of the sizes encountered in scrubbers. Diffusion is indicated to be a relatively minor mechanism for the particles larger than 0.1 μm that are of principal concern. Thermal deposition is negligible. Gravitational settling is ineffective because of the high gas velocities and short residence times used in scrubbers. Electrostatic deposition is unlikely to be important except in cases in which the dust particles or the water, or both, are being deliberately charged from an external power source to enhance collection. Deposition produced by Stefan flow can be significant when water vapor is condensing in a scrubber.

Despite numerous claims or speculations that wetting of dust particles by the scrubbing liquid plays a major role in the collection process, there is no unequivocal evidence that this is the case. The issue is whether wetting is an important factor in the adherence of a particle to a collecting droplet upon impact. From the body of general experience, it can be inferred that wettable particles probably are not collected much, if any, more readily than nonwettable particles of the same size. However, the available experimental techniques have not been adequate to permit any direct test to resolve the question. Changing from a wettable to a nonwettable test aerosol or from one scrubbing liquid to another is virtually certain to introduce other (and possibly unknown) factors into the scrubbing process. The most informative experimental studies appear to be some by Weber [*Staub,* English trans., **28,** 37 (November 1968); **29,** 12 (July 1969)], who bombarded single drops of various liquids with dust particles at different velocities and studied the behavior at impact by means of high-speed photography. Dust particles hitting the drops were invariably retained by the latter, regardless of their wettability by the liquid used.

The use of wetting agents in scrubbing water is equally controversial, and there has been no clear demonstration that it is beneficial.

A particulate scrubber may be considered as consisting of two parts: (1) a contactor stage, in which a spray is generated and the dust-laden gas stream is brought into contact with it; and (2) an entrainment separation stage, in which the spray and deposited dust particles are separated from the cleaned gas. These two stages may be separate or physically combined. The contactor stage may be of any form intended to bring about effective contacting of the gas and spray. The spray may be generated by the flow of the gas itself in contact with the liquid, by spray nozzles (pressure-atomizing or pneumatic-atomizing), by a motor-driven mechanical spray generator, or by a motor-driven rotor through which both gas and liquid pass.

Entrainment separation is accomplished with inertial separators, which are usually cyclones or impingement separators of various forms. If properly designed, these devices can remove virtually all droplets of the sizes produced in scrubbers. However, reentrainment of liquid can take place in poorly designed or overloaded separators.

Scrubber Types and Performance The diversity of particulate scrubber designs is so great as to defy any detailed and self-consistent system of classification based on configuration or principle of operation. However, it is convenient to characterize scrubbers loosely according to prominent constructional features, even though the modes of operation of different devices in a group may vary widely.

A relationship of power consumption to collection efficiency is characteristic of all particulate scrubbers. Attaining increased efficiency requires increased power consumption, and the power consumption required to attain a given efficiency increases as the particle size of the dust decreases. Experience generally indicates that the power consumption required to provide a specific efficiency on a given dust does not vary widely even with markedly different devices. The extent to which this generalization holds true has not been fully explored, but the known extent is sufficient to suggest that the underlying collection mechanism may be essentially the same in all types of particulate scrubbers.

Since some relationship of power consumption to performance appears to be a universal characteristic of particulate scrubbers, it is useful to characterize such devices broadly according to the source from which the energy is supplied to the gas-liquid contacting process. The energy may be drawn from (1) the gas stream itself, (2) the liquid stream, or (3) a motor driving a rotor. For convenience, devices in these classes may be termed respectively (1) gas-atomized spray scrubbers, (2) spray, or preformed-spray, scrubbers, and (3) mechanical scrubbers. In the spray scrubbers, all the energy may be supplied from the liquid, using a pressure nozzle, but some or all may be provided by compressed air or steam in a two-fluid nozzle or by a motor driving a spray generator.

Particulate scrubbers may also be classed broadly into low-energy and high-energy scrubbers. The distinction between the two classes is arbitrary, since the devices are not basically different and the same device may fall into either class depending on the amount of power it consumes. However, some differences in configuration are sometimes necessary to adapt a device for high-energy service. No specific level of power consumption is commonly agreed upon as the boundary between the two classes, but high-energy scrubbers may be regarded as those using sufficient power to give substantial efficiencies on submicrometer particles.

Scrubber Performance Models A number of investigators have made theoretical studies of the performance of venturi scrubbers and have sought to produce performance models, based on first principles, that can be used to design a unit for a given duty without recourse to experimental data other than the particle size and size distribution of the dust. Among these workers are Calvert [*Am. Inst. Chem. Eng. J.*, **16,** 392 (1970); *J. Air Pollut. Control Assoc.*, **24,** 929 (1974)], Boll [*Ind. Eng. Chem. Fundam.*, **12,** 40 (1973)], Goel and Hollands [*Atmos. Environ.*, **11,** 837 (1977)], and Yung et al. [*Environ. Sci. Technol.*, **12,** 456 (1978)]. Comparatively few efforts have been made to model the performance of scrubbers of types other than the venturi, but a number of such models are summarized by Yung and Calvert (U.S. EPA-600/8-78-005b, 1978).

The various venturi-scrubber models embody a variety of assumptions and approximations. The solutions of the equations for particulate collection must in general be determined numerically, although Calvert et al. [*J. Air Pollut. Control Assoc.*, **22,** 529 (1972)] obtained an explicit equation by making some simplifying assumptions and incorporating an empirical constant that must be evaluated experimentally; the constant may absorb some of the deficiencies in the model. Although other models avoid direct incorporation of empirical constants, use of empirical relationships is necessary to obtain specific estimates of scrubber collection efficiency. One of the areas of greatest uncertainty is the estimation of droplet size.

Most of the investigators have assumed the effective drop size of the spray to be the Sauter (surface-mean) diameter and have used the empirical equation of Nukiyama and Tanasawa [*Trans. Soc. Mech. Eng., Japan,* **5,** 63 (1939)] to estimate the Sauter diameter:

$$D_o = \frac{1920\sqrt{\sigma_L}}{V_o\sqrt{\rho_L/62.3}} + 75.4\left(\frac{\mu_L}{\sqrt{\sigma_L\rho_L/62.3}}\right)^{0.45}\left(\frac{1000Q_L}{Q_G}\right)^{1.5} \quad (17\text{-}3)$$

where D_o = drop diameter, μm; V_o = gas velocity, ft/s; σ_L = liquid surface tension, dyn/cm; ρ_L = liquid density, lb/ft^3; μ_L = liquid viscosity, cP; Q_L = liquid flow rate, ft^3/s; and Q_G = gas flow rate, ft^3/s.

The Nukiyama-Tanasawa equation, which is not dimensionally homogeneous, was derived from experiments with small, internal-mix pneumatic atomizing nozzles with concentric feed of air and liquid (Lapple et al., "Atomization: A Survey and Critique of the Literature," Stanford Res. Inst. Tech. Rep. No. 6, AD 821-314, 1967; Lapple, "Atomization," in *McGraw-Hill Encyclopedia of Science and Technology,* 5th ed., vol. 1, McGraw-Hill, New York, 1982, p. 858). The effect of nozzle size on the drop size is undefined. Even within the range of parameters for which the relationship was derived, the drop sizes reported by various investigators have varied by twofold to threefold from those predicted by the equation (Boll, op. cit.). The Nukiyama-Tanasawa equation has, nevertheless, been applied to large venturi and orifice scrubbers with configurations radically different from those of the atomizing nozzles for which the equation was originally developed.

Primarily because of the lack of adequate experimental techniques (particularly, the production of appropriate monodisperse aerosols), there has been no comprehensive experimental test of any of the venturi-scrubber models over wide ranges of design and operating variables. The models for other types of scrubbers appear to be essentially untested.

Contacting Power Correlation A scrubber design method that has achieved wide acceptance and use is based on correlation of the collection efficiency with the power dissipated in the gas-liquid contacting process, which is termed "contacting power." The method originated from an investigation by Lapple and Kamack [*Chem. Eng. Prog.*, **51,** 110 (1955)] and has been extended and refined in a series of papers by Semrau and coworkers [*Ind. Eng. Chem.*, **50,** 1615 (1958); *J. Air Pollut. Control Assoc.*, **10,** 200 (1960); **13,** 587 (1963); U.S. EPA-650/2-74-108, 1974; U.S. EPA-600/2-77-234, 1977; *Chem. Eng.*, **84**(20), 87 (1977); and "Performance of Particulate Scrubbers as Influenced by Gas-Liquid Contactor Design and by Dust Flocculation," EPA-600/9-82-005c, 1982, p. 43]. Other workers have made extensive independent studies of the correlation method [Walker and Hall, *J. Air Pollut. Control Assoc.*, **18,** 319 (1968)], and numerous studies of narrower scope have been made. The major conclusion from these studies is that the collection efficiency of a scrubber on a given dust is essentially dependent only on the contacting power and is affected to only a minor degree by the size or geometry of the scrubber or by the way in which the contacting power is applied. This contacting-power rule is strictly empirical, and the full extent of its validity has still not been explored. It has been best verified for the class of gas-atomized spray scrubbers, in which the contacting power is derived from the gas stream and takes the form of gas pressure drop. Tests of the equivalence of contacting power supplied from the liquid stream in pressure spray nozzles have been far less extensive and are strongly indicative but not yet conclusive. Evidence for the equivalence of contacting power from mechanically driven devices is also indicative but extremely limited in quantity.

Contacting power is defined as the power per unit of volumetric gas flow rate that is dissipated in gas-liquid contacting and is ultimately converted to heat. In the simplest case, in which all the energy is

obtained from the gas stream in the form of pressure drop, the contacting power is equivalent to the friction loss across the wetted equipment, which is termed "effective friction loss," F_E. The pressure drop may reflect kinetic-energy changes rather than energy dissipation, and pressure drops that result solely from kinetic-energy changes in the gas stream do not correlate with performance. Likewise, any friction losses taking place across equipment that is operating dry do not contribute to gas-liquid contacting and do not correlate with performance. The gross power input to a scrubber includes losses in motors, drive shafts, fans, and pumps that obviously should be unrelated to scrubber performance.

The effective friction loss, or "gas-phase contacting power," is easily determined by direct measurements. However, the "liquid-phase contacting power," supplied from the stream of scrubbing liquid, and the "mechanical contacting power," supplied by a mechanically driven rotor, are not directly measurable; the theoretical power inputs can be estimated, but the portions of these quantities effectively converted to contacting power can only be inferred from comparison with gas-phase contacting power. Such data as are available indicate that the contributions of contacting power from different sources are directly additive in their relation to scrubber performance.

Contacting power is variously expressed in units of MJ/1000 m^3 (SI), kWh/1000 m^3 (meter-kilogram-second system), and hp/(1000 ft^3/min) (U.S. customary). Relationships for conversion to SI units are

$$1.0 \text{ kWh}/1000 \text{ m}^3 = 3.60 \text{ MJ}/1000 \text{ m}^3$$

$$1.0 \text{ hp}/(1000 \text{ ft}^3/\text{min}) = 1.58 \text{ MJ}/1000 \text{ m}^3$$

The gas-phase contacting power P_G may be calculated from the effective friction loss by the following relationships:

SI units:

$$P_G = 1.0F_E \tag{17-4}$$

where F_E = kPa.

U.S. customary units:

$$P_G = 0.1575F_E \tag{17-5}$$

where F_E = in of water.

The power input from a liquid stream injected with a hydraulic spray nozzle may usually be taken as approximately equal to the product of the nozzle feed pressure p_F and the volumetric liquid rate. The liquid-phase contacting power P_L may then be calculated from the following formulas:

SI units:

$$P_L = 1.0p_F(Q_L/Q_G) \tag{17-6}$$

where p_F = kPa gauge, and Q_L and Q_G = m^3/s.

U.S. customary units:

$$P_L = 0.583p_F(Q_L/Q_G) \tag{17-7}$$

where p_G = lbf/in^2 gauge, Q_L = gal/min, and Q_G = ft^3/min.

The correlation of efficiency data is based on the total contacting power P_T, which is the sum of P_G, P_L, and any power P_M that may be supplied mechanically by a power-driven rotor.

In general, the liquid-to-gas ratio does not have an influence independent of contacting power on the collection efficiency of scrubbers of the venturi type. This is true at least of operation with liquid-to-gas ratios above some critical lower value. However, several investigations [Semrau and Lunn, "Performance of Particulate Scrubbers as Influenced by Gas-Liquid Contactor Design and by Dust Flocculation," EPA-600/9-82-005c, 1982, p. 43; and Muir et al., *Filtr. Sep.*, **15,** 332 (1978)] have shown that at low liquid-to-gas ratios relatively poor efficiencies may be obtained at a given contacting power. Such regions of operation are obviously to be avoided.

It has sometimes been asserted that multiple gas-liquid contactors in series will give higher efficiencies at a given contacting power than will a single contacting stage. However, there is little experimental evidence to support this contention. Lapple and Kamack (op. cit.) obtained slightly higher efficiencies with a venturi and an orifice in series than they did with a venturi alone. Muir and Mihisei [*Atmos. Environ.*, **13,** 1187 (1979)] obtained somewhat higher efficiencies on two redispersed dusts when using two venturis in series rather than one. The improvement obtained with two-stage scrubbing was greatest with the coarser of the two dusts and was relatively small with the finer dust. Flocculation or deflocculation of the dusts may have been responsible for some of the behavior encountered. Semrau et al. (EPA-600/2-77-234, 1977) compared the performance of a four-stage multiple-orifice contactor with that of a single-orifice contactor, using well-dispersed aerosols generated from ammonium fluorescein, The multiple-orifice contactor gave about the same efficiency as the single-orifice in the upper range of contacting power but lower efficiencies in the lower range. The deviations in performance in this case were probably characteristic of the particular multiple-orifice contactor rather than of multistage contacting as such.

Most scrubbers actually incorporate more than one stage of gas-liquid contacting even though these may not be identical (e.g., the contactor and the entrainment separator). The preponderance of evidence indicates that multiple-stage contacting is not inherently either more or less efficient than single-stage contacting. However, two-stage contacting may have practical benefits in dealing with abrasive or flocculated dusts.

Some investigators have proposed, mostly on the basis of mathematical modeling, to optimize the design of scrubbers to obtain a given efficiency with a minimum power consumption (e.g., Goel and Hollands, op. cit.). In fact, no optimum in performance appears to exist; apart from some avoidable regions of unfavorable operation, increased contacting power yields increased efficiency.

Scrubber Performance Curves The scrubber performance curve, which shows the relationship of scrubber efficiency to the contacting power, has been found to take the form

$$N_t = \alpha P_T^{\gamma} \tag{17-8}$$

where α and γ are empirical constants that depend primarily on the aerosol (dust or mist) collected. In a log-log plot of N_t versus P_T, γ is the slope of the performance curve and α is the intercept at $P_T = 1$. Figure 17-46 shows such a performance curve for the collection of coal fly ash by a pilot-plant venturi scrubber (Raben "Use of Scrubbers for Control of Emissions from Power Boilers," United States–U.S.S.R. Symposium on Control of Fine-Particulate Emissions from Industrial Sources, San Francisco, 1974). The scatter in the data reflects not merely experimental errors but actual variations in the particle-size characteristics of the dust. Because the characteristics of an industrial dust vary with time, the scrubber performance curve necessarily must represent an average material, and the scatter in the data is frequently greater than is shown in Fig. 17-46. For best definition, the curve should cover as wide a range of contacting power as possible. Obtaining the data thus requires pilot-plant equipment with the flexibility to operate over a wide range of conditions. Because scrubber performance is not greatly affected by the size of the unit, it is feasible to conduct the tests with a unit handling no more than 170 m^3/h (100 ft^3/min) of gas.

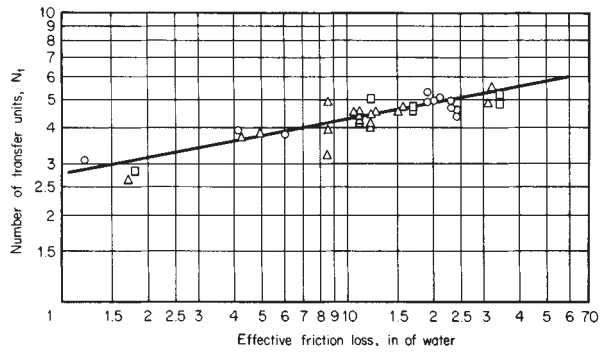

FIG. 17-46 Performance of pilot-plant venturi scrubber on fly ash. Liquid-to-gas ratio, gal/1000 ft^3: ○, 10; △, 15; □, 20. (*Raben, United States–U.S.S.R. Symposium on Fine-Particulate Emissions from Industrial Sources, San Francisco, 1974.*)

A clear interpretation of γ, the slope of the curve, is still lacking. Presumably, it should be related to the particle-size distribution of the dust. Because scrubbing preferentially removes the coarser particles, the fraction of the dust removed (or the increment of N_t) per unit of contacting power should decrease as the contacting power and efficiency increase, so that the value of γ should be less than unity. In fact, the value of γ has been less than unity for most dusts. Nevertheless, some data in the literature have displayed values of γ greater than unity when plotted on the transfer-unit basis, indicating that the residual fraction of dust became more readily collectible as contacting power and efficiency increased. More recent studies by Semrau et al. (EPA-650/2-74-108 and EPA-600/2-77-237) have revealed performance curves having two branches (typified by Fig. 17-47), the lower having a slope greater than unity and the upper a slope less than unity. This suggests that had the earlier tests been extended into higher contacting-power ranges, performance curves with flatter slopes might have appeared in those ranges.

Among the aerosols that gave performance curves with $\gamma > 1$, the only obvious common characteristic was that a large fraction of each was composed of submicrometer particles.

Cut-Power Correlation Another design method, also based on scrubber power consumption, is the cut-power method of Calvert [*J. Air Pollut. Control Assoc.*, **24,** 929 (1974); *Chem. Eng.*, **84**(18), 54 (1977)]. In this approach, the cut diameter (the particle diameter for which the collection efficiency is 50 percent) is given as a function of the gas pressure drop or of the power input per unit of volumetric gas flow rate. The functional relationship is presented as a log-log plot of the cut diameter versus the pressure drop (or power input). In principle, the function could be constructed by experimentally determining scrubber performance curves for discrete particle sizes and then plotting the particle sizes against the corresponding pressure drops necessary to give efficiencies of 50 percent. In practice, Calvert and coworkers evidently have in most cases constructed the cut-power functions for various scrubbers by modeling (Yung and Calvert, U.S. EPA-600/8-78-005b, 1978). They show a variety of curves, whereas empirical studies have indicated that different types of scrubbers generally have about the same performance at a given level of power consumption.

Condensation Scrubbing The collection efficiency of scrubbing can be increased by the simultaneous condensation of water vapor from the gas stream. Water-vapor condensation assists in particle removal by two entirely different mechanisms. One is the deposition of particles on cold-water droplets or other surfaces as the result of Stefan flow. The other is the condensation of water vapor on particles as nuclei, which enlarges the particles and makes them more readily collected by inertial deposition on droplets. Both mechanisms can operate simultaneously. However, for the buildup of particles by condensation to be effective, there must be adequate time for the particles to grow substantially before the principal gas-liquid-contacting operation takes place. Hence, if particle buildup is to be sought, the scrubber should be preceded by an appropriate gas-conditioning section. On the other hand, particle collection by Stefan flow can be induced simply by scrubbing the hot, humid gas with sufficient cold water to bring the gas below its initial dew point. Any practical method of inducing condensation on the dust particles will incidentally afford opportunities for the operation of the Stefan-flow mechanism. The hot gas stream must, of course, have a high initial moisture content, since the magnitude of the effects obtained is related to the quantity of water vapor condensed.

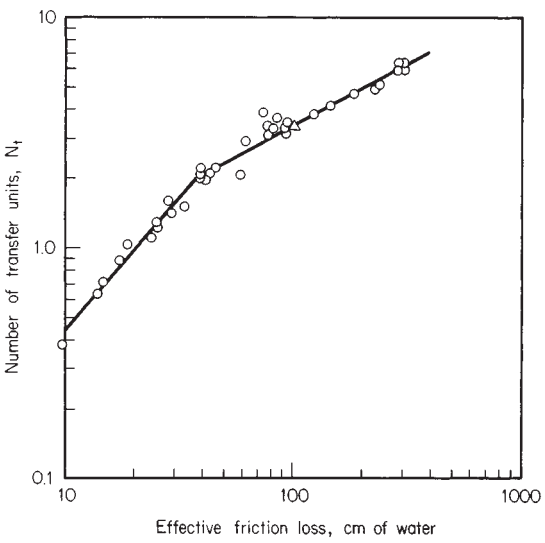

FIG. 17-47 Performance curve for orifice scrubber collecting ammonium fluorescin aerosol. (*Semrau et al., EPA 600/2-77-237, 1977.*)

Although there is a considerable body of literature on particle collection by condensation mechanisms, most of it is either theoretical or, if experimental, treats basic phenomena in simplified cases. Few studies have been made to determine what performance may be expected from condensation scrubbing under practical conditions in industrial applications. In a series of studies, Calvert and coworkers investigated several types of equipment for condensation scrubbing, generally emphasizing the use of the condensation center effect to build up the particles for collection by inertial deposition (Calvert and Parker, EPA-600/8-78-005c, 1978). From early estimates, they predicted that a condensation scrubber would require only about one-third or less of the power required by a conventional high-energy scrubber. A subsequent demonstration-plant scrubber system consisted of a direct-contact condensing tower fed with cold water followed by a venturi scrubber fed with recirculated water (Chmielewski and Calvert, EPA-600/7-81-148, 1981). The condensation and particle buildup took place in the cooling tower. In operation on humidified iron-foundry-cupola gas, this system still required about 65 percent as much power as for conventional high-energy scrubbing.

Semrau and coworkers [*Ind. Eng. Chem.*, **50,** 1615 (1958); *J. Air Pollut. Control Assoc.*, **13,** 587 (1963); EPA-650/2-74-108, 1974] investigated condensation scrubbing in pilot-plant studies in the field and, later, under laboratory conditions. Hot, humid gases were scrubbed directly with cold water under conditions that were favorable for the Stefan-flow mechanism but offered little or no opportunity for particle buildup. Some of the field studies indicated a contacting-power saving of as much as 50 percent for condensation scrubbing of Kraft-recovery-furnace fume. Laboratory tests on a predominantly submicrometer synthetic aerosol showed contacting-power savings of up to 40 percent with condensation scrubbing.

In the scrubbing of hot gases with high water content, condensation reduces contacting power and affords a direct power saving through the reduction of the gas volume by cooling and water-vapor condensation, but it incurs other costs for power and equipment for heat transfer and water cooling. However, condensation scrubbing may offer a net economic advantage if recovery of low-level heat is practical. It should also be advantageous when a hot gas must be not only cleaned but cooled and dehumidified as well; examples are the cleaning of blast-furnace gas for use as fuel and of SO_2-bearing waste gases for feed to a sulfuric acid plant.

Entrainment Separation The entrainment separator is a critical element of a scrubber, since the collection efficiency of the scrubber depends on essentially total removal of the spray from the gas stream. The sprays generated in scrubbers are generally large enough in droplet size that they can be readily removed by properly designed inertial separators. Primary collection of the spray is seldom the critical limitation on separator performance, but reentrainment is a common problem. In dust scrubbers it is essential that the entrainment separator not be of a form readily subject to blockage by solids deposits and that it be readily cleared of deposits if they should occur. Cyclone separators are advantageous in this respect and are widely used with venturi contactors. However, they cannot readily be made integral with scrubbers of some other configurations, which can be more conveniently fitted with various forms of impingement separators. Although separator design can be important, the most common

cause of reentrainment is simply the use of excessive gas velocities, and few data are available on the gas-handling capacities of separators. In the absence of good data, there is a frequent tendency to underdesign separators in an effort to reduce costs.

Venturi Scrubbers The venturi scrubber is one of the most widely used types of particulate scrubbers. The designs have become generally standardized, and units are manufactured by a large number of companies. Venturi scrubbers may be used as either high- or low-energy devices but are most commonly employed as high-energy units. The units originally studied and used were designed to the proportions of the classical venturis used for metering, but since it was discovered that these proportions have no special merits, simpler and more practical designs have been adopted. Most "venturi" contactors in current use are in fact not venturis but variable orifices of one form or another. Any of a wide range of devices can be used, including a simple pipe-line contactor. Although the venturi scrubber is not inherently more efficient at a given contacting power than other types of devices, its simplicity and flexibility favor its use. It is also useful as a gas absorber for relatively soluble gases, but because it is a cocurrent contactor, it is not well suited to absorption of gases having low solubilities.

Current designs for venturi scrubbers generally use the vertical downflow of gas through the venturi contactor and incorporate three features: (1) a "wet-approach" or "flooded-wall" entry section, to avoid dust buildup at a wet-dry junction; (2) an adjustable throat for the venturi (or orifice), to provide for adjustment of the pressure drop; and (3) a "flooded elbow" located below the venturi and ahead of the entrainment separator, to reduce wear by abrasive particles. The venturi throat is sometimes fitted with a refractory lining to resist abrasion by dust particles. The entrainment separator is commonly, but not invariably, of the cyclone type. An example of the "standard form" of venturi scrubber is shown in Fig. 17-48. The wet-approach entry section has made practical the recirculation of slurries. Various forms of adjustable throats, which may be under manual or automatic control, permit maintaining a constant pressure drop and constant efficiency under conditions of varying gas flow.

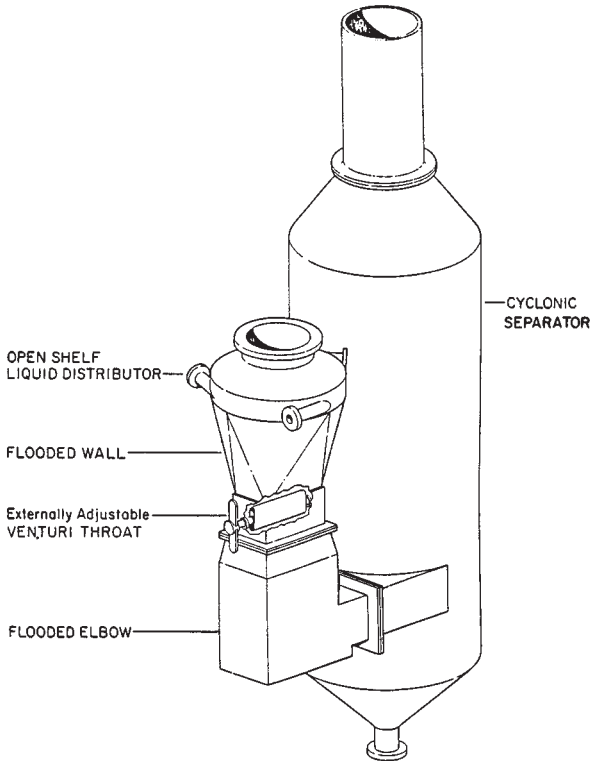

FIG. 17-48 Venturi scrubber. (*Neptune AirPol.*)

Self-Induced Spray Scrubbers Self-induced spray scrubbers form a category of gas-atomized spray scrubbers in which a tube or a duct of some other shape forms the gas-liquid-contacting zone. The gas stream flowing at high velocity through the contactor atomizes the liquid in essentially the same manner as in a venturi scrubber. However, the liquid is fed into the contactor and later recirculated from the entrainment separator section by gravity instead of being circulated by a pump as in venturi scrubbers. The scheme is well illustrated in Fig. 17-49*a*. A great many such devices using contactor ducts of various shapes, as in Fig. 17-49*b* are offered commercially. Although self-induced spray scrubbers can be built as high-energy units and sometimes are, most such devices are designed for only low-energy service.

The principal advantage of self-induced spray scrubbers is the elimination of a pump for recirculation of the scrubbing liquid. However, the designs for high-energy service are somewhat more complex and less flexible than those for venturi scrubbers.

Plate Towers Plate (tray) towers are countercurrent gas-atomized spray scrubbers using one or more plates for gas-liquid contacting. They are essentially the same as, if not identical to, the devices used for gas absorption and are frequently employed in applications in which gases are to be absorbed simultaneously with the removal of dust. Except possibly in cases in which condensation effects are involved, countercurrent operation is not significantly beneficial in dust collection.

The plates may be any of several types, including sieve, bubble-cap, and valve trays. The impingement baffle plate (Fig. 17-50) is commonly used for dust collection applications. Impingement on the baffles is not the controlling mechanism of particle collection; the principal collecting bodies are the droplets produced from the liquid by the gas as it flows through the perforations and around the baffles. The slot stage (Fig. 17-50) is in effect a miniature venturi contactor. Valve trays constitute multiple self-adjusting orifices that provide nearly constant gas pressure drop over considerable ranges of variation in gas flow. The gas pressure drop that can be taken across a single plate is necessarily limited, so that units designed for high contacting power must use multiple plates.

Plate towers are more subject to plugging and fouling than venturi-type scrubbers that have large passages for gas and liquid.

Packed-Bed Scrubbers Packed-bed scrubbers of the types used for gas absorption may also be used for dust collection but are subject to plugging by deposits of insoluble solids. Random packings, such as dumped Raschig rings and Berl saddles, are most seriously affected by plugging. Regular packings, such as stacked grids, are better in dust-collection service. When both a gas and particulate matter are to be collected, it is advisable to use a primary-stage scrubber of the venturi or similar type to collect the particulate matter ahead of a packed gas absorber.

Packed-bed scrubbers may be constructed for either vertical or horizontal gas flow. Vertical-flow units (packed towers) commonly use countercurrent flow of gas and liquid, although cocurrent flow is sometimes used. Packed scrubbers using horizontal gas flow usually employ cross-flow of liquid.

Scrubber packings are too large to serve as collecting bodies for any except very large dust particles. In the collection of fine particles, the packings serve primarily to promote fluid turbulence that aids the deposition of the dust particles on droplets. In a packed tower operating below the flooding point, with most of the liquid flowing in films and little spray formation, the relative efficiency in collection of particles may possibly be lower than that of a venturi-type scrubber operating at the same contacting power. However, no data are available to resolve the question.

Mobile-Bed Scrubbers Mobile-bed scrubbers (Fig. 17-51) are constructed with one or more beds of low-density spheres that are free to move between upper and lower retaining grids. The spheres are commonly 1.0 in (2.5 cm) or more in diameter and made from rubber or a plastic such as polypropylene. The plastic spheres may be solid or hollow. Gas and liquid flows are countercurrent, and the spherical packings are fluidized by the upward-flowing gas. The movement of

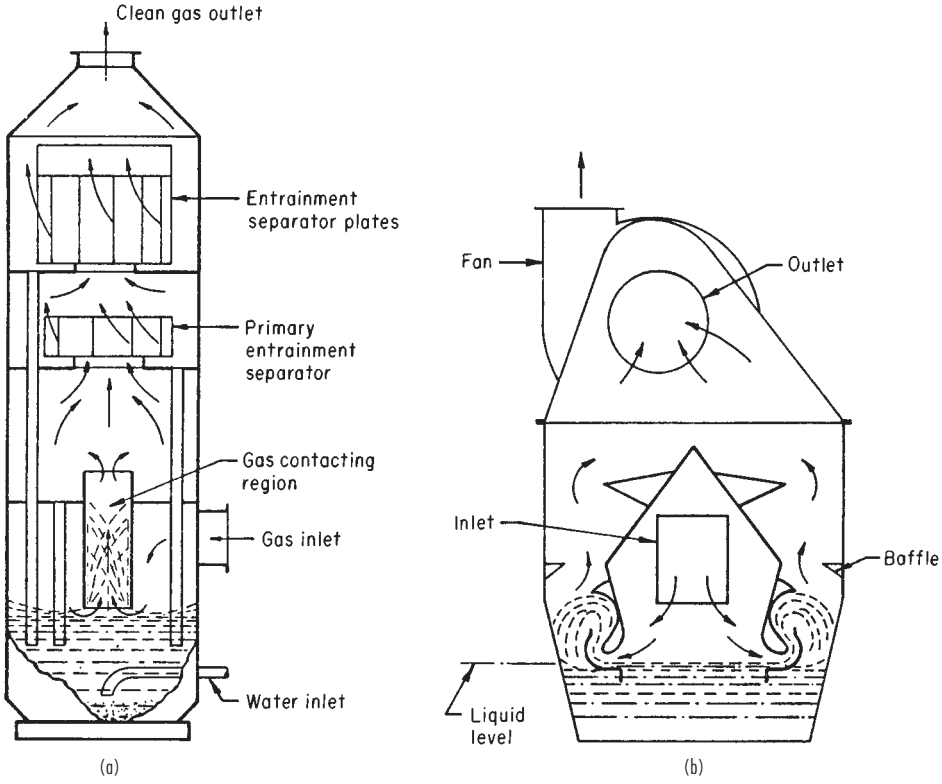

FIG. 17-49 Self-induced spray scrubbers. (*a*) Blaw-Knox Food & Chemical Equipment, Inc. (*b*) American Air Filter Co., Inc.

the packings is intended to minimize fouling and plugging of the bed. Mobile-bed scrubbers were first developed for absorbing gases from gas streams that also carry solid or semisolid particles.

The spherical packings are too large to serve as effective targets for the deposition of fine dust particles. In dust-collection service, the packings actually serve as turbulence promoters, while the dust particles are collected primarily by the liquid droplets.

The gas pressure drop through the scrubber may be increased by increasing the gas velocity, the liquid-to-gas ratio, the depth of the bed, the density of the packings, and the number of beds in series. In an experimental study, Yung et al. (EPA-600/7-79-071, 1979) determined that the collection efficiency of a mobile-bed scrubber was dependent only on the gas pressure drop and was not influenced independently by the gas velocity, the liquid-to-gas ratio, or the number of beds except as these factors affected the pressure drop. Yung et al. also reported that the mobile-bed scrubber was less efficient at a given pressure drop than scrubbers of the venturi type, but without offering comparable experimental supporting evidence.

Spray Scrubbers Spray scrubbers consist of empty chambers of some simple form in which the gas stream is contacted with liquid droplets generated by spray nozzles. A common form is a spray tower, in which the gas flows upward through a bank or successive banks of spray nozzles. Similar arrangements are sometimes used in spray chambers with horizontal gas flow. Such devices have very low gas pressure drops, and all but a small part of the contacting power is derived from the liquid stream. The required contacting power is obtained from an appropriate combination of liquid pressure and flow rate. Most spray scrubber are low-energy units. Collection of fine particles is possible but may require very high liquid-to-gas ratios, liquid feed pressures, or both. Plugging of the nozzles can be a persistent maintenance problem. Entrainment separators are necessary to prevent carry-over of spray into the exit gas.

Cyclone Scrubbers The vessels of cyclone scrubbers are all in the form of cyclones, which provide for entrainment separation. However, the gas-liquid-contacting devices may be of either the gas-atomized-spray or the preformed-spray type. The cyclone-spray scrubber shown in Fig. 17-52*a* has an axial spray tree, or manifold, equipped with hydraulic spray nozzles. Similar units are available with the spray nozzles mounted in the wall of the cyclone, discharging inward. This latter arrangement makes the nozzles more accessible for maintenance. In the cyclone scrubber shown in Fig. 17-52*b*, most of the gas-liquid contacting is accomplished in the swirl vanes, with the energy being supplied from the gas stream in the form of pressure drop. The swirl vanes serve the same function as do the trays in a tray tower. Higher contacting power can be provided by using additional sets of swirl vanes in series.

Ejector-Venturi Scrubbers In the ejector-venturi scrubber (Fig. 17-53) the cocurrent water jet from a spray nozzle serves both to scrub the gas and to provide the draft for moving the gas. No fan is required, but the equivalent power must be supplied to the pump that delivers water to the ejector nozzle. The water must be supplied in sufficient volume and at high enough pressure to provide both adequate draft and enough contacting power for the required scrubbing operation. Considered as a gas pump, the ejector is not a very efficient device, but the dissipated energy that is not effective in pumping does serve in gas-liquid contacting. The energy equivalent to any gas pressure rise across the scrubber is not part of the contacting power (Semrau et al., EPA-600/2-77-234, 1974).

The ejector-venturi scrubber is widely used as a gas absorber, but the combinations of water pressure and flow rate that are sufficient to provide the required draft usually do not also yield enough contacting power to give high collection efficiency on submicrometer particles. Other types of ejectors have been employed to provide higher contacting-power levels. In one, superheated water is discharged through

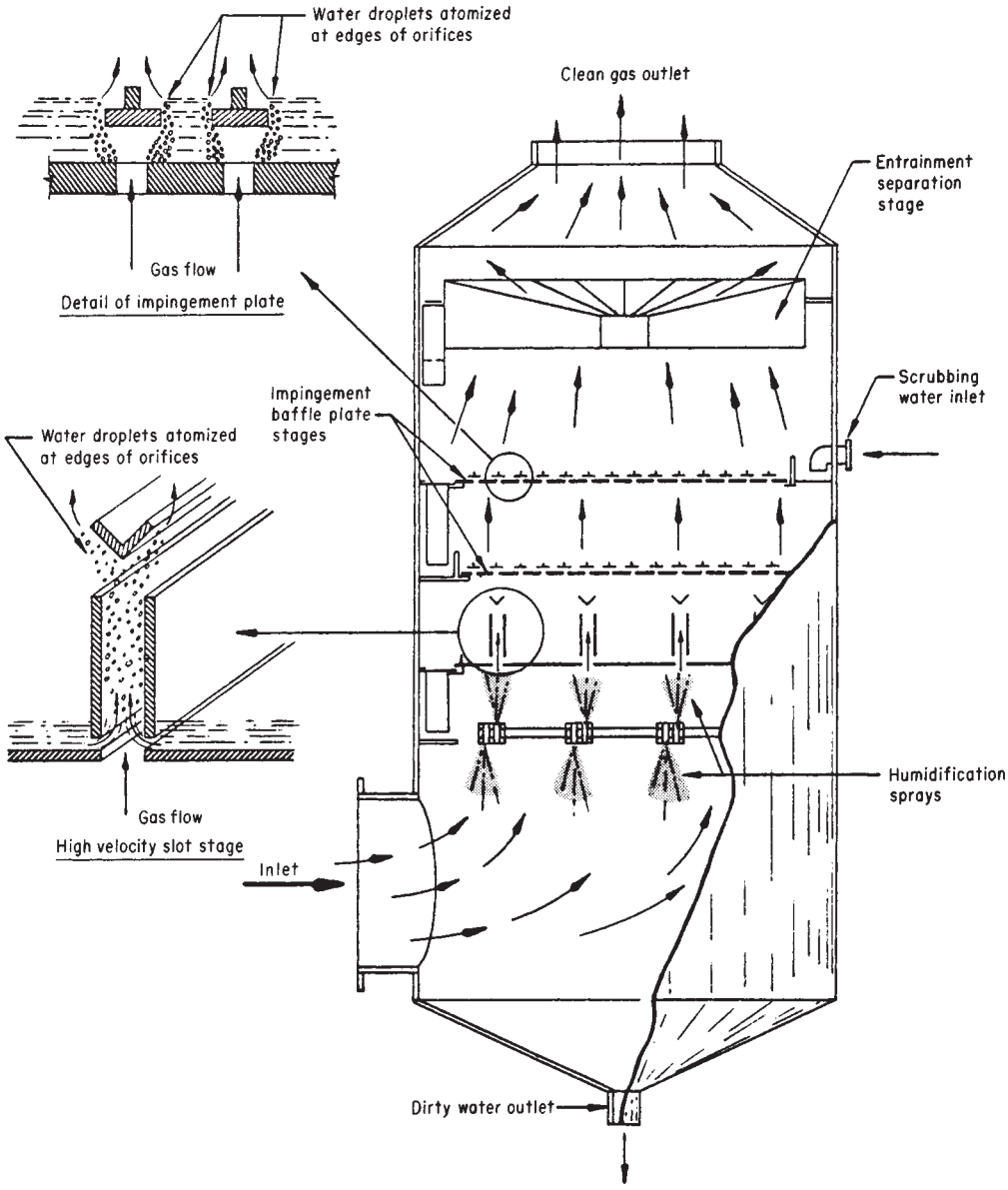

FIG. 17-50 Impingement-plate scrubber. (*Peabody Engineering Corp.*)

the nozzle, and part flashes to steam, increasing the mechanical energy available for scrubbing [Gardenier, *J. Air Pollut. Control Assoc.*, **24,** 954 (1974)]. Some units use two-fluid nozzles, with either compressed air or steam as the compressible fluid [Sparks, *J. Air Pollut. Control Assoc.*, **24,** 958 (1974)]. Most of the energy for gas movement and for atomizing the liquid and scrubbing the gas is derived from the compressed air or steam. In some ejector-venturi-scrubbers installations, part of the draft is supplied by a fan [Williams and Fuller, TAPPI, **60**(1), 108 (1977)].

Mechanical Scrubbers Mechanical scrubbers comprise those devices in which a power-driven rotor produces the fine spray and the contacting of gas and liquid. As in other types of scrubbers, it is the droplets that are the principal collecting bodies for the dust particles. The rotor acts as a turbulence producer. An entrainment separator must be used to prevent carry-over of spray. Among potential maintenance problems are unbalancing of the rotor by buildup of dust deposits and abrasion by coarse particles.

The simplest commercial devices of this type are essentially fans upon which water is sprayed. The unit shown in Fig. 17-54 is adapted to light duty, and heavy dust loads are avoided to minimize buildup on the rotor.

Fiber-Bed Scrubbers Fibrous-bed structures are sometimes used as gas-liquid contactors, with cocurrent flow of the gas and liquid streams. In such contactors, both scrubbing (particle deposition on droplets) and filtration (particle deposition on fibers) may take place. If only mists are to be collected, small fibers may be used, but if solid particles are present, the use of fiber beds is limited by the tendency of the beds to plug. For dust-collection service, the fiber bed must be composed of coarse fibers and have a high void fraction, so as to minimize the tendency to plug. The fiber bed may be made from metal or

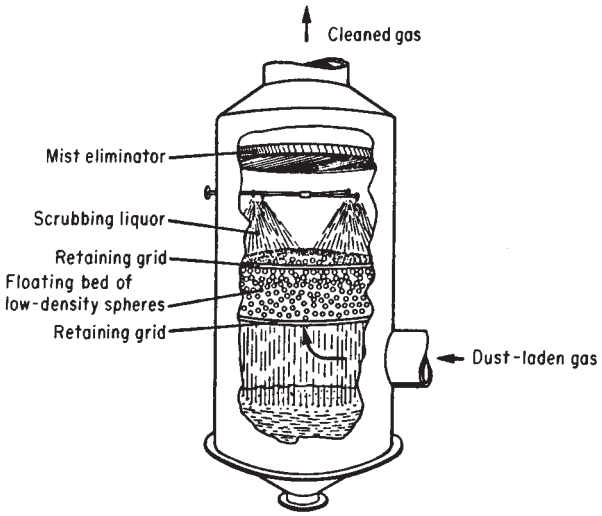

FIG. 17-51 Mobile-bed scrubber. (*Air Correction Division, UOP.*)

plastic fibers in the form of knitted structures, multiple layers of screens, or random-packed fibers. However, the bed must have sufficient dimensional stability so that it will not be compacted during operation.

Lucas and Porter (U.S. Patent 3,370,401, 1967) developed a fiber-bed scrubber in which the gas and scrubbing liquid flow vertically upward through a fiber bed (Fig. 17-55). The beds tested were composed of knitted structures made from fibers with diameters ranging from 89 to 406 μm. Lucas and Porter reported that the fiber-bed scrubber gave substantially higher efficiencies than did venturi-type scrubbers tested with the same dust at the same gas pressure drop. In similar experiments, Semrau (Semrau and Lunn, op. cit.) also found that a fiber-bed contactor made with random-packed steel-wool fibers gave higher efficiencies than an orifice contactor. However, there were indications that the fiber bed would have little advantage in the collection of submicrometer particles, presumably because of the large fiber size feasible for dust-collection service.

Despite their potential for increased collection efficiency, fiber-bed scrubbers have had only limited commercial acceptance for dust collection because of their tendency to become plugged. Their principal use has been in small units such as engine-intake-air cleaners, for which it is feasible to remove the fiber bed for cleaning at frequent intervals.

Electrically Augmented Scrubbers In some types of wet collectors, attempts are made to apply the electrostatic-deposition mechanism by charging the dust particles, the water droplets, or both. The objective is to combine in a scrubber high efficiency in collecting fine particles and the moderate power consumption characteristic of an electrical precipitator. Successful devices of this type have been essentially wet electrical precipitators and should properly be discussed in that category (see "Electrical Precipitators"). So far, there has been no clear demonstration of a device that combines the small size, compactness, and high efficiency of a high-energy scrubber with the relatively low power consumption of an electrical precipitator.

Dry Scrubbing *Dry scrubbing* is an umbrella term used to associate several different unit operations and types of hardware that can be used in combinations to accomplish the unit process of dry scrubbing. They all utilize scrubbing, in which mass transfer takes place between the gas phase and an active liquidlike surface, and they all discharge the resulting products separately as a gas and a solidlike "dry" product for reuse or disposal.

It is helpful to recognize three phases in the development of systems using dry scrubbing. The first phase used mainly good contactors and relatively expensive sorbents, which were tailored to catch targeted compounds with high efficiency (>99 percent). The second phase used mainly minimal contactors and cheap sorbents in order to get enough sulfur dioxide capture (>60 percent) to justify using cheaper higher sulfur coal. The third phase is ongoing; it uses mainly better contactors, sorbents, and fabric filters in order to get not only high SO_2 capture (>90 percent), but also substantial capture of other regulated emissions such as metals and dioxins.

The principle of dry scrubbing was first recognized by Lamb and Wilson [*I&EC*, **11**(5), 420 (1919)] and Wilson [*I&EC*, **12**(10), 1000 (1920)] at MIT during their World War I program to develop better

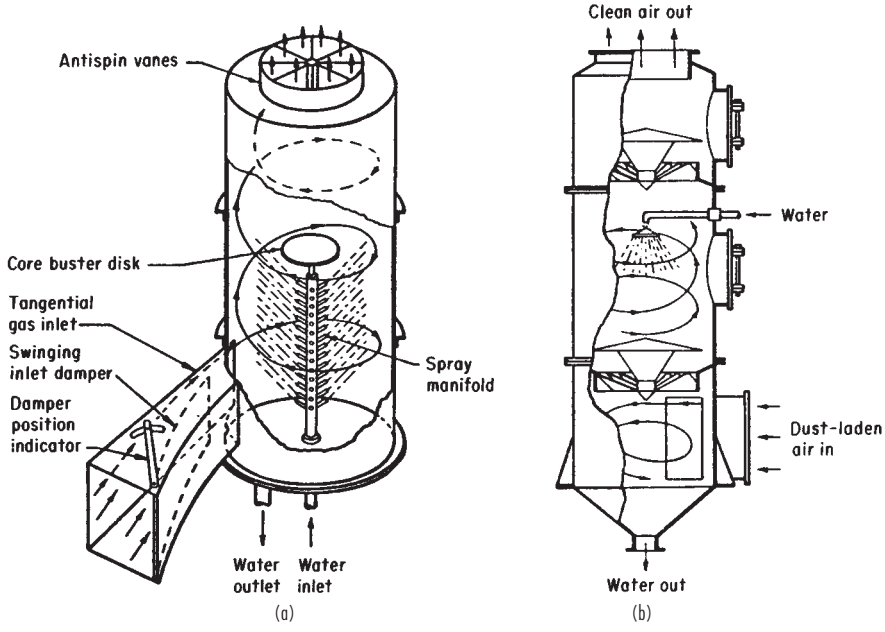

FIG. 17-52 Cyclone scrubbers. (*a*) Chemico Air Pollution Control Corp. (*b*) Ducon Co., Inc.

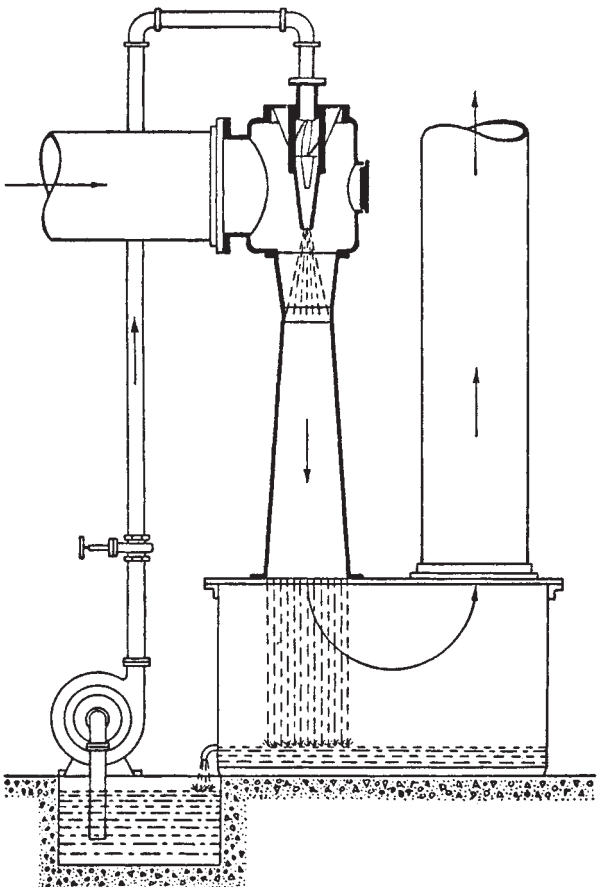

FIG. 17-53 Ejector-venturi scrubber. (*Schutte & Koerting Division, Amtek, Inc.*)

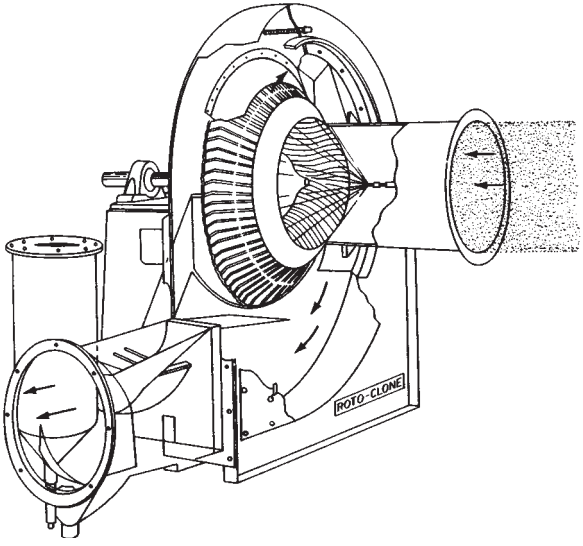

FIG. 17-54 Mechanical scrubber. (*American Air Filter Co., Inc.*)

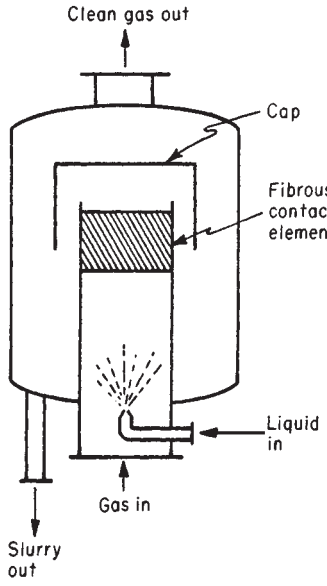

FIG. 17-55 Fibrous-bed scrubber. (*Lucas and Porter, U.S. Patent 3,370,401, 1967.*)

media for military gas masks. The preferred medium turned out to be a mixture of granular activated carbon with a new kind of porous granular hydrated lime, which they dubbed *activated soda-lime.* What activated it was a small but critical amount of sodium hydroxide, which was enough to maintain in use on French battlefields an equilibrium moisture film a few molecules thick on the surface of pores within lime particles. That film enhanced surface hydrolysis, diffusion, and neutralization of acid gases such as Cl_2 and SO_2, to the point that their removal became controlled by fast external gas-film diffusion, up to substantial utilization of the potential stoichiometric capacity. The better varieties of army activated soda-lime used in gas masks captured more than 99 percent of Cl_2 or SO_2 even after using up more than 10 percent of alkalinity. Gas-mask-canister sorbent beds typically used 8×14 mesh granules 10 cm deep, and tests were run with 1 percent acid gas at space velocities of 3000 to 7400 l/hr. Carbon dioxide was tested to higher penetrations; its capture was more than 50 percent even after using up more than 50 percent of available alkalinity.

With good dry scrubbing sorbents, the controlling resistance for gas cleaning is external turbulent diffusion, which also depends on energy dissipated by viscous and by inertial mechanisms. It turns out to be possible to correlate mass-transfer rate as a function of the friction factor.

It turns out that packed beds much less than a hundred particles thick behave as if they were well-stirred due to the entrance effect. Although it may seem odd that a packed bed can behave as if well-stirred, it typically takes at least a 100-particle bed depth in order for a plug-flow concentration wave to develop.

Integration of the Ergun equation for well stirred flow gives

$$\frac{C_2 - C_1}{C^* - C_2} = F_k \frac{\rho D_v (1 - \varepsilon_v) L}{\mu \varepsilon_v D_p} \tag{17-9}$$

Recognition of dry scrubbing as a mechanism useful in treating large gas flows first came in the 1960s as regulations were tightening on fly ash emissions from utility boilers. Dry scrubbing turns out to be the appropriate way to describe the interactions of sulfuric acid vapor with fly ash from pulverized coal combustion. On one hand, powdered sodium bicabonate was added to some flue gases in order to protect fabric filter bags from attack by sulfuric acid films on ash from high sulfur coal combustion. On the other hand, sulfur trioxide was added to other flue gases in order to generate sulfuric acid films that would improve the performance of electrostatic precipitators collecting inherently high resistivity ash from low sulfur coal. From Eq. (17-9),

it is readily apparent that the way to get more gas cleaning per unit pressure drop is to optimize the particle size and void fraction, and use relatively fewer particles operating at higher velocity. Such an arrangement runs out of stoichiometric capacity quickly, which leads naturally to transported bed contactors fed with fresh sorbent.

The actual name "dry scrubbing" was first publicized by Teller [U.S. Patent no. 3,721,066 (1973)]. He worked both with classical Army-type soda-lime and with his patented water-activated form of the alkaline feldspar nepheline syenite as a flow agent and feedstock sorbent for HF and SO_2 in hot, sticky fumes from glass melting furnaces. He claimed capture of more than 99 percent of 180 ppm HF and SO_2 for more than 20 hours in a packed bed of 200 × 325 mesh hydrated nepheline syenite at 42,000/hr.

Teller [U.S. Patent no. 3,997,652 (1976)] also patented a number of "chromatographic sorbents" using semivolatile liquid coatings similar to mobile phases used in capillary columns for gas chromatographs. For simple acid gases, Teller generally used a flash-drying-type venturi injector and pneumatic transport system to disperse fresh sorbent into hot gas to be treated and to provide time for turbulent mixing. He then typically used a baghouse to collect the loaded sorbent for inclusion with other feeds into the glass melting system.

Aluminum producers were also early users of another type of dry scrubbing for the difficult cleaning problem of acid gases in hot, sticky fumes from aluminum reduction potlines. Bazhenov et al. [*Tsvetn. Met.—Russia,* (6) 44 (1975)] described the use of a fluidized bed of feedstock aluminum oxide to clean potline offgas in an arrangement where there was an integral freeboard baghouse. Loaded sorbent was purged from the bed for feed into the aluminum reduction system. In that anhydrous system there was no water film as such inside the pores, but there was high specific surface, having liquidlike mobile active sites with a strong affinity for binding fluoride. The potential for achieving significant gas cleaning at very high space velocities led to dry scrubbing being applied both for incremental desulfurization of flue gases from coal-fired utility boilers and for removal of trace acid gases from solid waste incineration. A number of different hardware arrangements were tested all the way to full scale in order to determine accurately the various effects that must be optimized in order to achieve minimum net cost to be carried by the rate-paying public.

It was apparent from the very earliest tests that control of thin moisture films on the surface of reactive particles was the key to success. The main three competing arrangements, as compared by Statnick et al. [4th Annual Pitt. Coal Conf. (1987)] involved slurry spray dryers, where lime and water were injected together, versus systems where the gas was humidified by water injection before or after injection of limey dry powder reagents. It turns out that there are tradeoffs among the costs of hardware, reagent, and water dispersion and reagent purchase and disposal. Systems where water evaporates in the presence of active particles are usually less expensive overall.

The evaporation lifetimes of pure water droplets are described by Marshall and Seltzer [*CEP,* **46**(10), 501 and **46**(11), 575 (1950)] and by Duffie and Marshall [*CEP,* **49**(8), 417 (1953) and **49**(9), 480 (1953)]. Figure 17-56 is easy to use to estimate the necessary spray dispersion. For typical humidifier conditions of 300°F gas inlet temperature and a 20°F approach to adiabatic saturation at the outlet, a 60-micrometer droplet will require about 0.9 seconds to evaporate, while a 110-micrometer droplet will require about 3 seconds. If the time available for drying is no more than 3 seconds, it therefore follows that the largest droplets in a humidifier spray should be no larger than 100 micrometers. If the material being dried contains solids, droplet top size will need to be smaller due to slower evaporation rates. Droplets this small not only require considerable expensive power to generate, but since they have inherent penetration distances of less than a meter, they require expensive dispersion arrangements to get good mixing into large gas flows without allowing damp, sticky particles to reach walls.

The economics seem to be better for systems where dry powdered fresh lime plus ground recycled lime is injected along with a relatively coarse spray which impinges on and dries out from the reagent, as described by Stouffer et al. [*I&EC Res.,* **28**(1) 20 (1989)]. Withum et al. [9th Ann. Pitt. Coal Prep. Util. Env. Control Contractors Conf. (1993)] describes an advanced version of that system that has been further optimized to the point that it is competitive with wet limestone scrubbing for >90 percent flue gas desulfurization.

The most popular dry scrubbing systems for incinerators have involved the spray drying of lime slurries, followed by dry collection in electrostatic precipitators or fabric filters. Moller and Christiansen [Air Poll. Cont. Assoc. 84-9.5 (1984)] published data on early European technology. Moller et al. [U.S. Patent no. 4,889,698 (1989)] describe the newer extension of that technology to include both spray-dryer absorption and dry scrubbing with powdered, activated carbon injection. They claim greatly improved removal of mercury, dioxins, and NOx.

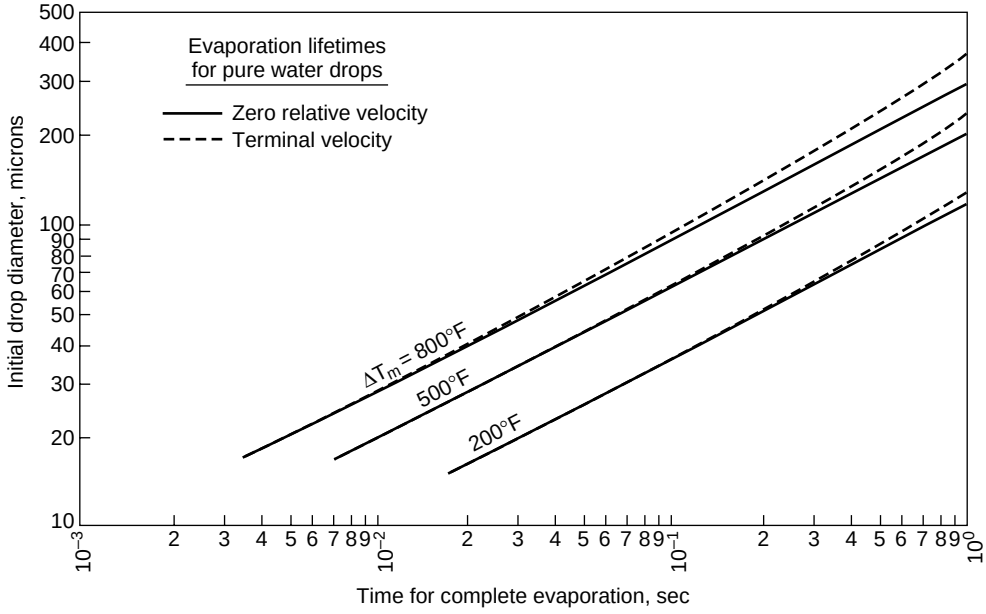

FIG. 17-56 Effect of drop diameter on time for complete evaporation of water drops.

Optimized modern dry scrubbing systems for incinerator gas cleaning are much more effective (and expensive) than their counterparts used so far for utility boiler flue gas cleaning. Brinckman and Maresca [ASME Med. Waste Symp. (1992)] describe the use of dry hydrated lime or sodium bicarbonate injection followed by membrane filtration as preferred treatment technology for control of acid gas and particulate matter emissions from modular medical waste incinerators, which have especially high dioxin emissions.

Kreindl and Brinckman [Air Waste Man. Assoc., paper 93-RP-154.04 (1993)] describe the three conventional flue-gas cleaning-process concepts (standard dry scrubbing, quasi-dry scrubbing, and wet scrubbing) as being inherently inadequate to meet the emerging European incinerator metal and organic emissions limits. Standard dry scrubbing can be upgraded by using powdered carbon along with lime, and switching to membrane filter media. Quasi-dry scrubbing can be upgraded by using powdered carbon along with lime spray drying [as also described by Moller (1989)], and switching to membrane filter media. Wet scrubbing can be upgraded by post-treatment following the wet scrubber with a circulating fluidized bed of granular activated carbon, again followed by a membrane filter.

Control of metal and organic emissions by dry scrubbing involves more than the simple acid gas neutralization discussed so far. Capture of metals other than mercury is mainly a matter of using a fabric filter having the capability of retaining unagglomerated submicron particles that are relatively enriched in toxic metals such as cadmium. Use of membrane-coated filter media is almost essential to do that well. Capture of mercury and dioxins is mainly achieved with activated carbon, which is more effective when used in combination with chlorine inhibitors. Karasek [U.S. Patent no. 4,793,270 (1988)] describes the inhibiting effects of sulfur compounds, which is why dioxins are rarely a problem in flue gases from coal-fired combustion. Naikwadi and Karasek [*Chemosphere,* **27**(1–3), 335 (1993)] describe the potent inhibiting effect of amines. That is presumably why German experience is finding that dioxins are rarely a problem in flue gases that have undergone some form of ammonia deNOx treatment, as described by Hahn [*Chemosphere,* **25**(1–2), 57 (1992)]. Hahn, like Kreindl and Brinckman, also argues that classical wet scrubbers will need to be upgraded with modern dry scrubbers and fabric filters.

Fabric Filters Fabric filters, commonly termed "bag filters" or "baghouses," are collectors in which dust is removed from the gas stream by passing the dust-laden gas through a fabric of some type (e.g., woven cloth, felt, or porous membrane). These devices are "surface" filters in that dust collects in a layer on the surface of the filter medium, and the dust layer itself becomes the effective filter medium. The pores in the medium (particularly in woven cloth) are usually many times the size of the dust particles, so that collection efficiency is low until sufficient particles have been collected to build up a "precoat" in the fabric pores (Billings and Wilder, *Handbook of Fabric Filter Technology,* vol. I, EPA No. APTD-0690, NTIS No. PB-200648, 1979). During this initial period, particle deposition takes place mainly by inertial and flow-line interception, diffusion, and gravity. Once the dust layer has been fully established, sieving is probably the dominant deposition mechanism, penetration is usually extremely low except during the fabric-cleaning cycle, and only limited additional means remain for influencing collection efficiency by filter design. Filter design is related mainly to choices of gas filtration velocities and pressure drops and of fabric-cleaning cycles.

Because of their inherently high efficiency on dusts in all particle-size ranges, fabric filters have been used for collection of fine dusts and fumes for over 100 years. The greatest limitation on filter application has been imposed by the temperature limits of available fabric materials. The upper limit for natural fibers is about 90°C (200°F). The major new developments in filter technology that have been made since 1945 have followed the development of fabrics made from glass and synthetic fibers, which has extended the temperature limits to about 230 to 260°C (450 to 500°F). The capabilities of available fibers to resist high temperatures are still among the most severe limitations on the possible applications of fabric filters.

Gas Pressure Drops The filtration, or superficial face, velocities used in fabric filters are generally in the range of 0.3 to 3 m/min (1 to 10 ft/min), depending on the types of fabric, fabric supports, and cleaning methods used. In this range, gas pressure drops conform to Darcy's law for streamline flow in porous media, in which the pressure drop is directly proportional to the flow rate. The pressure drop across the fabric and the collected dust layer may be expressed (Billings and Wilder, op. cit.) by

$$\Delta p = K_1 V_f + K_2 w V_f \tag{17-10}$$

where Δp = kPa, or in of water; V_f = superficial velocity through filter, m/min, or ft/min; w = dust loading on filter, g/m^2, or lbm/ft^2; and K_1 and K_2 are resistance coefficients for the "conditioned" fabric and the dust layer respectively. The conditioned fabric is that fabric in which a relatively consistent dust load remains deposited in depth following cycles of filtration and cleaning. K_1, expressed in units of kPa/(m/min) or in water/(ft/min), may be more than 10 times the value of the resistance coefficient for the original clean fabric. If the depth of the dust layer on the fabric is greater than about 0.2 cm (1/16 in), corresponding to a fabric dust loading on the order of 500 g/m^2 (0.1 lbm/ft^2), the pressure drop across the fabric (including the dust in the pores) is usually negligible relative to that across the dust layer.

The specific resistance coefficient for the dust layer K_2 was originally defined by Williams et al. [*Heat. Piping Air Cond.,* **12,** 259 (1940)], who proposed estimating values of the coefficient by use of the Kozeny-Carman equation [Carman, *Trans. Inst. Chem. Eng. (London),* **15,** 150 (1937)]. In practice, K_1 and K_2 are measured directly in filtration experiments. The K_1 and K_2 values can be corrected for temperature by multiplying by the ratio of the gas viscosity at the desired condition to the gas viscosity at the original experimental conditions. Values of K_2 determined for certain dusts by Williams et al. (op. cit.) are presented in Table 17-5.

Lapple (in Perry, *Chemical Engineers' Handbook,* 3d ed., McGraw-Hill, New York, 1950) presents an alternative form of Eq. (17-10) in which the gas-viscosity term is explicit instead of being incorporated into the resistance coefficients:

$$\Delta p_i = K_c \mu V_f + K_d \mu w V_f \tag{17-11}$$

where Δp_i = in water, μ = cP, V_f = ft/min, w = gr/ft^2, K_c = cloth resistance coefficient = (in water)/(cP)(ft/min), and K_d = dust-layer resistance coefficient = (in water)/(cP)(gr/ft^2)(ft/min). K_d may be expressed in the same units, using the Kozeny-Carman equation:

$$K_d = \frac{160.0(1-\varepsilon_v)}{\phi_s^2 D_p^2 \rho_s \varepsilon_v^3} \tag{17-12}$$

where D_p = μm and ρ_s = lbm/ft^3.

Data sufficient to permit reasonable predictions of K_d from Eq. (17-12) are seldom available. The range in the values of K_d that may be encountered in practice is illustrated in Fig. 17-57 in which avail-

TABLE 17-5 Specific Resistance Coefficients for Certain Dusts*

	K_2† for particle size less than						
Dust	20 mesh	140 mesh	375 mesh	90 μm	45 μm	20 μm	2 μm
Granite	1.58	2.20				19.8	
Foundry	0.62	1.58	3.78				
Gypsum			6.30			18.9	
Feldspar			6.30			27.3	
Stone	0.96			6.30			
Lampblack							47.2
Zinc oxide							15.7‡
Wood				6.30			
Resin (cold)		0.62				25.2	
Oats	1.58			9.60	11.0		
Corn	0.62		1.58	3.78	8.80		

*Data from Williams et al., *Heat. Piping Air Cond.,* **12,** 259–263 (1940).

†$K_2 = \dfrac{\Delta p_i}{V_f w}, \dfrac{\text{in water}}{(\text{ft/min})(\text{lbm/ft}^2)}$.

NOTE: These data were obtained when filtering air at ambient conditions. For gases other than atmospheric air, the Δp_i values predicted from Table 17-5 should be multiplied by the actual gas viscosity divided by the viscosity of atmospheric air.

‡Flocculated material not dispersed; size actually larger.

able experimental determinations of K_d reported in the literature for a variety of dusts are plotted against particle size. In most cases no accurate particle-size data were reported, and the curves represent the estimated range of particle size involved. The data of Williams et al. (op. cit.) are related to a wide variety of dusts, and only the approximate limits enclosing these data are shown. Also included are curves predicted from Eq. (17-12) for specific values of ϕ_s, ρ_s, and ε_v. It is apparent from these curves that smaller particles tend toward higher values of ε_v, which is consistent with the observation that fine dusts (particularly those smaller than 10 μm) have lower bulk densities than coarser fractions, apparently because of the effects of surface forces. For coarse dusts, K_d varies approximately inversely as the square of the particle diameter, which implies that the void fraction (or bulk density) does not change with particle size. However, for particles finer than 10 μm, the value of K_d appears to become constant, increased voids compensating for the reduction in size. In addition to the increased voidages encountered with small particles, slip flow also contributes to the relative constancy of the experimental values of K_d for particle sizes under 5 μm.

Because of the assumptions underlying its derivation, the Kozeny-Carman equation is not valid at void fractions greater than 0.7 to 0.8 (Billings and Wilder, op. cit.). In addition, in situ measurement of the void fraction of a dust layer on a filter fabric is extremely difficult and has seldom even been attempted. The structure of the layer is dependent on the character of the fabric surface as well as on the characteristics of the dust, whereas the application of Eq. (17-12) implicitly assumes that K_2 is dependent only on the properties of the dust. A smooth fabric surface permits the dust to become closely packed, leading to a relatively high value of K_2. If the surface is napped or has numerous extended fibrils, the dust cake formed will be more porous and have a lower value of K_2 [Billings and Wilder, op. cit.; Snyder and Pring, *Ind. Eng. Chem.*, **47,** 960 (1955); and K. T. Semrau, unpublished data, SRI International, Menlo Park, Calif., 1952–1953].

Equation (17-10) indicates that for filtration at a given velocity the pressure drop is a linear function of the fabric dust loading w. In some cases, particularly with smooth-surfaced fabrics, this is at least approximately the case, but in other instances the function displays an upward curvature with increases in w, indicating compression of the dust layer, the fabric, or both, and a consequent increase in K_2 (Snyder and Pring, op. cit.; Semrau, op. cit.). Several investigations have shown K_2 to be increased by increases in the filtration velocity [Billings and Wilder, op. cit.; Spaite and Walsh, *Am. Ind. Hyg. Assoc. J.*, **24,** 357 (1968)]. However, the various investigators do not agree on the magnitude of the velocity effects. Billings and Wilder suggest assuming as an approximation that K_2 is directly proportional to the filtration velocity, but the actual relationship is probably dependent on the nature of the fabric and fabric surface, the characteristics of the dust, the dust loading on the fabric, and the pressure drop.

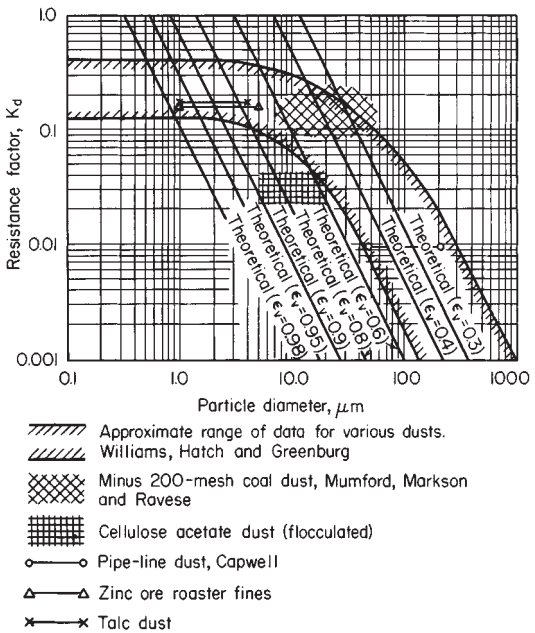

FIG. 17-57 Resistance factors for dust layers. Theoretical curves given are based on Eq. (20-78) for a shape factor of 0.5 and a true particle specific gravity of 2.0. [*Williams, Hatch, and Greenburg,* Heat. Piping Air. Cond., ***12,*** *259 (1940); Mumford, Markson, and Ravese,* Trans. Am. Soc. Mech. Eng., ***62,*** *271 (1940); Capwell, Gas,* ***15,*** *31 (August 1939)*].

Clearly, the factors determining K_2 are far more complex than is indicated by a simple application of the Kozeny-Carman equation, and when possible, filter design should be based on experimental determinations made under conditions approximating those expected in the planned installation.

Types of Filters Current fabric-filter designs fall into three types, depending on the method of cleaning used: (1) shaker-cleaned, (2) reverse-flow-cleaned, and (3) reverse-pulse-cleaned. The shaker-cleaned filter is the earliest form of bag filter (Fig. 17-58). The open lower ends of the bags are fastened over openings in the tube sheet that separates the lower dirty-gas inlet chamber from the upper clean-gas chamber. The bag supports from which the bags are suspended are connected to a shaking mechanism. The dirty gas flows upward into the filter bags, and the dust collects on the inside surfaces of the bags. When the gas pressure drop rises to a chosen upper limit as the result of dust accumulation, the gas flow is stopped and the shaker is operated, giving a whipping motion to the bags. The dislodged dust falls into the dust hopper located below the tube sheet. If the filter is to be operated continuously, it must be constructed with multiple compartments, so that the individual compartments can be sequentially taken off line for cleaning while the other compartments continue in operation (Fig. 17-59).

Shaker-cleaned filters are available as standard commercial units, although large baghouses for heavy-duty service are commonly custom-designed and -fabricated. The oval or round bags used in the standard units are usually 12 to 20 cm (5 to 8 in) in diameter and 2.5 to 5 m (8 to 17 ft) long. The large, heavy-duty baghouses may use bags up to 30 cm (12 in) in diameter and 9 m (30 ft) long. The bags must be made of woven fabrics to withstand the flexing and stretching involved in shaking. The fabrics may be made from natural fibers (cotton or wool) or synthetic fibers. Fabrics of glass or mineral fibers are generally too fragile to be cleaned by shaking and are usually used in reverse-flow-cleaned filters.

Large units (other than custom units) are usually built up of standardized rectangular sections in parallel. Each section contains on the order of 1000 to 2000 ft^2 of cloth, and the sections are assembled in the field to form a single filter housing. In this manner, the filter can be partitioned so that one or more sections at a time can be cut out of service for shaking or general maintenance.

Ordinary shaker-cleaned filters may be shaken every ¼ to 8 h, depending on the service. A manometer connected across the filter is useful in determining when the filter should be shaken. Fully automatic filters may be shaken as frequently as every 2 min, but bag maintenance will be greatly reduced if the time between shakings can be increased to 15 or 20 min without developing excessive pressure drop. Cleaning may be actuated automatically by a differential-pressure switch. It is essential that the gas flow through the filter be stopped when shaking in order to permit the dust to fall off. With very fine dust, it may even be necessary to equalize the pressure across the cloth [Mumford, Markson, and Ravese, *Trans. Am. Soc. Mech. Eng.*, **62,** 271 (1940)]. In practice this can be accomplished without interrupting the operation by cutting one section out of service at a time, as shown in Fig. 17-59. In automatic filters this operation involves closing the dampers, shaking the filter units either pneumatically or mechanically, sometimes with the addition of a reverse flow of cleaned gas through the filter, and lastly reopening the dampers. For compressed-air-operated automatic filters, this entire operation may take only 2 to 10 s. For ordinary mechanical filters equipped for automatic control, the operation may take as long as 3 min.

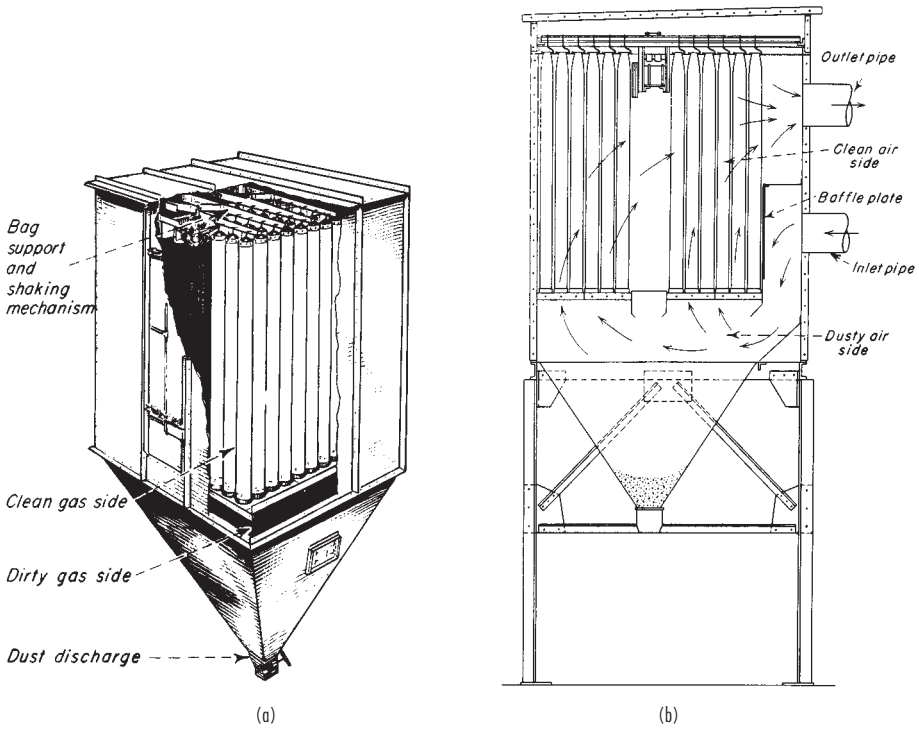

FIG. 17-58 Typical shaker-type fabric filters. (*a*) Buell Norblo (cutaway view). (*b*) Wheelabrator-Frye Inc. (sectional view).

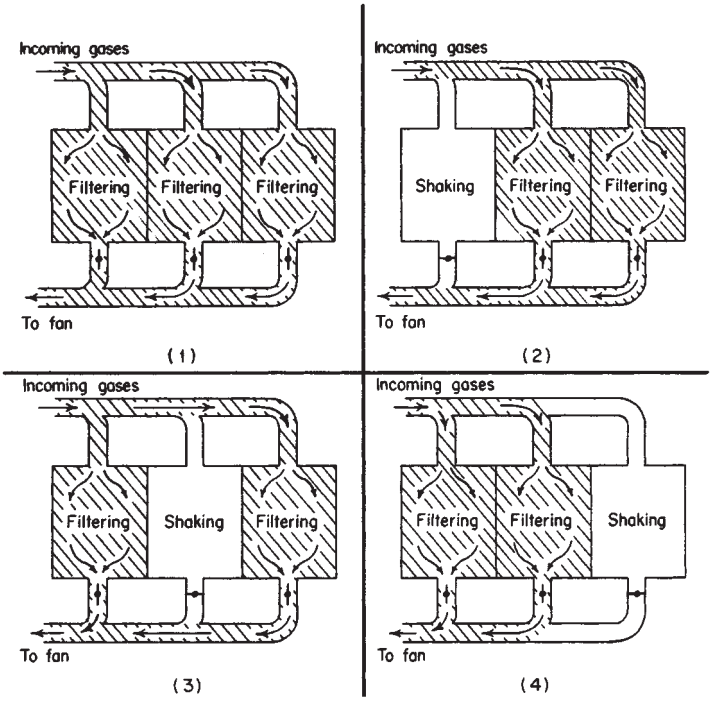

FIG. 17-59 Three-compartment bag filter at various stages in the cleaning cycle. (*Wheelabrator-Frye Inc.*)

Equation (17-11) may be rewritten as

$$\Delta p_i = K_d \mu c_d V_f^2 t_m \qquad (17\text{-}13)$$

where c_d = dust concentration in dirty gas, gr/ft^3; and t_m = filtration time, min. This shows that the pressure drop due to dust accumulation varies as the square of the gas velocity through the filter. (The actual effect of velocity on pressure drop may be even greater in some instances.) Greater cloth area and reduced filtration velocity therefore afford substantial reductions in shaking frequency and in bag wear. Consequently, it is generally economical to be conservative in specifying cloth area. Shaker-cleaned filters are generally operated at filtration velocities of 0.3 to 2.5 m/min (1 to 8 ft/min) and at pressure drops of 0.5 to 1.5 kPa (2 to 6 in water). For very fine dusts or high dust concentrations, filtration velocities should not exceed 1 m/min (3 ft/min). For fine fumes and dusts in heavy-duty installations, filtration velocities of 0.3 to 0.6 m/min (1 to 2 ft/min) have long been accepted on the basis of operating experience.

Cyclone precleaners are sometimes used to reduce the dust load on the filter or to remove large hot cinders or other materials that might damage the bags. However, reducing the dust load on the filter by this means may not reduce the pressure drop, since the increase in K_2 produced by the reduction in average particle size may compensate for the decrease in the fabric dust loading.

In filter operation, it is essential that the gas be kept above its dew point to avoid water-vapor condensation on the bags and resulting plugging of the bag pores. However, fabric filters have been used successfully in steam atmospheres, such as those encountered in vacuum dryers. In such cases, the housing is generally steam-traced.

Reverse-flow-cleaned filters are generally similar to the shaker-cleaned filters except for the elimination of the shaker. After the flow of dirty gas has stopped, a fan is used to force clean gas through the bags from the clean-gas side. This flow of gas partly collapses the bags and dislodges the collected dust, which falls to the dust hopper. Rings are usually sewn into the bags at intervals along the length to prevent complete collapse, which would obstruct the fall of the dislodged dust. The principal applications of reverse-flow cleaning are in units using fiberglass fabric bags for dust collection at temperatures above 150°C (300°F). Collapsing and reinflation of the bags can be made sufficiently gentle to avoid putting excessive stresses on the fiberglass fabrics [Perkins and Imbalzano, "Factors Affecting the Bag Life Performance in Coal-Fired Boilers," 3d APCA Specialty Conference on the User and Fabric Filtration Equipment, Niagara Falls, N.Y., 1978; and Miller, *Power,* **125**(8), 78 (1981)]. As with shaker-cleaned filters, compartments of the baghouse are taken off line sequentially for bag cleaning. The gas for reverse-flow cleaning is commonly supplied in an amount necessary to give a superficial velocity through the bags of 0.5 to 0.6 m/min (1.5 to 2.0 ft/min), which is the same range as the filtration velocities frequently used.

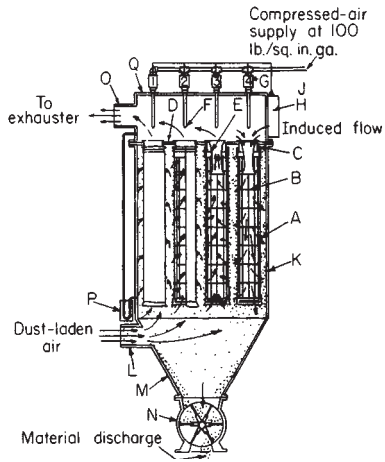

FIG. 17-60 Reverse-pulse fabric filter: (*a*) filter cylinders; (*b*) wire retainers; (*c*) collars; (*d*) tube sheet; (*e*) venturi nozzle; (*f*) nozzle or orifice; (*g*) solenoid valve; (*h*) timer; (*j*) air manifold; (*k*) collector housing; (*l*) inlet; (*m*) hopper; (*n*) air lock; (*o*) upper plenum. (*Mikropul Division, U.S. Filter Corp.*)

In the reverse-pulse filter (frequently termed a reverse-jet filter), the filter bag forms a sleeve that is drawn over a wire cage, which is usually cylindrical (Fig. 17-60). The cage supports the fabric on the clean-gas side, and the dust is collected on the outside of the bag. A venturi nozzle is located in the clean-gas outlet from the bag. For cleaning, a jet of high-velocity air is directed through the venturi nozzle and into the bag, inducing a flow of cleaned gas to enter the bag and flow through the fabric to the dirty-gas side. The high-velocity jet is released in a sudden, short pulse (typical duration 100 ms or less) from a compressed-air line by a solenoid valve. The pulse of air and clean gas expands the bag and dislodges the collected dust. Rows of bags are cleaned in a timed sequence by programmed operation of the solenoid valves. The pressure of the pulse is sufficient to dislodge the dust without cessation of the gas flow through the filter unit.

It has been a common practice to clean the bags on line (i.e., without stopping the flow of dirty gas into the filter), and reverse-pulse bag filters have been built without division into multiple compartments. However, investigations [Leith et al., *J. Air Pollut. Control Assoc.,* **27,** 636 (1977)] and experience have shown that, with online cleaning of reverse-pulse filters, a large fraction of the dust dislodged from the bag being cleaned may redeposit on neighboring bags rather than fall to the dust hopper. As a result, there is a growing trend to off-line cleaning of reverse-pulse filters. The baghouse is sectionalized so that the outlet-gas plenum serving the bags in a section can be closed off from the clean-gas exhaust, thereby stopping the flow of inlet gas through the bags. On the dirty-gas side of the tube sheet, the bags of the section are separated by partitions from the neighboring sections, where filtration is continuing. Sections of the filter are cleaned in rotation, as in shaker and reverse-flow filters.

Some manufacturers are using relatively low-pressure air (100 kPa, or 15 lbf/in^2, instead of 690 kPa, or 100 lbf/in^2) and are eliminating the venturi tubes for clean-gas induction. Others have eliminated the separate jet nozzles located at the individual bags and use a single jet to inject a pulse into the outlet-gas plenum.

Reverse-pulse filters are typically operated at higher filtration velocities (air-to-cloth ratios) than shaker or reverse-flow filters designed for the same duty. Filtration velocities may range from 1 to 4.5 m/min (3 to 15 ft/min), depending on the dust being collected, but for most dusts the commonly used range is about 1.2 to 2.5 m/min (4 to 8 ft/min). The frequency of cleaning is also dependent on the nature and concentration of the dust, with the intervals between pulses varying from about 2 to 15 min.

The cleaning action of the pulse is so effective that the dust layer may be completely removed from the surface of the fabric. Consequently, the fabric itself must serve as the principal filter medium for at least a substantial part of the filtration cycle. Woven fabrics are unsuitable for such service, and felts of various types must be used. The bulk of the dust is still removed in a surface layer, but the felt ensures that an adequate collection efficiency is maintained until the dust layer has formed.

Filter Fabrics The cost of the filter bags represents a substantial part of the erected cost of a bag filter—typically 5 to 20 percent, depending on the bag material [Reigel and Bundy, *Power,* **121**(1), 68 (1977)]. The cost of bag repair and replacement is the largest component of the cost of bag-filter maintenance. Consequently, the proper choice of filter fabric is critical to both the technical performance and the economics of operating a filter. With the advent of synthetic fibers, it has become possible to produce fabrics having a wide range of properties. However, demonstrating the acceptability of a fabric still depends on experience with prolonged operation under the actual or simulated conditions of the proposed application. The choice of a fabric material for a given service is necessarily a compromise, since no single material possesses all the properties that may be desired. Following the choice of material, the type of fabric construction is critical.

Two principal types of fabric are adaptable to filter use: woven fabrics, which are used in shaker and reverse-flow filters; and felts, which are used in reverse-pulse filters. The felts made from synthetic fibers are needle felts (i.e., felted on a needle loom) and are normally rein-

forced with a woven insert. The physical properties and air permeabilities of some typical woven and felt filter fabrics are presented in Tables 17-6 and 17-7. The "air permeability" of a filter fabric is defined as the flow rate of air in cubic feet per minute (at 70°F, 1 atm) that will pass through 1 ft^2 of clean fabric under an applied differential pressure of ½ in water. The resistance coefficient K_F of the clean fabric is defined by the equation in Table 17-6, which may be used to calculate the value of K_F from the air permeability. If Δp_i is taken as 0.5 in water, μ as 0.0181 cP (the viscosity of air at 70°F and 1 atm), and V_f as the air permeability, then $K_F = 27.8$/air permeability.

Collection Efficiency The inherent collection efficiency of fabric filters is usually so high that, for practical purposes, the precise level has not commonly been the subject of much concern. Furthermore, for collection of a given dust, the efficiency is usually fixed by the choices of filter fabric, filtration velocity, method of cleaning, and cleaning cycle, leaving few if any controllable variables by which efficiency can be further influenced. Inefficiency usually results from bags that are poorly installed, torn, or stretched from excessive dust loading and pressure drop. Of course, certain types of fabrics may simply be unsuited for filtration of a particular dust, but usually this will soon become obvious.

Few basic studies of the efficiency of bag filters have been made. Increased dust penetration immediately following cleaning has been readily observed while the dust layer is being reestablished. However,

TABLE 17-6 Resistance Factors and Air Permeabilities for Typical Woven Fabrics

Cloth	Pore size,* in	Threads/in	Weight, oz/yd^2	Thread* diameter, in	K_F†	Air permeability, (ft^3/min)/ft^2 at Δp_i = ½ in H_2O
Osnaburg cotton	0.01	32 × 28		0.02	0.51	55
Osnaburg cotton (soiled)‡		32 × 28			4.80	5.8
Drill cotton	0.01	68 × 40	5.28	0.01	0.093	300
Cotton§		46 × 56			1.39	20
Cotton§		104 × 68			1.54	18
Cotton sateen (unnapped)	0.007	96 × 56	6.88	0.009	0.27	103
Cotton sateen (unnapped)	0.005	96 × 64	8.23	0.01	0.88	32
Cotton sateen (unnapped)		96 × 60		0.012	1.63	17
Cotton sateen (unnapped)	0.004	96 × 56	10.2	0.011	1.12	25
Wool					0.25	111
Wool		40 × 50	11.5	0.014	0.33	84
Wool, white§		36 × 32			0.15	185
Wool, black§		28 × 30			0.25	110
Wool§		30 × 26			0.51	55
Vinyon§		37 × 37			0.12	23
Nylon tackle twill		72 × 196		0.010	0.66	42
Nylon sailcloth		130 × 130		0.007	1.66	17
Nylon§		37 × 37			1.74	16
Nylon§					3.71	7.5
Asbeston§					0.56	50
Orlon§		72 × 72			0.66	42
Orlon§		74 × 38			0.75	37
Orlon§					1.16	24
Orlon§					1.98	14
Smoothtex nickel screen		(300 mesh)			0.16	174
Glass		32 × 28		0.03	1.60	17
Dacron		60 × 40	5.8		0.84	33
Dacron		76 × 48	13.4		0.29	9.5
Teflon		76 × 70	8.7		1.39	20

*Estimates based on microscopic examination.

†Measured with atmospheric air. This value will be constant only for streamline flow, which is the case for values of $\rho V_f/\mu$ of less than approximately 100.

$$K_F = \Delta p_i/\mu V_f$$

where Δp_i = pressure drop, in water; μ = gas viscosity, cP; V_f = superficial gas velocity through cloth, ft/min; and ρ = gas density, lb/ft^3.

‡Cloth, similar to previous one, that had been in service and contained dust in pores although free of surface accumulation.

§Data from Pring, *Air Pollution*, McGraw-Hill, New York, 1952, p. 280.

TABLE 17-7 Physical Properties of Selected Felts for Reverse-Pulse Filters

Fiber	Weight, oz/yd^2	Thickness, in	Breaking strength, lbf/in width	Elongation, % to rupture	Air permeability, (ft^3/min)/ft^2 at Δp_i = ½ in water	K_F
Wool	23.1	0.135			27.1	1.03
Wool	21.2	0.129			29.8	0.93
Orlon*	10.9	0.045	65	18	20–25	1.11–1.39
Orlon*	17.9	0.088	85	18	15–20	1.39–1.85
Orlon*	24	0.125	110	60	10–20	1.39–2.78
Acrilan*	17.9	0.075	100	22	15–20	1.39–1.85
Dynel*	24	0.125	60	80	30–40	0.70–0.93
Dacron*	17.9	0.080	125	22	15–20	1.39–1.85
Dacron*	9.9	0.250	20	150	200–225	0.11–0.14
Dacron*	24	0.125	175	80	20–30	0.93–1.39
Nylon*	24	0.125	100	100	30–40	0.70–0.93
Arnel*	24	0.125	60	80	30–40	0.70–0.93
Teflon	15.6	0.053			82.5	0.34
Teflon	43.5	0.119			21.6	1.29

*These data courtesy of American Felt Co.

field and laboratory studies have indicated that during the rest of the filtration cycle the effluent-dust concentration tends to remain constant regardless of the inlet concentration [Dennis, *J. Air Pollut. Control Assoc.,* **24,** 1156 (1974)]. In addition, there has been little indication that the penetration is strongly related to dust-particle size, except possibly in the low-submicrometer range. These observations appear to be generally consistent with sieving being the principal collection mechanism.

Leith and First [*J. Air Pollut. Control Assoc.,* **27,** 534 (1977); **27,** 754 (1977)] studied the collection efficiency of reverse-pulse filters and concluded that once the dust cake has been established, "straight-through" penetration by dust particles that pass through the filter without being stopped is negligible by comparison with penetration by dust that actually deposits initially and then "seeps" through the fabric to be reentrained into the exit air stream. They also noted that "pinholes" may form in the dust cake, particularly over pores between yarns in a woven fabric, and that particles may subsequently penetrate straight through at the pinholes. The formation of pinholes, or "cake puncture," had been observed earlier by Stephan et al. [*Am. Ind. Hyg. Assoc. J.,* **21,** 1 (1960)], but without measurement of the associated loss of collection efficiency. When a supported flat filter medium with extremely fine pores (e.g., glass-fiber paper, membrane filter) was used, no cake puncture took place even with very high pressure differentials across the cake. However, puncture did occur when a cotton-sateen filter fabric was used as the cake support. The formation of pinholes with certain combinations of dusts, fabrics, and filtration conditions was also observed by Koscianowski et al. (EPA-600/7-78-056, 1978). Evidently puncture occurs when the local cake structure is not strong enough to maintain a bridge over the aperture represented by a large pore and the portion of the cake covering the pore is blown through the fabric. This suggests that formation of pinholes will be highly dependent on the strength of the surface forces between particles that produce flocculation of dusts. The seepage of a dust through a filter is probably also closely related to the strength of the surface forces.

Surface pores can be greatly reduced in size by coating what will become the dusty side of the filter fabric with a thin microporous membrane that is supported by the underlying fabric. That has the effect of decreasing the effective penetration, both by eliminating cake pinholes, and by preventing the seepage of dust that is dragged through the fabric by successive cleanings. A variety of different membrane-forming polymers can be used in compatible service. The most versatile and effective surface filtration membranes are microfibrous Teflon as already described by Brinckman and Maresca [ASME Med. Waste Symp. (1992)] in the section on dry scrubbing.

Granular-Bed Filters Granular-bed filters may be classified as "depth" filters, since dust particles deposit in depth within the bed of granules. The granules themselves present targets for the deposition of particles by inertia, diffusion, flow-line interception, gravity, and electrostatic attraction, depending on the dust and filter characteristics and the operating conditions. Other deposition mechanisms are minor at most. Although it is physically possible under some circumstances for a dust layer to form on the inlet face of the filter, the practical limits of gas pressure drop will normally have been reached long before a surface dust layer can be established.

Granular-bed filters may be divided into three classes:

1. *Fixed-bed, or packed-bed, filters.* These units are not cleaned when they become plugged with deposited dust particles but are broken up for disposal or simply abandoned. If they are constructed from fine granules (e.g., sand particles), they may be designed to give high collection efficiencies on fine dust particles. However, if such a filter is to have a reasonable operating life, it can be used only on a gas containing a low concentration of dust particles.

2. *Cleanable granular-bed filters.* In these devices provisions are made to separate the collected dust from the granules either continuously or periodically, so that the units can operate continuously on gases containing moderate to high dust concentrations. The necessity for cleaning and recycling the granules generally restricts the practical lower granule size to about 3 to 10 mm. This in turn makes it difficult to attain high collection efficiencies on fine particles with granule beds of reasonable depth and gas pressure drop.

3. *Fluidized-bed filters.* Fluidized beds of granules have received considerable study on theoretical and experimental levels but have not been applied on a practical commercial scale.

Fixed Granular-Bed Filters Fixed-bed filters composed of granules have received considerable theoretical and experimental study [Thomas and Yoder, *AMA Arch. Ind. Health,* **13,** 545 (1956); **13,** 550 (1956); Knettig and Beeckmans, *Can. J. Chem. Eng.,* **52,** 703 (1974); Schmidt et al., *J. Air Pollut. Control Assoc.,* **28,** 143 (1978); Tardos et al., *J. Air Pollut. Control Assoc.,* **28,** 354 (1978); and Gutfinger and Tardos, *Atmos. Environ.,* **13,** 853 (1979)]. The theoretical approach is the same as that used in the treatment of deep-bed fibrous filters.

Fibers for filter applications can be produced with diameters smaller than it is practical to obtain with granules. Consequently, most concern with filtration of fine particles has been focused on fibrous-bed rather than granular-bed filters. However, for certain specialized applications granular beds have shown some superior properties, such as greater dimensional stability. Granular-bed filters of special design (deep-bed sand filters) have been used since 1948 for removing radioactive particles from waste air and gas streams in atomic energy plants (Lapple, "Interim Report—200 Area Stack Contamination," U.S. AEC Rep. HDC-743, Oct. 11, 1948; Juvinall et al., "Sand-Bed Filtration of Aerosols: A Review of Published Information," U.S. AEC Rep. ANL-7683, 1970; and Burchsted et al., *Nuclear Air Cleaning Handbook,* U.S. ERDA 76-21, 1976). The filter characteristics needed included high collection efficiency on fine particles, large dust-holding capacity to give long operating life, and low maintenance requirements. The sand filters are as much as 2.7 m (9 ft) in depth and are constructed in graded layers with about a 2:1 variation in the granule size from one layer to the next. The air-flow direction is upward, and the granules decrease in size in the direction of the air flow. The bottom layer is composed of rocks about 5 to 7.5 cm (2 to 3 in) in diameter, and granule sizes in successive layers decrease to 0.3 to 0.6 mm (50 to 30 mesh) in the finest layer. With superficial face velocities of about 1.5 m/min (5 ft/min), gas pressure drops of clean filters have ranged from 1.7 to 2.8 kPa (7 to 11 in water). Collection efficiencies of up to 99.98 percent with a polydisperse dioctyl phthalate aerosol of 0.7-μm mean diameter have been reported (Juvinall et al., op. cit.). Operating lives of 5 years or more have been attained.

Cleanable Granular-Bed Filters The principal objective in the development of cleanable granular-bed filters is to produce a device that can operate at temperatures above the range that can be tolerated with fabric filters. In some of the devices, the granules are circulated continuously through the unit, then are cleaned of the collected dust and returned to the filter bed. In others, the granular bed remains in place but is periodically taken out of service and cleaned by some means, such as backflushing with air.

A number of moving-bed granular filters have used cross-flow designs. One form of cross-flow moving-granular-bed filter, produced by the Combustion Power Company (Fig. 17-61), is currently in commercial use in some applications. The granular filter medium consists of ⅛- to ¼-in (3- to 6-mm) pea gravel. Gas face velocities range from 30 to 46 m/min (100 to 150 ft/min), and reported gas pressure drops are in the range of 0.5 to 3 kPa (2 to 12 in water). The original form of the device [Reese, TAPPI, **60**(3), 109 (1977)] did not incorporate electrical augmentation. Collection efficiencies for submicrometer particles were low, and the electrical augmentation was added to correct the deficiency (Parquet, "The Electroscrubber Filter: Applications and Particulate Collection Performance," EPA-600/9-82-005c, 1982, p. 363). The electrostatic grid immersed in the bed of granules is charged to a potential of 20,000 to 30,000 V, producing an electric field between the grid and the inlet and outlet louvers that enclose the bed. No ionizing electrode is used to charge particles in the incoming gas; reliance is placed on the existence of natural charges on the dust particles. Individual dust particles commonly carry positive or negative charges even though the net charge on the dust as a whole is normally neutral. Depending on their charges, dust particles are attracted or repelled by the electrical field and are therefore caused to deposit on the rocks in the bed.

Self et al. ("Electrical Augmentation of Granular Bed Filters," EPA-600/9-80-039c, 1980, p. 309) demonstrated in theoretical studies and

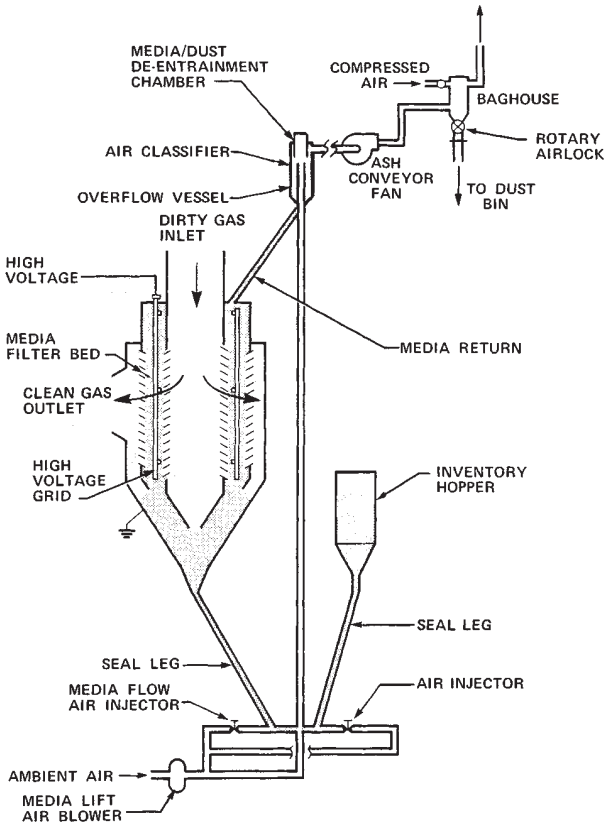

FIG. 17-61 Electrically augmented granular-bed filter. (*Combustion Power Company.*)

laboratory experiments that such an augmentation system should yield substantial increases in the collection efficiency for fine particles if the particles carry significant charges. Significant improvements in the performance of the Combustion Power units with electrical augmentation have been reported by the manufacturer (Parquet, op. cit.).

Another type of gravel-bed filter, developed by GFE in Germany, has had limited commercial application in the United States [Schueler, *Rock Prod.*, **76**(7), 66 (1973); **77**(11), 39 (1974)]. After precleaning in a cyclone, the gas flows downward through a stationary horizontal filter bed of gravel. When the bed becomes loaded with dust, the gas flow is cut off, and the bed is backflushed with air while being stirred with a double-armed rake that is rotated by a gear motor. The backflush air also flows backward through the cyclone, which then acts as a dropout chamber. Multiple filter units are constructed in parallel so that individual units can be taken off the line for cleaning. The dust dislodged from the bed and carried by the backflush air is flocculated, and part is collected in the cyclone. The backflush air with the remaining suspended dust is cleaned in the other gravel-bed filter units that are operating on line. Performance tests made on one installation for the U.S. Environmental Protection Agency (EPA-600/7-78-093, 1978) did not give clear results but indicated that collection efficiencies were low on particles under 2 μm and that some of the dust in the backflush air was redispersed sufficiently to penetrate the operating filter units.

Air Filters The types of equipment previously described are intended primarily for the collection of process dusts, whereas air filters comprise a variety of filtration devices designed for the collection of particulate matter at low concentrations, usually atmospheric dust. The difference in the two categories of equipment is not in the principles of operation but in the adaptations required to deal with the different quantities of dust. Process-dust concentrations may run as high as several hundred grams per cubic meter (or grains per cubic foot) but usually do not exceed 45 g/m^3 (20 gr/ft^3). Atmospheric-dust concentrations that may be expected in various types of locations are shown in Table 17-8 and are generally below 12 mg/m^3 (5 gr/1000 ft^3).

TABLE 17-8 Average Atmospheric-Dust Concentrations*
1 gr/1000 ft^3 = 2.3 mg/m^3

Location	Dust concentration, gr/1000 ft^3
Rural and suburban districts	0.02–0.2
Metropolitan districts	0.04–0.4
Industrial districts	0.1–2.0
Ordinary factories or workrooms	0.2–4.0
Excessive dusty factories or mines	4.0–400

**Heating Ventilating Air Conditioning Guide,* American Society of Heating, Refrigerating and Air-Conditioning Engineers, New York, 1960, p. 77.

The most frequent application of air filters is in cleaning atmospheric air for building ventilation, which usually requires only moderately high collection-efficiency levels. However, a variety of industrial operations developed mostly since the 1940s require air of extreme cleanliness, sometimes for pressurizing enclosures such as clean rooms and sometimes for use in a process itself. Examples of applications include the manufacture of antibiotics and other pharmaceuticals, the production of photographic film, and the manufacture and assembly of semiconductors and other electronic devices. Air cleaning at the necessary efficiency levels is accomplished by the use of high-efficiency fibrous filters that have been developed since the 1940s.

Air filters are also used to protect internal-combustion engines and gas turbines by cleaning the intake air. In some locations and applications, the atmospheric-dust concentrations encountered are much higher than those normally encountered in air-conditioning service.

High-efficiency air filters are sometimes used for emission control when particulate contaminants are low in concentration but present special hazards; cleaning of ventilation air and other gas streams exhausted from nuclear plant operations is an example.

Air-Filtration Theory Current high-efficiency air- and gas-filtration methods and equipment have resulted largely from the development of filtration theory since about 1930 and particularly since the 1940s. Much of the theoretical advance was originally encouraged by the requirements of the military and atomic energy programs. The fibrous filter has served both as a practical device and as a model for theoretical and experimental investigation. Extensive reviews and new treatments of air-filtration theory and experience have been presented by Chen [*Chem. Rev.*, **55,** 595 (1955)], Dorman ("Filtration," in Davies, *Aerosol Science,* Academic, New York, 1966), Pich (*Theory of Aerosol Filtration by Fibrous and Membrane Filters,* in ibid.), Davies (*Air Filtration,* Academic, New York, 1973), and Kirsch and Stechkina ("The Theory of Aerosol Filtration with Fibrous Filters," in Shaw, *Fundamentals of Aerosol Science,* Wiley, New York, 1978). The theoretical treatment of filtration starts with the processes of dust-particle deposition on collecting bodies, as outlined in Fig. 17-35 and Table 17-2. All the mechanisms shown in Table 17-2 may come into play, but inertial deposition, flow-line interception, and diffusional deposition are usually dominant. Electrostatic precipitation may become a major mechanism if the collecting body, the dust particle, or both, are charged. Gravitational settling is a minor influence for particles in the size range of usual interest. Thermal precipitation is nil in the absence of significant temperature gradients. Sieving is a possible mechanism only when the pores in the filter medium are smaller than or approximately equal to the particle size and will not be encountered in fibrous filters unless they are loaded sufficiently for a surface dust layer to form.

The theoretical prediction of the efficiency of collection of dust particles by a fibrous filter consists of three steps (Chen, op. cit.):

1. Calculation of the target efficiency η_o of an isolated fiber in an air stream having a superficial velocity the same as that in the filter
2. Determining the difference between the target efficiency of the isolated fiber and that of an individual fiber in the filter array η_t

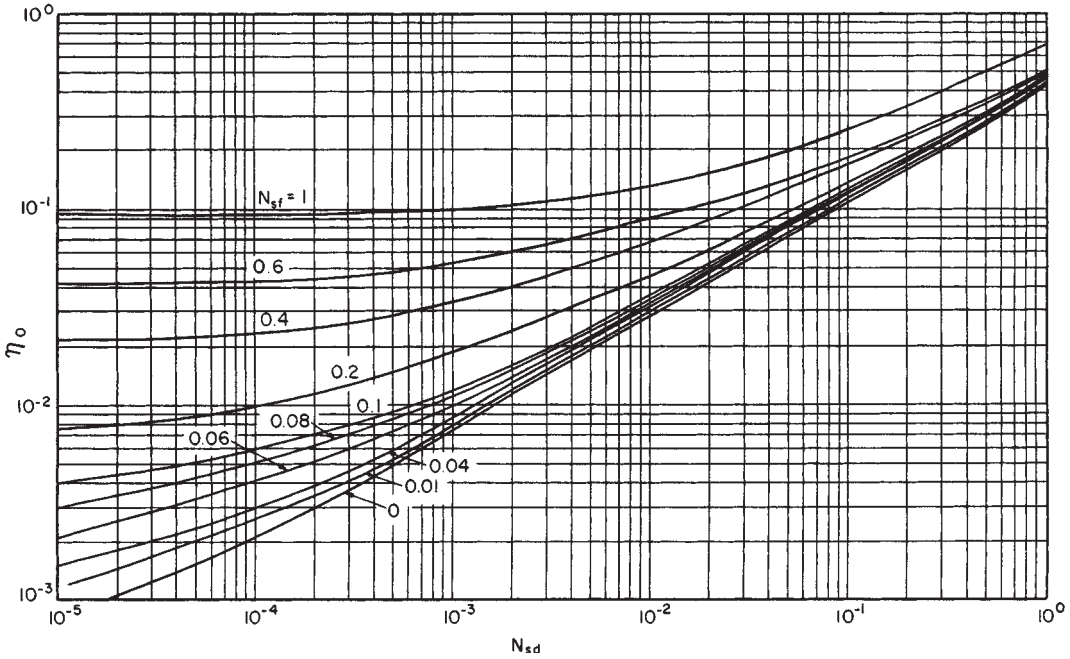

FIG. 17-62 Isolated fiber efficiency for combined diffusion and interception mechanism at $N_{Re} = 10^{-2}$. [*Chen,* Chem. Rev., ***55,*** *595 (1955).*]

3. Determining the collection efficiency of the filter η from the target efficiency of the individual fibers

The results of computations of η_o for an isolated fiber are illustrated in Figs. 17-62 and 17-63. The target efficiency η_t of an individual fiber in a filter differs from η_o for two main reasons (Pich, op. cit.): (1) the average gas velocity is higher in the filter, and (2) the velocity field around the individual fibers is influenced by the proximity of neighboring fibers. The interference effect is difficult to determine on a purely theoretical basis and is usually evaluated experimentally. Chen (op. cit.) expressed the effect with an empirical equation:

$$\eta_t = \eta_o[1 + K_\alpha(1 - \varepsilon_v)] \tag{17-14}$$

This indicates that the target efficiency of the fiber is increased by the proximity of other fibers. The value of K_α averaged 4.5 for values of the void fraction ε_v, ranging from 0.90 to 0.99. Extending use of the equation to values of ε_v lower than 0.90 may result in large errors.

The collection efficiency of the filter may be calculated from the fiber target efficiency and other physical characteristics of the filter (Chen, op. cit.):

$$N_t = \frac{4\eta_t L(1 - \varepsilon_v)}{\pi D_b \varepsilon_v} \tag{17-15}$$

where D_b = fiber diameter and L = filter thickness. The derivation of Eq. (17-15) assumes that (1) η_t is the same throughout the filter, (2) all fibers are of the same diameter D_b, are cylindrical and are normal to the direction of the gas flow, (3) the fraction of the particles deposited in any one layer of fiber is small, and (4) the gas passing through the filter is essentially completely remixed after it leaves one layer of the filter and before it enters the next. The first assumption requires that Eq. (17-15) apply only for particles of a single size for which there are corresponding values of η_t, η, and N_t.

For filters of high porosity, ε_v approaches unity and Eq. (17-15) reduces to the expression used by Wong et al. [*J. Appl. Phys.*, **27,** 161 (1956)] and Thomas and Lapple [*Am. Inst. Chem. Eng. J.*, **7,** 203 (1961)]:

$$N_t = \frac{4\eta_t L(1 - \varepsilon_v)}{\pi D_b} \tag{17-16}$$

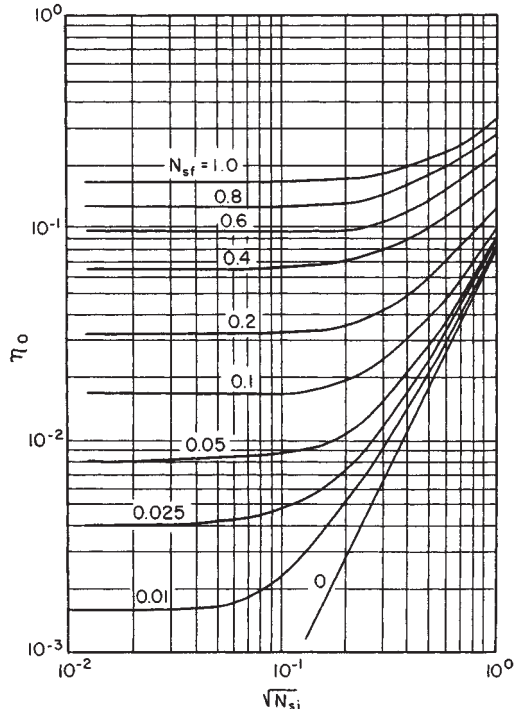

FIG. 17-63 Isolated fiber efficiency for combined inertia and interception mechanisms at $N_{Re} = 0.2$. [*Chen,* Chem. Rev., ***55,*** *595 (1955).*]

The foregoing procedure is commonly employed in reverse to determine or confirm fiber target efficiencies from the experimentally determined efficiencies of fibrous filter pads.

Filtration theory assumes that a dust particle that touches a collector body adheres to it. This assumption appears to be valid in most cases, but evidence of nonadherence, or particle bouncing, has appeared in some instances. Wright et al. ("High Velocity Air Filters," WADC TR 55-457, ASTIA Doc. AD-142075, 1957) investigated the performance of fibrous filters at filtration velocities of 0.091 to 3.05 m/s (0.3 to 10 ft/s), using 0.3-μm and 1.4-μm supercooled liquid aerosols and a 1.2-μm solid aerosol. The collection efficiencies agreed well with theoretical predictions for the liquid aerosols and apparently also for the solid aerosol at filtration velocities under 0.3 m/s (1 ft/s). But at filtration velocities above 0.3 m/s some of the solid particles failed to adhere. With a filter composed of 30-μm glass fibers and a filtration velocity of 9.1 m/s (30 ft/s), there were indications that 90 percent of the solid aerosol particles striking a fiber bounced off.

Bouncing may be regarded as a defect in the particle-deposition process. However, particles that have been deposited in filters may subsequently be blown off and reentrained into the air stream (Corn, "Adhesion of Particles," in Davies, *Aerosol Science,* Academic, New York, 1966; and Davies, op. cit.).

The theories of filtration by a fibrous filter relate only to the initial efficiency of the clean filter in the "static" period of filtration before the deposition of any appreciable quantity of dust particles. The deposition of particles in a filter increases the number of targets available to intercept particles, so that collection efficiency increases as the filter loads. At the same time, the filter undergoes clogging and the pressure drop increases. No theory is available for dealing with the "dynamic" period of filtration in which collection efficiency and pressure drop vary with the loading of collected dust. The theoretical treatment of this filtration period is incomparably more complex than that for the "static" period. Investigators have noted that both the increase in collection efficiency and the increase in pressure drop are exponential functions of the loading of collected dust or are at least roughly so (Davies, op. cit.). Some empirical relationships have been derived for correlating data in particular instances.

The dust particles collected by a fibrous filter do not deposit in uniform layers on fibers but tend to deposit preferentially on previously deposited particles (Billings, "Effect of Particle Accumulation in Aerosol Filtration," Ph.D. dissertation, California Institute of Technology, Pasadena, 1966), forming chainlike agglomerates termed "dendrites." The growth of dendritic deposits on fibers has been studied experimentally [Billings, op. cit.; Bhutra and Payatakes, *J. Aerosol Sci.,* **10,** 445 (1979)], and Payatakes and coworkers [Payatakes and Tien, *J. Aerosol Sci.,* **7,** 85 (1976); Payatakes, *Am. Inst. Chem. Eng. J.,* **23,** 192 (1977); and Payatakes and Gradon, *Chem. Eng. Sci.,* **35,** 1083 (1980)] have attempted to model the growth of dendrites and its influence on filter efficiency and pressure drop.

Air-Filter Types Air filters may be broadly divided into two classes: (1) panel, or unit, filters; and (2) automatic, or continuous, filters. Panel filters are constructed in units of convenient size (commonly 20- by 20-in or 24- by 24-in face area) to facilitate installation, maintenance, and cleaning. Each unit consists of a cleanable or replaceable cell or filter pad in a substantial frame that may be bolted to the frames of similar units to form an airtight partition between the source of the dusty air and the destination of the cleaned air.

Panel filters may use either viscous or dry filter media. Viscous filters are so called because the filter medium is coated with a tacky liquid of high viscosity (e.g., mineral oil and adhesives) to retain the dust. The filter pad consists of an assembly of coarse fibers (now usually metal, glass, or plastic). Because the fibers are coarse and the media are highly porous, resistance to air flow is low and high filtration velocities can be used.

Dry filters are usually deeper than viscous filters. The dry filter media use finer fibers and have much smaller pores than the viscous media and need not rely on an oil coating to retain collected dust. Because of their greater resistance to air flow, dry filters must use lower filtration velocities to avoid excessive pressure drops. Hence, dry media must have larger surface areas and are usually pleated or arranged in the form of pockets (Fig. 17-64), generally sheets of cellulose pulp, cotton, felt, or spun glass.

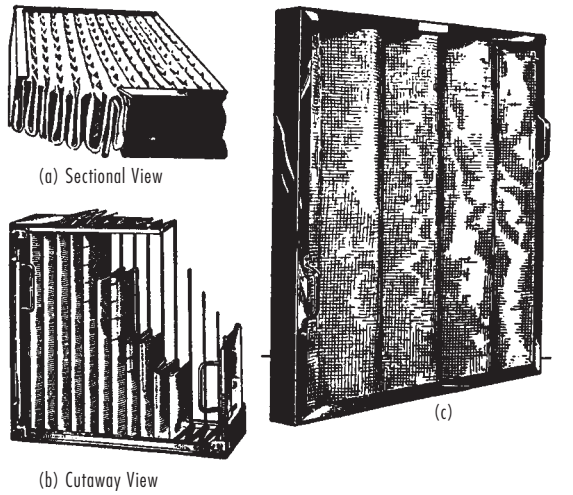

FIG. 17-64 Typical dry filters. (*a*) Throwaway type, Airplex. (*Davies Air Filter Corporation.*) (*b*) Replaceable medium type, Airmat PL-24, cutaway view. (*American Air Filter Co., Inc.*) (*c*) Cleanable type, Amirglass sawtooth. (*Amirton Company.*)

Automatic filters are made with either viscous-coated or dry filter media. However, the cleaning or disposal of the loaded medium is essentially continuous and automatic. In most such devices the air passes horizontally through a movable filter curtain. As the filter loads with dust, the curtain is continuously or intermittently advanced to expose clean media to the air flow and to clean or dispose of the loaded medium. Movement of the curtain can be provided by a hand crank or a motor drive. Movement of a motor-driven curtain can be actuated automatically by a differential-pressure switch connected across the filter.

High-Efficiency Air Cleaning Air-filter systems for nuclear facilities and for other applications demanding extremely high standards of air purity require filtration efficiencies well beyond those attainable with the equipment described above. The *Nuclear Air Cleaning Handbook* (Burchsted et al., op. cit.) presents an extensive treatment of the requirements for and the design of such air-cleaning facilities. Much of the material is pertinent to high-efficiency air-filter systems for applications to other than nuclear facilities.

HEPA (high-efficiency particulate air) filters were originally developed for nuclear and military applications but are now widely used and are manufactured by numerous companies. By definition, an HEPA filter is a "throwaway, extended-medium dry-type" filter having (1) a minimum particle-removal efficiency of not less than 99.97 percent for 0.3-μm particles, (2) a maximum resistance, when clean, of 1.0 in water when operated at rated air-flow capacity, and (3) a rigid casing extending the full depth of the medium (Burchsted et al., op. cit.). The filter medium is a paper made of submicrometer glass fibers in a matrix of larger-diameter (1- to 4-μm) glass fibers. An organic binder is added during the papermaking process to hold the fibers and give the paper added tensile strength. Filter units are made in several standard sizes (Table 17-9).

TABLE 17-9 Standard HEPA Filters*

Face dimensions, in	Depth, less gaskets, in	Design air-flow capacity at clean-filter resistance of 1.0 in water (standard ft³/min)
24 × 24	11½	1000
24 × 24	5⅞	500
12 × 12	5⅞	125
8 × 8	5⅞	20
8 × 8	3¹⁄₁₆	25

*Burchsted et al., *Nuclear Air Cleaning Handbook,* ERDA 76-21, Oak Ridge, Tenn., 1976.

Because HEPA filters are designed primarily for high efficiency, their dust-loading capacities are limited, and it is common practice to use prefilters to extend their operating lives. In general, HEPA filters should be protected from (1) lint, (2) particles larger than 1 to 2 μm in diameter, and (3) dust concentrations greater than 23 mg/m^3 (10 gr/1000 ft^3). Air filters used in nuclear facilities as prefilters and building-supply air filters are classified as shown in Table 17-10. The standard of the American Society of Heating, Refrigerating and Air-Conditioning Engineers (*Method of Testing Air Cleaning Devices Used in General Ventilation for Removing Particulate Matter,* ASHRAE 52-68, 1968) requires both a dust-spot (dust-stain) efficiency test made with atmospheric dust and a weight-arrestance test made with a synthetic test dust. A more precise comparison of the different groups of filters, based on removal efficiencies for particles of specific sizes, is presented in Table 17-11.

Table 17-12 presents the relative performance of Group I, II, and III filters with respect to air-flow capacity, resistance, and dust-holding capacity. The dust-holding capacities correspond to the manufacturers' recommended maximum allowable increases in air-flow resistance. The values for dust-holding capacity are based on tests with a synthetic dust and hence are relative. The actual dust-holding capacity in a specific application will depend on the characteristics of the dust encountered. In some instances it may be appropriate to use two or more stages of precleaning in air-filter systems to achieve a desired combination of operating life and efficiency. In very dusty locations, inertial devices such as multiple small cyclones may be used as first-stage separators.

Electrical Precipitators When particles suspended in a gas are exposed to gas ions in an electrostatic field, they will become charged and migrate under the action of the field. The functional mechanisms of electrical precipitation may be listed as follows:

1. Gas ionization
2. Particle collection
   - *a.* Production of electrostatic field to cause charging and migration of dust particles
   - *b.* Gas retention to permit particle migration to a collection surface
   - *c.* Prevention of reentrainment of collected particles
   - *d.* Removal of collected particles from the equipment

TABLE 17-10 Classification of Common Air Filters*

Group	Efficiency	Filter type	Stain test efficiency, %	Arrestance, %
I	Low	Viscous impingement, panel type	<20†	40–80†
II	Moderate	Extended medium, dry type	20–60†	80–96†
III	High	Extended medium, dry type	60–98‡	96–99†
HEPA	Extreme	Extended medium, dry type	100§	100†

*Burchsted et al., *Nuclear Air Cleaning Handbook,* ERDA 76-21, Oak Ridge, Tenn., 1976.
†Test using synthetic dust.
‡Stain test using atmospheric dust.
§ASHRAE/52-68, American Society of Heating, Refrigerating and Air-Conditioning Engineers.

TABLE 17-11 Comparison of Air Filters by Percent Removal Efficiency for Various Particle Sizes*

Group	Efficiency	Removal efficiency, %, for particle size of 0.3 μm	1.0 μm	5.0 μm	10.0 μm
I	Low	0–2	10–30	40–70	90–98
II	Moderate	10–40	40–70	85–95	98–99
III	High	45–85	75–99	99–99.9	99.9
HEPA	Extreme	99.97 min	99.99	100	100

*Burchsted et al., *Nuclear Air Cleaning Handbook,* ERDA 76-21, Oak Ridge, Tenn., 1976.

TABLE 17-12 Air-Flow Capacity, Resistance, and Dust-Holding Capacity of Air Filters*

Group	Efficiency	Air-flow capacity, ft^3/(min·ft^2 of frontal area)	Resistance, in water: Clean filter	Resistance, in water: Used filter	Dust-holding capacity, g/(1000 ft^3·min of air-flow capacity)
I	Low	300–500	0.05–0.1	0.3–0.5	50–1000
II	Moderate	250–750	0.1–0.5	0.5–1.0	100–500
III	High	250–750	0.20–0.5	0.6–1.4	50–200

*Burchsted et al., *Nuclear Air Cleaning Handbook,* ERDA 76-21, Oak Ridge, Tenn., 1976.

There are two general classes of electrical precipitators: (1) single-stage, in which ionization and collection are combined; (2) two-stage, in which ionization is achieved in one portion of the equipment, followed by collection in another. Various types in each class differ essentially in the details by which each function is accomplished.

The underlying theory presented in the following paragraphs assumes that the dust concentration is small, since only very incomplete evaluations for conditions of high dust concentration have been made.

Field Strength Whereas the applied potential or voltage is the quantity commonly known, it is the field strength that determines behavior in an electrostatic field. When the current flow is low (i.e., before the onset of spark or corona discharge), these are related by the following equations for two common forms of electrodes:

Parallel plates:

$$\mathscr{E} = E/B_e \tag{17-17}$$

Concentric cylinders (wire-in-cylinder):

$$\mathscr{E} = \frac{E}{r \ln (D_t/D_d)} \tag{17-18}$$

The field strength is uniform between parallel plates, whereas it varies in the space between concentric cylinders, being highest at the surface of the central cylinder. After corona sets in, the current flow will become appreciable. The field strength near the center electrode will be less than given by Eq. (17-18) and that in the major portion of the clearance space will be greater and more uniform [see Eqs. (17-23) and (17-24)].

Potential and Ionization In order to obtain gas ionization it is necessary to exceed, at least locally, the electrical breakdown strength of the gas. Corona is the name applied to such a local discharge that fails to propagate itself. Sparking is essentially an advanced stage of corona in which complete breakdown of the gas occurs along a given path. Since corona represents a local breakdown, it can occur only in a nonuniform electrical field (Whitehead, *Dielectric Phenomena—Electrical Discharge in Gases,* Van Nostrand, Princeton, N.J., 1927, p. 40). Consequently, for parallel plates, only sparking occurs at a field strength or potential difference given by the empirical expressions

$$\mathscr{E}_s = \mathscr{E}_o k_\rho \left[1 + \left(\frac{K_o}{k_\rho B_e}\right)\right] \tag{17-19}$$

$$E_s = \mathscr{E}_o k_\rho B_e + K_o \mathscr{E}_o \tag{17-20}$$

For air in the range of $k_\rho B_e$ from 0.1 to 2, $\mathscr{E}_o = 111.2$ and $K_o = 0.048$. Thornton [*Phil. Mag.,* **28**(7), 666 (1939)] gives values for other gases. For concentric cylinders (Loeb, *Fundamental Processes of Electrical Discharge in Gases,* Wiley, New York, 1939; Peek, *Dielectric Phenomena in High-Voltage Engineering,* McGraw-Hill, New York, 1929; and Whitehead, op. cit.), corona sets in at the central wire when

$$\mathscr{E}_c = \mathscr{E}_o k_\rho \left(1 + \sqrt{\frac{K_o}{k_\rho D_d}}\right) \tag{17-21}$$

$$E_c = \left(\frac{\mathscr{E}_o k_\rho D_d}{2}\right)\left(1 + \sqrt{\frac{K_o}{k_\rho D_d}}\right) \ln\left(\frac{D_t}{D_d}\right) \tag{17-22}$$

TABLE 17-13 Sparking Potentials* (Small Wire Concentric in Pipe)

Pipe diameter, in	Sparking potential,† volts	
	Peak	Root mean square
4	59,000	45,000
6	76,000	58,000
9	90,000	69,000
12	100,000	77,000

*Data reported by Anderson in Perry, "Chemical Engineers' Handbook," 2d ed., p. 1873, McGraw-Hill, New York, 1941.

†For gases at atmospheric pressure, 100°F, containing water vapor, air, CO_2, and mist, and negative-discharge-electrode polarity.

For air approximate values are $\mathscr{E}_o = 110$, $K_o = 0.18$. Corona, however, will set in only if $(D_t/D_d) > 2.718$. If this ratio is less than 2.718, no corona occurs, and only sparking will result, following the laws given by Eqs. (17-21) and (17-22) (Peek, op. cit.).

In practice, precipitators are usually operated at the highest voltage practicable without sparking, since this increases both the particle charge and the electrical precipitating field. The sparking potential is generally higher with a negative charge on the discharge electrode and is less erratic in behavior than a positive corona discharge. It is the consensus, however, that ozone formation with a positive discharge is considerably less than with a negative discharge. For these reasons negative discharge is generally used in industrial precipitators, and a positive discharge is utilized in air-conditioning applications. In Table 17-13 are given some typical values for the sparking potential for the case of small wires in pipes of various sizes. The sparking potential varies approximately directly as the density of the gas but is very sensitive to the character of any material collected on the electrodes. Even small amounts of poorly conducting material on the electrodes may markedly lower the sparking voltage. For positive polarity of the discharge electrode, the sparking voltage will be very much lower. The sparking voltage is greatly affected by the temperature and humidity of the gas, as shown in Fig. 17-65.

Current Flow Corona discharge is accompanied by a relatively small flow of electric current, typically 0.1 to 0.5 mA/m^2 of collecting-electrode area (projected, rather than actual area). Sparking usually involves a considerably larger flow of current which cannot be tolerated except for occasional periods of a fraction of a second duration, and then only when suitable electrical controls are provided to limit the current. However, when suitable controls are provided, precipitators have been operated continuously with a small amount of sparking

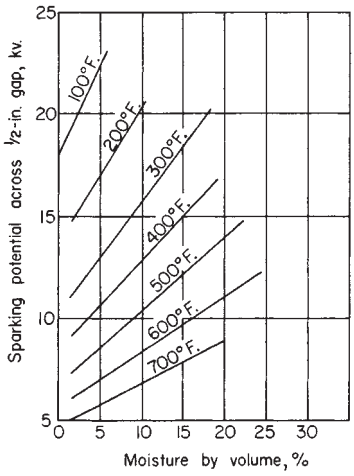

FIG. 17-65 Sparking potential for negative point-to-plane ½-in (1.3-cm) gap as a function of moisture content and temperature of air at 1-atm (101.3-kPa) pressure. [*Sproull and Nakada,* Ind. Eng. Chem., ***43,*** *1356 (1951).*]

to ensure that the voltage is in the correct range to ensure corona. Besides disruptive effects on the electrical equipment and electrodes, sparking will result in low collection efficiency because of reduction in applied voltage, redispersion of collected dust, and current channeling. Although an exact calculation can be made for the current flow for a direct-current potential applied between concentric cylinders, the following simpler expression, based on the assumption of a constant space charge or ion density, gives a good approximation of corona current [Ladenburg, *Ann. Phys.*, **4**(5), 863 (1930)]:

$$I = \frac{8\lambda_i E(E - E_c)}{D_t^2 \ln (D_t/D_d)} \tag{17-23}$$

and the average space charge is given by (Whitehead, op. cit.)

$$\sigma_{avg} = \frac{4(E - E_c)}{\pi D_t^2 \varepsilon} \tag{17-24}$$

In the space outside the immediate vicinity of corona discharge, the field strength is sensibly constant, and an average value is given by

$$\mathscr{E} = \sqrt{2I/\lambda_i} \tag{17-25}$$

which applies if the potential difference is above the critical potential required for corona discharge so that an appreciable current flows.

Ionic mobilities are given by Loeb (*International Critical Tables,* vol. 6, McGraw-Hill, New York, 1929, p. 107). For air at 0°C, 760 mmHg, $\lambda_i = 624$ (cm/s)/(statV/cm) for negative ions. Positive ions usually have a slightly lower mobility. Loeb (*Basic Processes of Gaseous Electronics,* University of California Press, Berkeley and Los Angeles, 1955, p. 53) gives a theoretical expression for ionic mobility of gases which is probably good to within ±50 percent:

$$\lambda_i = \frac{100.0}{k_p \sqrt{(\delta_g - 1)M}} \tag{17-26}$$

In general, ionic mobilities are inversely proportional to gas density. Ionic velocities in the usual electrostatic precipitator are on the order of 30.5 m/s (100 ft/s).

Electric Wind By virtue of the momentum transfer from gas ions moving in the electrical field to the surrounding gas molecules, a gas circulation, known as the "electric" or "ionic" wind, is set up between the electrodes. For conditions encountered in electrical precipitators, the velocity of this circulation is on the order of 0.6 m/s (2 ft/s). Also, as a result of this momentum transfer, the pressure at the collecting electrode is slightly higher than at the discharge electrode (Whitehead, op. cit., p. 167).

Charging of Particles [Deutsch, *Ann. Phys.*, **68**(4), 335 (1922); **9**(5), 249 (1931); **10**(5), 847 (1931); Ladenburg, op. cit.; and Mierdel, *Z. Tech. Phys.*, **13,** 564 (1932).] Three forces act on a gas ion in the vicinity of a particle: attractive forces due to the field strength and the ionic image; and repulsive forces due to the Coulomb effect. For spherical particles larger than 1-μm diameter, the ionic image effect is negligible, and charging will continue until the other two forces balance according to the equation

$$N_o = \left(\frac{\zeta \mathscr{E} D_p^2}{4\varepsilon}\right)\left(\frac{\pi\sigma\varepsilon t\lambda_i}{1 + \pi\sigma\varepsilon\lambda_i t}\right) \tag{17-27}$$

The ultimate charge acquired by the particle is given by

$$N_o = \zeta \mathscr{E} D_p^2/4\varepsilon \tag{17-28}$$

and is very nearly attained in a fraction of a second. For particles smaller than 1-μm diameter, the initial charging will occur according to Eq. (17-27). However, owing to the ionic-image effect, the ultimate charge will be considerably greater because of penetration resulting from the kinetic energy of the gas ions. For charging times of the order encountered in electrical precipitation, the ultimate charge acquired by spherical particles smaller than about 1-μm diameter may be approximated (±30 percent) by the empirical expression

$$N_o = 3.4 \times 10^3 D_p T \tag{17-29}$$

Values of N_o for various sized particles are listed in Table 17-14 for 70°F, $\zeta = 2$, and $\mathscr{E} = 10$ statV/cm.

Particle Mobility By equating the electrical force acting on a

TABLE 17-14 Charge and Motion of Spherical Particles in an Electric Field

For $\zeta = 2$, and $\varepsilon = \varepsilon_i = \varepsilon_p = 10$ statV/cm

Particle diam., μ	Number of elementary electrical charges, N_0	Particle migration velocity,* u_e, ft/sec
0.1	10	0.27
.25	25	.15
.5	50	.12
1.0	105	.11
2.5	655	.26
5.0	2,620	.50
10.0	10,470	.98
25.0	65,500	2.40

NOTE: To convert feet per second to meters per second, multiply by 0.3048.

particle to the resistance due to air friction, as expressed by Stokes' law, the particle velocity or mobility may be expressed by

1. For particles larger than 1-μm diameter:

$$\lambda_p = \left(\frac{u_e}{\mathscr{E}_p}\right) = \frac{\zeta D_p \mathscr{E}_i K_m}{12\pi\mu} \tag{17-30}$$

2. For particles smaller than 1-μm diameter:

$$\lambda_p = \left(\frac{u_e}{\mathscr{E}_p}\right) = \frac{360 K_m \varepsilon T}{\mu} \tag{17-31}$$

For single-stage precipitators, $\mathscr{E}_i$ and $\mathscr{E}_p$ may be considered as essentially equal. It is apparent from Eq. (17-31) that the mobility in an electric field will be almost the same for all particles smaller than about 1-μm diameter, and hence, in the absence of reentrainment, collection efficiency should be almost independent of particle size in this range. Very small particles will actually have a greater mobility because of the Stokes-Cunningham correction factor. Values of u_e are listed in Table 17-14 for 70°F, $\zeta = 2$, and $\mathscr{E} = \mathscr{E}_i = \mathscr{E}_p = 10$ statV/cm.

Collection Efficiency Although actual particle mobilities may be considerably greater than would be calculated on the basis given in the preceding paragraph because of the action of the electric wind in single-stage precipitators, the latter acts in a compensating fashion, and the overall effect of the electric wind is probably to provide an equalization of particle concentration between the electrodes similar to the action of normal turbulence (Mierdel, op. cit.). On this basis Deutsch (op. cit.) has derived the following equations for collection efficiency, the form of which had previously been suggested by Anderson on the basis of experimental data:

$$\eta = 1 - e^{-(u_e A_c/q)} = 1 - e^{-K a u_e} \tag{17-32}$$

For the concentric-cylinder (or wire-in-cylinder) type of precipitator, $K_e = 4L_e/D_t V_e$; for rod-curtain or wire-plate types, $K_e = L_e/B_e V_e$. Strictly speaking, Eq. (17-32) applies only for a given particle size, and the overall efficiency must be obtained by an integration process for a specific dust distribution, as described in the subsection "Cyclone Separators." However, over limited ranges of performance conditions, Eq. (17-32) has been found to give a good approximation of overall collection efficiency, with the term for particle migration velocity representing an empirical average value. Such values, calculated from overall collection-efficiency measurements, are given in Table 17-15 for specific installations.

For two-stage precipitators with close collecting-plate spacings (Figs. 20-152, 20-153), the gas flow is substantially streamline, and no electric wind exists. Consequently, with reentrainment neglected, collection efficiency may be expressed as [Penny, *Electr. Eng*, **56,** 159 (1937)]

$$\eta = u_e L_e / V_e B_e \tag{17-33}$$

which holds for values of $\eta \leqq 1.0$. In practice, however, extraneous factors may cause the actual efficiency to approach a relationship of the type given by Eq. (17-32).

Application The theoretical considerations that have been expounded should be used only for order-of-magnitude estimates, since a number of extraneous factors may enter into actual performance. In actual installations rectified alternating current is employed. Hence the electric field is not fixed but varies continuously, depending on the waveform of the rectifier, although Schmidt and Anderson [*Electr. Eng.*, **57,** 332 (1938)] report that the waveform is not a critical factor. Allowances for high dust concentrations have not been fully studied, although Deutsch (op. cit.) has presented a theoretical approach. In addition, irregularities on the discharge electrode will result in local discharges. Such irregularities can readily result from dust incrustation on the discharge electrodes due to charging of particles with opposite polarity within the thin but appreciable flow or ionization layer surrounding this electrode. Very high dust loadings increase the potential difference required for corona and reduce the current due to the space charge of the particles. This tends to reduce the average particle charge and reduces collection efficiency. This can be compensated for by increasing the potential difference when high dust loadings are involved.

TABLE 17-15 Performance Data on Typical Single-Stage Electrical Precipitator Installations*

Type of precipitator	Type of dust	Gas volume, cu ft/min	Average gas velocity, ft/sec	Collecting electrode area, sq ft	Over-all collection efficiency, %	Average particle migration velocity, ft/sec
Rod curtain	Smelter fume	180,000	6	44,400	85	0.13
Tulip type	Gypsum from kiln	25,000	3.5	3,800	99.7	.64
Perforated plate	Fly ash	108,000	6	10,900	91	.40
Rod curtain	Cement	204,000	9.5	26,000	91	.31

*Research-Cottrell, Inc. To convert cubic feet per minute to cubic meters per second, multiply by 0.00047; to convert feet per second to meters per second, multiply by 0.3048; and to convert square feet to square meters, multiply by 0.0929.

Several investigators have attempted to modify the basic Deutsch equation so that it would more nearly describe precipitator performance. Cooperman ("A New Theory of Precipitator Efficiency," Pap. 69-4, APCA meeting, New York, 1969) introduced correction factors for diffusional forces arising from variations in particle concentration along the precipitator length and also perpendicular to the collecting surface. Robinson [*Atmos. Environ.* **1**(3), 193 (1967)] derived an equation for collection efficiency in which two erosion or reentrainment terms are introduced.

An analysis of precipitator performance based on theoretical considerations was undertaken by the Southern Research Institute for the National Air Pollution Control Administration (Nichols and Oglesby, "Electrostatic Precipitator Systems Analysis," AIChE annual meeting, 1970). A mathematical model was developed for calculating the particle charge, electric field, and collection efficiency based on the Deutsch-Anderson equation. The system diagram is shown in Fig. 17-66. This system-analysis method, using high-speed computers, makes it possible to analyze what takes place in each increment of precipitator length. Collection efficiency versus particle size is computed for each 1 ft (0.3 m) of gas travel, and the inlet particle-size distribution is modified accordingly. Computed overall efficiencies compare well with measured values on three precipitators. The model assumes that field charging is the only charging mechanism. The authors considered the addition of several refinements to the program: the influence of diffusion charging; reentrainment effects due to rapping and erosion; and loss of efficiency due to maldistribution of gas, dust resistivity, and gas-property effects. The modeling technique appeared promising, but much more work was needed before it could be used for design. The same authors prepared a general treatise (Oglesby and Nichols, *A Manual of Electrostatic Precipitator Technology,* parts I and II, Southern Research Institute, Birmingham, Ala., U.S. Government Publications PB196360, 196381, 1970).

High-Pressure-High-Temperature Electrostatic Precipitation In general, increased pressure increases precipitation efficiency, although a somewhat higher potential is required, because it reduces ion mobility and hence increases the potential required for corona

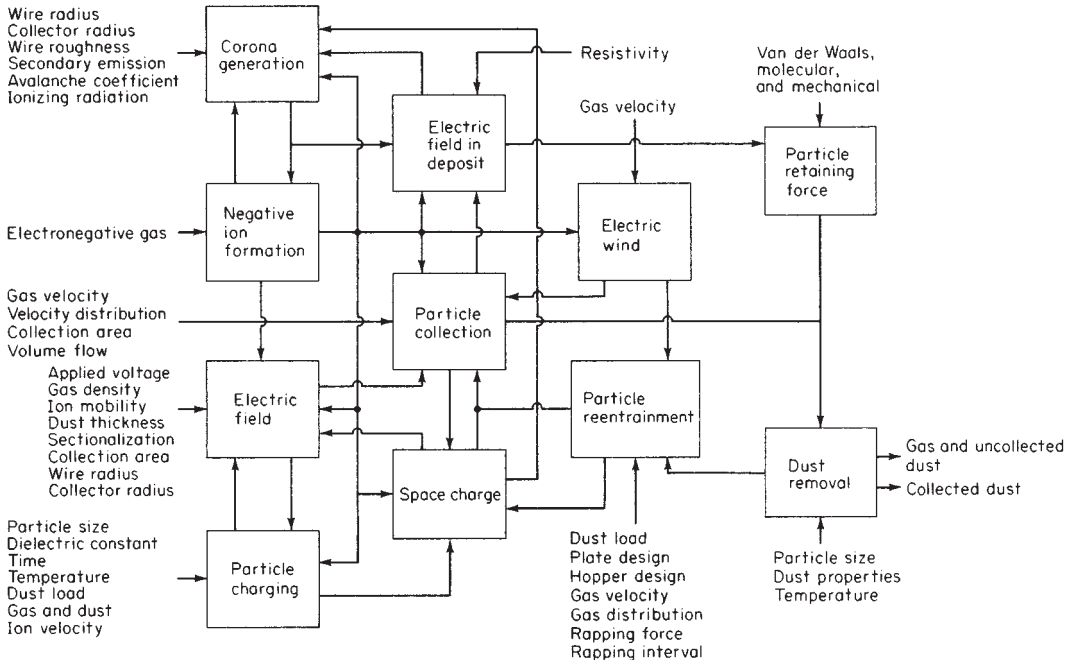

FIG. 17-66 Electrostatic-precipitator-system model. (*Nichols and Oglesby, "Electrostatic Precipitator Systems Analysis," AIChE annual meeting, 1970.*)

and sparking. Increased temperature reduces collection efficiency because ion mobility is increased, lowering critical potentials, and because gas viscosity is increased, reducing migration velocities.

Precipitators have been operated at pressures up to 5.5 MPa (800 psig) and temperatures to 800°C.

The effect of increasing gas density on sparkover voltage has been investigated by Robinson [*J. Appl. Phys.*, **40,** 5107 (1969); *Air Pollution Control*, part 1, Wiley-Interscience, New York, 1971, chap. 5]. Figure 17-67 shows the effect of gas density on corona-starting and sparkover voltages for positive and negative corona in a pipe precipitator. The sparkover voltages are experimental and are given by the solid points. Experimental corona-starting voltages are given by the hollow points. The solid lines are corona-starting voltage curves calculated from Eq. (17-33). This is an empirical relationship developed by Robinson.

$$\frac{E_c}{\rho'} = A\frac{B}{\sqrt{D_d\,\rho'/2}} \tag{17-34}$$

E_c is the corona-starting field, kV/cm. ρ' is the relative gas density, equal to the actual gas density divided by the density of air at 25°C, 1 atm. D_d is the diameter of the ionizing wire, cm. A and B are constants which are characteristics of the gas. In dry air, $A = 32.2$ kV/cm and $B = 8.46$ kV/cm$^{1/2}$. Agreement between experimental and calculated starting voltages is good for the case of positive corona, but in the case of negative corona the calculated line serves as an upper limit for the data. This lower-than-expected starting-voltage characteristic of negative corona is confirmed by Hall et al. [*Oil Gas J.*, **66,** 109 (1968)] in a report of an electrostatic precipitator which removes lubricating-oil mist from natural gas at 5.5 MPa (800 psig) and 38°C (100°F). The use of electrostatic precipitators at elevated pressure is expected to in-

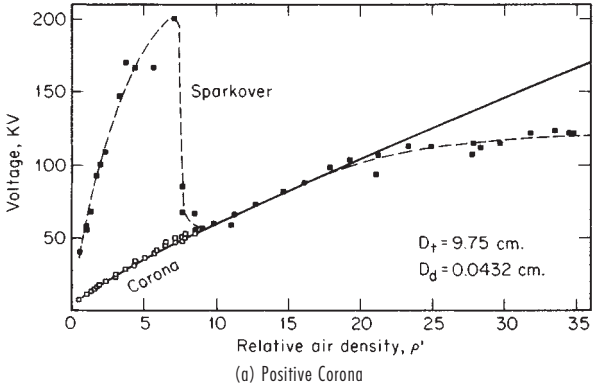

(a) Positive Corona

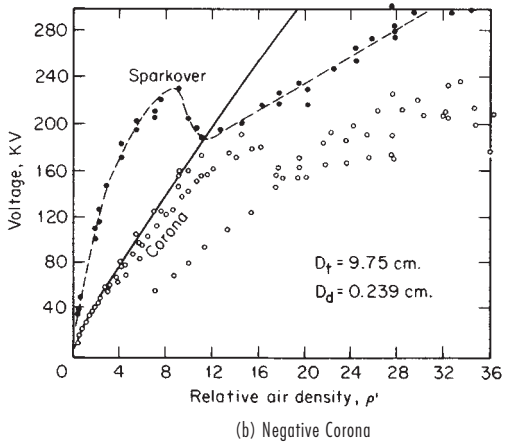

(b) Negative Corona

FIG. 17-67 Corona-starting and sparkover voltages for coaxial wire-pipe electrodes in air (25°C). D_t and D_d are the respective pipe and wire diameters. The voltage is unvarying direct current. (*Robinson,* Air Pollution Control, *part 1, Wiley-Interscience, New York, 1971, chap. 5.*)

crease, because the method requires very low pressure drop [approximately 69 Pa (0.1 lbf/in^2)]. This results from the fact that the electric separation forces are applied directly to the particles themselves rather than to the entire mass of the gas, as in inertial separators. The use of electrostatic precipitators at temperatures up to 400°C is well developed for the powerhouse fly-ash application, but in the range of 600 to 800°C they are still in the experimental phase. The U.S. Bureau of Mines has tested a pilot-scale tubular precipitator for fly ash. See Shale [*Air Pollut. Control Assoc. J.*, **17,** 159 (1967)] and Shale and Fasching (*Operating Characteristics of a High-Temperature Electrostatic Precipitator,* U.S. Bur. Mines Rep. 7276, 1969). It operated over a temperature range of 27 to 816°C (80 to 1500°F) and a pressure range of 552 kPa (35 to 80 psig). Initial collection efficiencies ranged from 90 to 98 percent at 793°C (1460°F), 552 kPa (80 psig), but continuous operation was not achieved because of excessive thermal expansion of internal parts.

Resistivity Problems Optimum performance of electrostatic precipitators is achieved when the electrical resistivity of the collected dust is sufficiently high to result in electrostatic pinning of the particles to the collecting surface, but not so high that dielectric breakdown of the dust layer occurs as the corona current passes through it. The optimum resistivity range is generally considered to be from 10^8 to 10^{10} Ω·cm, measured at operating conditions. As the dust builds up on the collecting electrode, it impedes the flow of current, so that a voltage drop is developed across the dust layer:

$$E_d = j\rho_d L_d \qquad (17\text{-}35)$$

If E_d/L_d exceeds the dielectric strength of the dust layer, sparks occur in the deposit and form back-corona craters. Ions of both polarities are formed. Positive ions formed in the craters are attracted to the negatively charged particles in the gas stream, whose charge level is reduced so that collection efficiency decreases. Some of the positive ions neutralize part of the negative-space-charge cloud normally present near the wire, thereby increasing total current. Collection efficiency under these conditions will not correlate with total power input (Owens, E. I. du Pont de Nemours & Co. internal communication, 1971). Under normal conditions, collection efficiency is an exponential function of corona power (White, *Industrial Electrostatic Precipitation,* Addison-Wesley, Reading, Mass., 1963). With typical ion density in the range of 10^9/cm^3, overall voltage gradient would be about 4000 V/cm, and current about 1 μA/cm^2. Dielectric breakdown of the dust layer (at about 10,000 V/cm) would therefore be expected for dusts with resistivities above 10^{10} Ω·cm.

Problems due to high resistivity are of great concern in **fly-ash** precipitation because air-pollution regulations require that coals have low (<1 percent) sulfur content. Figure 17-68 shows that the resistivity of low-sulfur coal ash exceeds the threshold of 10^{10} Ω·cm at common operating temperatures. This has resulted in the installation of a number of precipitators which have failed to meet guaranteed performance. This has occurred to an alarming extent in the United States but has also been encountered in Australia, where the sulfur content is typically 0.3 to 0.6 percent. Maartmann (Pap. EN-34F, 2d International Clean Air Congress, Washington, 1970) reports the installation of a number of precipitators which performed below guarantees, so that the Electricity Commission of New South Wales decided that each manufacturer wishing to bid on a new station must first make pilot tests to prove performance on the actual coal to be burned in that station. Problems of back corona and excessive sparking with low-sulfur coal usually require that the operating voltage be reduced. This reduces the migration velocity and leads to larger precipitators. Ramsdell (*Design Criteria for Precipitators for Modern Central Station Power Plants,* American Power Conference, Chicago, 1968) developed the curves in Fig. 17-69. They show the results of extensive field tests by the Consolidated Edison Co. In another paper ("Antipollution Program of Consolidated Edison Co. of New York," ASCE, May 13–17, 1968), Ramsdell traces the remarkable growth in the size of precipitators required for high efficiency on low-sulfur coals. The culmination of this work was the precipitator at boiler 30 at Ravenswood Station, New York. Resistivity problems were avoided by operating at high temperature [343°C (650°F)]. The mechanical

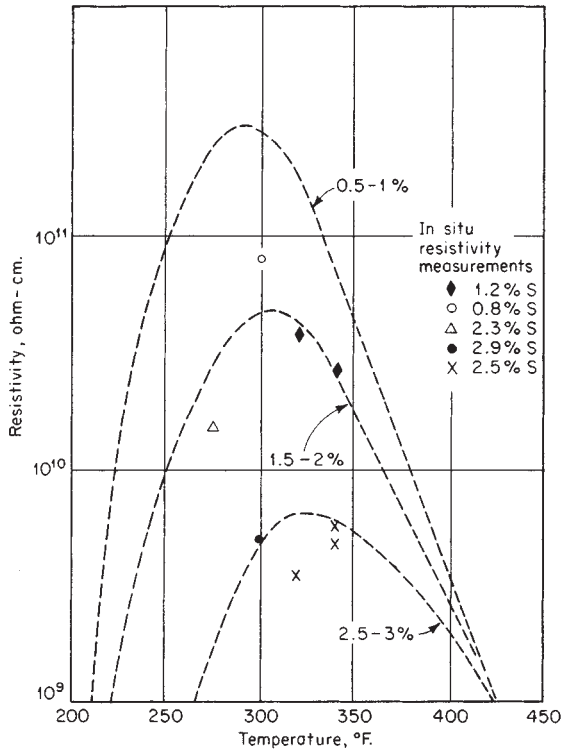

FIG. 17-68 Trends in resistivity of fly ash with variations in flue-gas temperature and coal sulfur content. °C = (°F − 32) × 5/9. (*Oglesby and Nichols,* A Manual of Electrostatic Precipitator Technology, *part II, Southern Research Institute, Birmingham, Ala., 1970.*)

(cyclone) collector was installed after the precipitator to clean up puffs due to rapping.

Maartmann (op. cit.) agrees that sulfur content is important but feels that it should not be the sole criterion for the determination of collecting surface. He points to specific collecting-surface requirements as high as 500 ft^2/(1000 ft^3·min) for 95 percent collection efficiency with high-resistivity Australian ash.

Schmidt and Anderson (op. cit.) and Anderson [*Physics,* **3,** 23 (July 1932)] claim that resistivity of the collected dust may be a controlling factor which is very sensitive to moisture. They state that an increase in relative humidity of 5 percent may double the precipitation rate because of its effect on the conductivity of the collected dust layer.

Conditioning agents have been added to the flue gas to alter dust resistivity. Steam, sodium chloride, sulfur trioxide, and ammonia have all been successfully used. Research by Chittum and others [Schmidt, *Ind. Eng. Chem.,* **41,** 2428 (1949)] led to a theory of conditioning by alteration of the moisture-adsorption properties of dust surfaces. Chittum proposed that an intermediate chemical-adsorption film, which was strongly bound to the particle and which in turn strongly adsorbed water, would be an effective conditioner. This explains how acid conditioners, such as SO_3, help resistivity problems associated with basic dusts, such as many types of fly ash, whereas ammonia is a good additive for acidic dusts such as alumina. Moisture alone can be used as a conditioning agent. This is shown in Fig. 17-65. Moisture is beneficial in two ways: it reduces the electrical resistivity of most dusts (an exception is powdered sulfur, which apparently does not absorb water), and it increases the voltage which may safely be employed without sparking, as shown in Fig. 17-65.

Low resistivity can sometimes be a problem. If the resistivity is below 10^4 Ω·cm, the collected particles are so conductive that their charges leak to ground faster than they are replenished by the corona. The particles are no longer electrostatically pinned to the plate, and

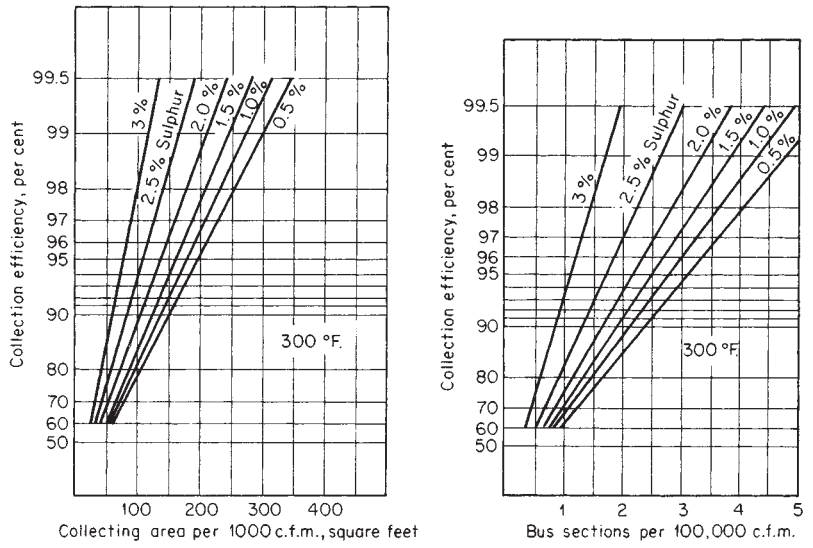

FIG. 17-69 Design curves for electrostatic precipitators for fly ash. Collection efficiency for various levels of percent sulfur in coal versus (*a*) specific collecting surface, and (*b*) bus sections per 100,000 ft^3/min (4.7 m^3/s). °C = (°F − 32) × 5/9. (*Ramsdell,* Design Criteria for Precipitators for Modern Central Station Power Plants, *American Power Conference, Chicago, Ill., 1968.*)

they may then be swept away and reentrained in the exit gas. The particles may even pick up positive charges from the collecting plate and then be repelled. Low-resistivity problems are common with dusts of high carbon content and may also occur in fly-ash precipitators which handle the ash from high-sulfur coal and operate at low gas temperatures. Low resistivity in this case results from excessive condensation of electrically conductive sulfuric acid.

Single-Stage Precipitators The single-stage type of unit, commonly known as a Cottrell precipitator, is most generally used for dust or mist collection from industrial-process gases. The corona discharge is maintained throughout the precipitator and, besides providing initial ionization, serves to prevent redispersion of precipitated dust and recharges neutralized or discharged particle ions. Cottrell precipitators may be divided into two main classes, the so-called plate type (Fig. 17-70), in which the collecting electrodes consist of parallel plates, screens, or rows of rods, chains, or wires; and the pipe type (Fig. 17-71), in which the collecting electrodes consist of a nest of parallel pipes which may be square, round, or of any other shape. The discharge or precipitating electrodes in each case are wires or rods, either round or edged, which are placed midway between the collecting electrodes or in the center of the pipes and may be either parallel or perpendicular to the gas flow in the case of plate precipitators. When the collecting electrodes are screens or rows of rods or wires, the gases are usually passed parallel to the plane of each but may also be passed through it. In pipe precipitators, the gas flow is generally vertical up through the pipe, although downflow is not unusual. The pipe-type precipitator is usually used for the removal of liquid particles and volatilized fumes [Beaver, op. cit.; and Cree, *Am. Gas J.*, **162,** 27 (March 1945)], and the plate type is used mainly on dusts. In the pipe type, the discharge electrodes are usually suspended from an insulated support and kept taut by a weight at the bottom. Cree (op.

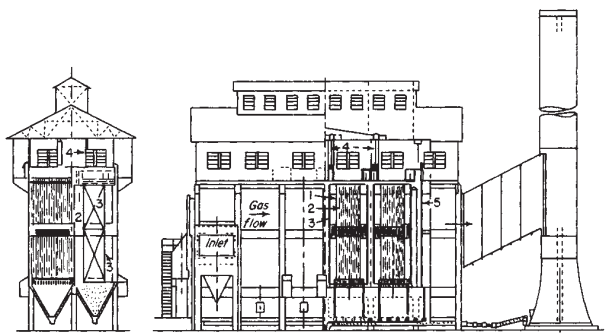

FIG. 17-70 Horizontal-flow plate precipitator used in a cement plant. (*Western Precipitation Division, Joy Manufacturing Company.*)

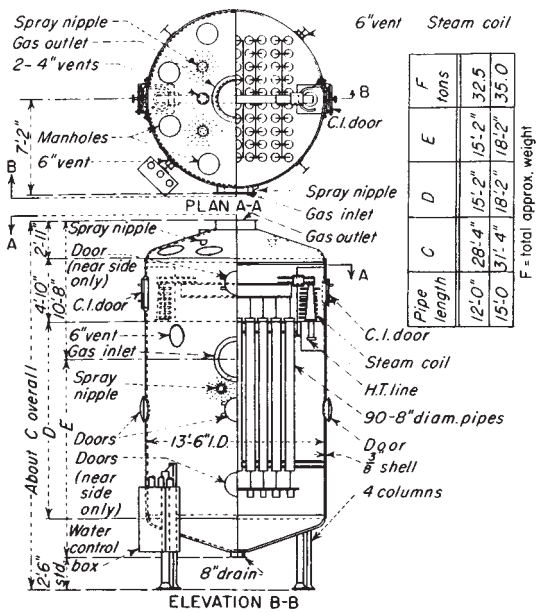

FIG. 17-71 Blast-furnace pipe precipitator. (*Research-Cottrell, Inc.*)

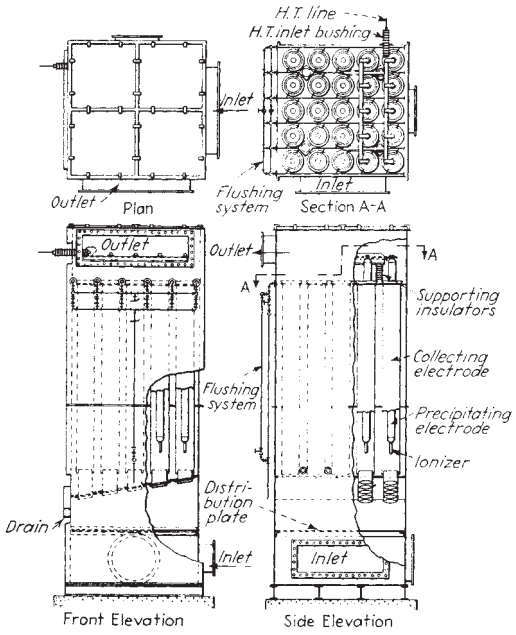

FIG. 17-72 Two-stage water-film pipe precipitator. (*Western Precipitation Division, Joy Manufacturing Company.*)

cit.) discusses the application of electrical precipitators to tar removal in the gas industry.

Rapping Except when liquid dispersoids are being collected or, in the case of film precipitators, when a liquid is circulated over the collecting-electrode surface (Fig. 17-72), thus continuously removing the precipitated material, the collected dust is dislodged from the electrodes either periodically or continuously by mechanical rapping or scraping, which may be performed automatically or manually. Automatic rapping with either impact-type or vibrator-type rappers is common practice. White (op. cit.) recommends fairly continuous rapping with magnetic-impulse rappers. Rapping with excessive force leads to dust reentrainment and possible mechanical failure of the plates, while insufficient rapping leads to excessive dust buildup with poor electrical operation and reduced collection efficiency. Intermittent rapping at intervals of an hour or more causes heavy puffs of reentrained dust. Sproull [*Air Pollut. Control Assoc. J.*, **15,** 50 (1965)] reports the importance of electrode acceleration and shows that it varies with the type of dust, whether the electrode is rapped perpendicularly (normally) to the plate or parallel to it. Figure 17-73 shows the accelerations required for rapping normally to the plate. Difficult dusts may require as much as 100 G acceleration for 90 percent removal, and even higher accelerations are required when the vibrating force is applied in the plane of the plate.

Perforated-plate or rod-curtain precipitators are frequently rapped without shutting off the gas flow and with the electrodes energized. This procedure, however, results in a tendency for reentrainment of collected dust. Sectional or composite-plate collecting electrodes (sometimes known as hollow, pocket, or tulip electrodes) are used to minimize this tendency in the continuous removal of the precipitated material, provided that it is free-flowing. These are generally designed for vertical gas flow and comprise a collecting electrode containing a dead air space and provided with horizontal protruding slots that guide the dust into this space (see Fig. 17-74), although some types use horizontal flow.

The choice of size, shape, and type of electrode is based on economic considerations and is usually determined by the characteristics of the gas and suspended matter and by mechanical considerations such as flue arrangement, the available space, and previous experience with the electrodes on similar problems. The spacing between collecting electrodes in plate-type precipitators and the pipe diameter

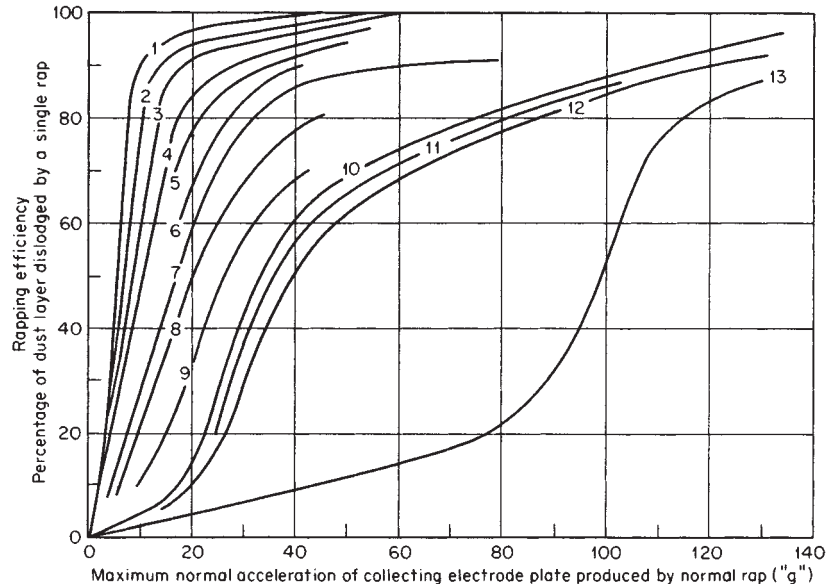

FIG. 17-73 Normal (perpendicular) rapping efficiency for various precipitated dust layers having about 0.03 g dust/cm^2 (0.2 g dust/in^2) as a function of maximum acceleration in multiples of *g*. Curve 1, fly ash, 200 or 300°F, power off. Curve 2, fly ash, 70°F, power off; also 200 or 300°F, power on. Curve 3, fly ash, 70°F, power on. Curve 4, cement-kiln feed, 300°F, power off. Curve 5, cement dust, 300°F, power off. Curve 6, same as 5, except power on. Curve 7, cement-kiln feed, 300°F, power on. Curve 8, cement dust, 200°F, power off. Curve 9, same as 8, except power on. Curve 10, cement-kiln feed, 200°F, power off. Curve 11, same as 10, except at 70°F. Curve 12, cement-kiln feed, 200°F, power on. Curve 13, cement-kiln feed, 70°F, power on. °C = (°F − 32) × 5/9. [*Sproull,* Air Pollut. Control Assoc. J., ***15,*** *50 (1965).*]

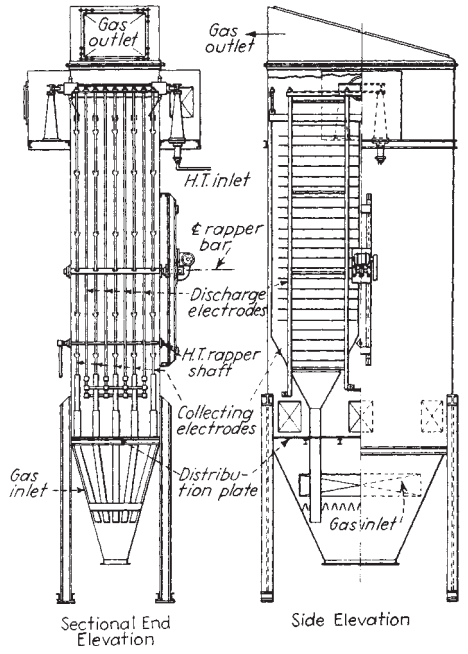

FIG. 17-74 Vertical-flow heavy-duty plate precipitator. (*Western Precipitation Division, Joy Manufacturing Company.*)

in pipe-type precipitators usually ranges from 15 to 38 cm (6 to 15 in). The smaller the spacing, the lower the necessary voltage and overall equipment size, but the greater the difficulties involved in maintaining proper alignment and resulting from disturbances due to collected material. Large spacings are usually associated with high dust concentration in order to minimize sparkover due to dust buildup. For very high dust concentrations, such as those encountered in fluid-catalyst plants, it is advantageous to use greater spacings in the first half of the precipitator than in the second half. Precipitators, especially of the plate type, are frequently built with groups of collecting electrodes in series in a common housing. Collecting electrodes are generally on the order of 0.9 to 1.8 m (3 to 6 ft) wide and 3 to 5.5 m (10 to 18 ft) high in plate-type precipitators and 1.8 to 4.6 m (6 to 15 ft) high in pipe types. It is essential for good collection efficiency that the gas be evenly distributed across the various electrode elements. Although this can be achieved by proper gas-inlet transitions and guide vanes, perforated plates or screens located on the upstream side of the electrodes are generally used for distribution. Perforated plates or screens located on the downstream side may be used in special cases.

Electrical precipitators are generally designed for collection efficiency in the range of 90 to 99.9 percent. It is essential, however, that the units be properly maintained in order to achieve the required collection efficiency. Electric power consumption is generally 0.2 to 0.6 kW/(1000 ft^3·min) of gas handled, and the pressure drop across the precipitator unit is usually less than 124 Pa (0.5 in water), ranging from 62 to 248 Pa (¼ to 1 in) and representing primarily distributor and entrance-exit losses. Applied potentials range from 30,000 to 100,000 V. Gas velocities and retention times are generally in the range of 0.9 to 3 m/s (3 to 10 ft/s) and 1 to 15 s respectively. Velocities are kept low in conventional precipitators to avoid reentrainment of dust. There are, however, precipitator installations on carbon black in which the precipitator acts to flocculate the dust so that it may be subsequently collected in multiple small-diameter cyclone collectors. By not attempting to collect the particles in the precipitator, higher velocities may be used with a correspondingly lower investment cost.

Power Supply Electrical precipitators are generally energized by rectified alternating current of commercial frequency. The voltage is stepped up to the required value by means of a transformer and then rectified. The rectifying equipment has undergone an evolution which began with the synchronous mechanical rectifier in 1904 and was followed by mercury-vapor rectifiers in the 1920s; the first solid-state selenium rectifiers were introduced about 1939. Silicon rectifiers are the latest and most widely used type, since they provide high efficiency and reliability. Automatic controls commonly are tied to voltage, current, spark rate, or some combination of these parameters. Modern precipitators use control circuits similar to those on Fig. 17-75. A high-voltage silicon rectifier is used together with a saturable reactor and means for limiting current and controlling voltage and/or spark rate. One popular method adjusts the voltage to give a specified sparking frequency (typically 50 to 150 sparks per minute per bus section). Half-wave rectification is sometimes used because of its lower equipment requirements and power consumption. It also has the advantage of longer decay periods for sparks to extinguish between current pulses.

Electrode **insulators** must also be designed for a particular service. The properties of the dust or mist and gas determine their design as well as the physical details of the installation. Conducting mists require special allowances such as oil seals, energized shielding cups, or air bleeds. With saturated gas, steam coils are frequently used to prevent condensation on the electrodes.

Typical applications in the chemical field (Beaver, op. cit.) include detarring of manufactured gas, removal of acid mist and impurities in contact sulfuric acid plants, recovery of phosphoric acid mists, removal of dusts in gases from roasters, sintering machines, calciners, cement and lime kilns, blast furnaces, carbon-black furnaces, regenerators on fluid-catalyst units, chemical-recovery furnaces in soda and sulfate pulp mills, and gypsum kettles. Figure 17-74 shows a vertical-flow steel-plate-type precipitator similar to a type used for catalyst-dust collection in certain fluid-catalyst plants.

A development of interest to the chemical industry is the tubular precipitator of reinforced-plastic construction (Wanner, *Gas Cleaning Plant after TiO_2 Rotary Kilns,* technical bulletin, Lurgi Corp., Frankfurt, Germany, 1971). Tubes made of polyvinyl chloride plastic are reinforced on the outside with polyester-fiber glass. The use of modern economical materials of construction to replace high-maintenance materials such as lead has been long awaited for corrosive applications.

Electrical precipitators are probably the most versatile of all types of dust collectors. Very high collection efficiencies can be obtained regardless of the fineness of the dust, provided that the precipitators are given proper maintenance. The chief disadvantages are the high initial cost and, in some cases, high maintenance costs. Furthermore, caution must be exercised with dusts that are combustible in the carrier gas.

Two-Stage Precipitators In two-stage precipitators, corona discharge takes place in the first stage between two electrodes having a nonuniform field (see Fig. 17-76). This is generally obtained by a fine-wire discharge electrode and a large-diameter receiving electrode. In this stage the potential difference must be above that required for corona discharge. The second stage involves a relatively uniform electrostatic field in which charged particles are caused to migrate to a collecting surface. This stage usually consists of either alternately charged parallel plates or concentric cylinders with relatively close clearances compared with their diameters. The only voltage requirement in this stage is that no sparking occur, though higher voltages will result in increased collection efficiency. Since collection occurs in the absence of corona discharge, there is no way of recharging reentrained and discharged particles. Consequently, some means must be provided for avoiding reentrainment of particles from the collecting surface. It is also essential that there be sufficient time and mixing between the first and second stages to secure distribution of gas ions across the gas stream and proper charging of the dust particles.

A unit is available in which electrostatic precipitation is combined with a dry-air filter of the type shown in Fig. 17-64*b*. In another unit an electrostatic field is superimposed on an automatic filter. In this case the ionizer wires are located on the leading face of the unit, and the collecting electrodes consist of alternate stationary and rotating parallel plates. Cleaning in this case is automatic and continuous.

Although intended primarily for air-conditioning applications, these units have been successfully applied to the collection of relatively nonconducting mists such as oil. However, other process applications

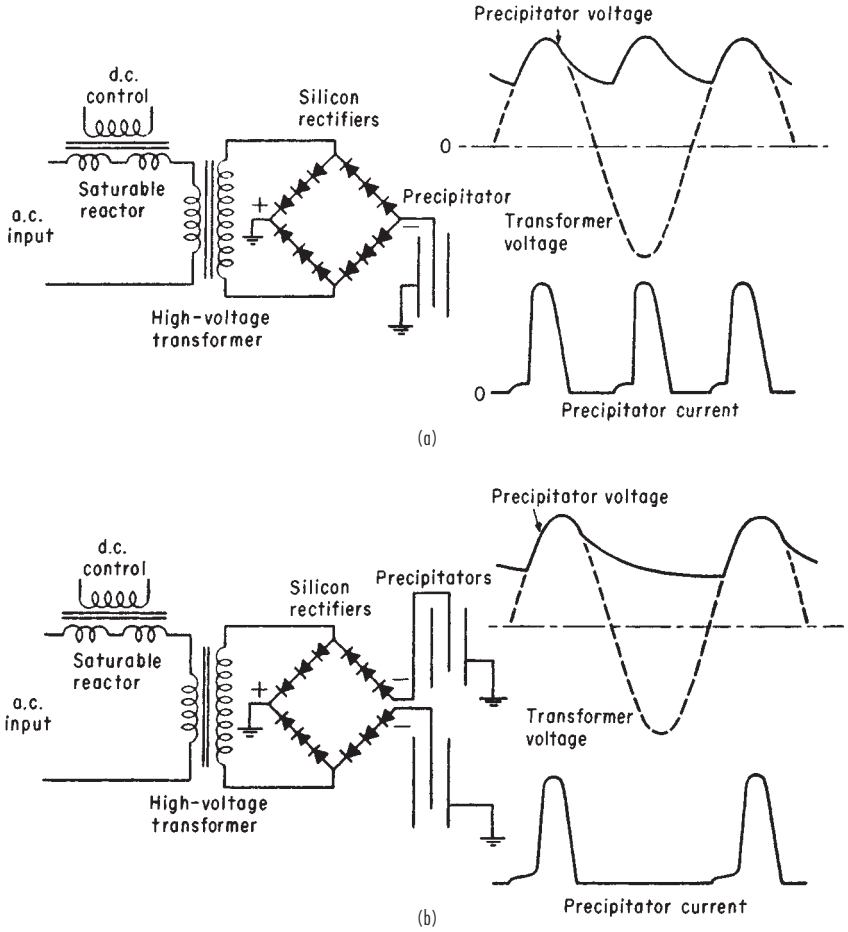

FIG. 17-75 Schematic circuits for silicon rectifier sets with saturable reactor control. (*a*) Full-wave silicon rectifier. (*b*) Half-wave silicon rectifier. (*White,* Industrial Electrostatic Precipitation, *Addison-Wesley, Reading, Mass., 1963.*)

have been limited largely to experimental installations. The large cost advantage of these units over the Cottrell precipitator lies in the smaller equipment size made possible by the close plate spacing, in the lower power consumption due to the two-stage operation, and primarily in the mass production of standardized units. In process applications, the close plate spacing is objectionable because of the relatively high dust concentrations involved. Special material or weight requirements for the structural members may eliminate the mass-production advantage except for individual wide applications.

Alternating-Current Precipitators High-voltage alternating current may be employed for electrical precipitation. Corona discharge will result in a net rectification, provided that no spark gaps are used in series with the precipitator. However, the equipment capacity for a given efficiency is considerably lower than for direct current. In addition, difficulties due to induced high-frequency currents may be encountered. The simplicity of an ac system, on the other hand, has permitted very satisfactory adaptation for laboratory and sampling purposes [Drinker, Thomson, and Fitchet, *J. Ind. Hyg.*, **5,** 162 (September 1923)].

Some promising work with alternating current has been undertaken at the University of Karlsruhe. Lau [*Staub,* English ed., **29,** 10 (1969)] and coworkers found that ac precipitators operated at 50 Hz were more effective than dc precipitators for dusts with resistivities higher than 10^{11} Ω·cm. An insulating screen covering the collecting electrode permitted higher-voltage operation without sparkover.

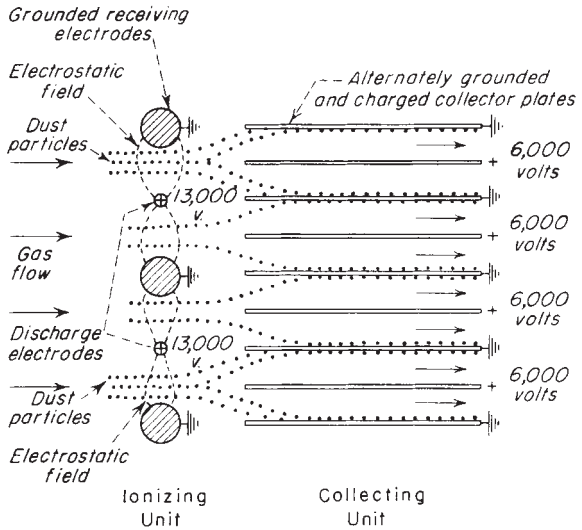

FIG. 17-76 Two-stage electrical-precipitation principle.